

SCUOLA DI SCIENZE
Dipartimento di Chimica Industriale “Toso Montanari”

Corso di Laurea Magistrale in

Chimica Industriale

Classe LM-71 - Scienze e Tecnologie della Chimica Industriale

Synthesis of novel cobalt and iron
complexes for sustainable catalytic
hydrogenations

Tesi di laurea sperimentale

CANDIDATO

Andrea Cingolani

RELATORE

Chiar.mo Prof. Valerio Zanotti

CORRELATORE

Dr. Cristiana Cesari

Dr. Kathrin Junge

Dr. Rita Mazzoni

Sessione II

Anno Accademico 2013-2014

ABSTRACT

Scopo del presente lavoro di tesi è la sintesi di nuovi complessi basati su metalli non nobili allo scopo di essere impiegati in reazioni redox attraverso un meccanismo cooperativo cooperativo metallo-legante. La necessità di sostituire i metalli preziosi, costosi e tossici con altri più disponibili ed ambientalmente compatibili, ha portato allo sviluppo di nuovi composti basati sul cobalto e sul ferro, i quali sono i metalli sotto il presente studio.

Il complesso carbonil-tetraidrobolato-bis[(2-diisopropilfosfino)etil]ammino-cobalto è stato sintetizzato tramite un percorso in tre passaggi. Tentativi di ottimizzazione del percorso di reazione sono stati valutati in modo da ridurre i tempi di reazione e l'utilizzo di solvente.

Il nuovo complesso di cobalto è stato testato nell'idrogenazione di esteri e nel ADC (Acceptorless Dehydrogenative Coupling) di etanolo. Altre varietà di substrati sono stati testate in modo tale da valutare altre possibili applicazioni.

Riguardo al complesso di ferro, dicarbonil-(η^4 -3,4-bis(4-metossifenil)-2,5-difenilciclopenta-2,4-dienone)(1,3-dimetil-ilidene)ferro è stato sintetizzato attraverso un percorso in tre passaggi, che comprendendo una transmetallazione da un complesso d'argento, derivante da un sale d'imidazolio, al complesso di ferro. In modo tale da evitare l'utilizzo di solventi, è stata valutata una possibile ottimizzazione. Studi sono stati effettuati per valutare l'attività del precursore tricarbonile di ferro verso i composti del sale d'imidazolio e d'argento.

SUMMARY

Aim of the present work of thesis is to synthesize new non-noble metal based complexes to be employ in redox reactions by a metal-ligand cooperative mechanism. The need of replacing toxic and expensive precious metal complexes with more available and benign metals, has led to the development of new compounds based on cobalt and iron, which are the metals investigated in this study.

A carbonyl-tetrahydroborato-bis[(2-diisopropylphosphino)ethyl]amine-cobalt complex bearing a PNP-type ligand is synthesized by a three-step route. Optimization attempt of reaction route were assessed in order to lowering reaction times and solvent waste.

New cobalt complex has been tested in esters hydrogenation as well as in acceptorless dehydrogenative coupling of ethanol. Other varieties of substrates were also tested in order to evaluate any possible applications.

Concerning iron complex, dicarbonyl-(η^4 -3,4-bis(4-methoxyphenyl)-2,5-diphenylcyclopenta-2,4-dienone)(1,3-dimethyl-ilidene)iron is synthesized by a three steps route, involving transmetallation of a silver complex, derived from an imidazolium salt, to iron complex. In order to avoid solvent waste, optimization is assessed. Studies were performed to assess activity of triscarbonyl iron precursor toward imidazolium salt and silver complexes.

1. INTRODUCTION	1
1.1 HYDROGENATION	1
1.1.1 Molecular hydrogen activation	2
1.2 DEHYDROGENATION	3
1.3 PINCER LIGANDS	5
1.4 RUTHENIUM COMPLEXES FOR ESTERS HYDROGENATION	8
1.4.1 Triphos ligands	8
1.4.2 Polydentate ligands	10
1.5 IRON PINCER COMPLEXES	12
1.5.1 Methanol dehydrogenation	14
1.5.2 Esters hydrogenation	15
1.6 COBALT PINCER COMPLEXES	16
AIM OF THE THESIS WORK	20
2. RESULTS AND DISCUSSION	21
2.1 COBALT COMPLEXES	21
2.1.1 Synthesis of dichloride-bis[(2-diisopropylphosphino)ethyl]amine-cobalt(II) (A)	21
2.1.2 Synthesis of carbonyl-dichloride-bis[(2-diisopropylphosphino)ethyl]amine-cobalt(II) (B)	22
2.1.3 Synthesis of carbonyl-hydrido-tetrahydroborato-bis[(2-diisopropylphosphino)ethyl]amine-cobalt(II) (C)	24
2.1.4 Synthesis of dibromide-bis[(2-diisopropylphosphino)ethyl]amine-cobalt(II) (D)	26
2.1.5 Synthesis of carbonyl-dibromide-bis[(2-diisopropylphosphino)ethyl]amine-cobalt(II) (E)	28
2.1.6 Synthesis of carbonyl-tetrahydroborato-bis[(2-diisopropylphosphino)ethyl]amine-cobalt (I) (F)	30
Attempt of synthesis of carbonyl-dibromide-bis[(2-diisopropylphosphino)ethyl]amine-cobalt(II) <i>in situ</i>	33
2.2 HYDROGENATION REACTIONS	35
2.3 ADC	41
2.4 SYNTHESIS OF A NOVEL IRON N-HETEROCYCLIC CARBENE COMPLEX	43
2.4.1 SHVO'S CATALYST	43
2.4.1.1 Reactivity	43
2.4.1.2 Structure	44
2.4.1.3 Discovery	44

2.4.1.4 Synthesis	45
2.4.1.5 Microwave assisted synthesis	46
2.4.1.6 Applications	48
2.4.1.7 Upgrading of bio-oil	48
2.4.1.8 Hydrogenation of HMF	50
2.4.1.9 Iron analogous	50
2.4.2 SYNTHESIS OF IRON COMPLEX	53
2.4.2.1 Synthesis of tricarbonyl-(η^4 -3,4-bis(4-methoxyphenyl)-2,5-diphenylcyclopenta-2,4-dienone)iron (G)	53
2.4.2.2 Synthesis of dicarbonyl-(η^4 -3,4-bis(4-methoxyphenyl)-2,5-diphenylcyclopenta-2,4-dienone)(acetonitrile)iron (H)	55
2.4.2.3 Synthesis of dicarbonyl-(η^4 -3,4-bis(4-methoxyphenyl)-2,5-diphenylcyclopenta-2,4-dienone)(1,3-dimethyl-ilidene)iron (I)	56
2.4.2.4 Attempts of synthesis of dicarbonyl-(η^4 -3,4-bis(4-methoxyphenyl)-2,5-diphenylcyclopenta-2,4-dienone)(1,3-dimethyl-ilidene)iron <i>in situ</i>	57
3. CONCLUSIONS	60
4. EXPERIMENTAL SECTION	63
4.1 GENERAL PROCEDURE	63
4.1.1 LIKAT (Rostock)	63
4.1.2 Bologna	64
4.2 COBALT COMPLEXES	66
4.2.1 Synthesis of dichloride-bis[(2-diisopropylphosphino)ethyl]amine-cobalt(II) (A)	66
4.2.2 Synthesis of carbonyl-dichloride-bis[(2-diisopropylphosphino)ethyl]amine-cobalt(II) (B)	67
4.2.3 Attempt of synthesis of carbonyl-hydrido-tetrahydroborato-bis[(2-diisopropylphosphino)ethyl]amine-cobalt(II) (C)	70
4.2.4 Synthesis of dibromide-bis[(2-diisopropylphosphino)ethyl]amine-cobalt(II) (D)	71
4.2.5 Synthesis of carbonyl-dibromide-bis[(2-diisopropylphosphino)ethyl]amine-cobalt(II) (E)	72
4.2.6 Synthesis of Carbonyl-dibromide-Bis[(2-diisopropylphosphino)ethyl]amine-Cobalt(II) (E)	75
4.2.7 Attempt of synthesis of carbonyl-dibromide-bis[(2-diisopropylphosphino)ethyl]amine-cobalt(II) (E) <i>in situ</i>	76
4.2.8 Synthesis of carbonyl-tetrahydroborato-bis[(2-diisopropylphosphino) ethyl]amine-cobalt(I) (F)	77
4.3 HYDROGENATION REACTION	80
4.4 ACCEPTORLESS DEHYDROGENATIVE COUPLING OF ETHANOL	82
4.5 IRON COMPLEXES	83

4.5.1 Synthesis of tricarbonyl-(η^4 -3,4-bis(4-methoxyphenyl)-2,5-diphenylcyclopenta-2,4-dienone)iron (G)	83
4.5.2 Synthesis of dicarbonyl-(η^4 -3,4-bis(4-methoxyphenyl)-2,5-diphenylcyclopenta-2,4-dienone)(acetonitrile)iron (H)	84
4.5.3 Synthesis of dicarbonyl-(η^4 -3,4-bis(4-methoxyphenyl)-2,5-diphenylcyclopenta-2,4-dienone)(1,3-dimethyl-ilidene)iron (I)	85
4.5.4 Attempt of synthesis of dicarbonyl-(η^4 -3,4-bis(4-methoxyphenyl)-2,5-diphenylcyclopenta-2,4-dienone)(1,3-dimethyl-ilidene)iron <i>in situ</i>	86
4.5.5 Attempt of synthesis of dicarbonyl-(η^4 -3,4-bis(4-methoxyphenyl)-2,5-diphenylcyclopenta-2,4-dienone)(1,3-dimethyl-ilidene)iron <i>in situ</i>	87
5. BIBLIOGRAPHY	88

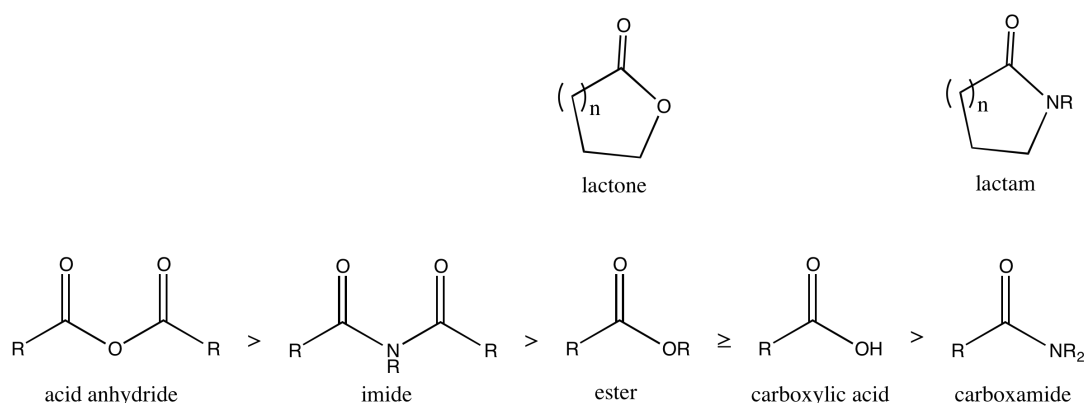
1. INTRODUCTION

1.1 HYDROGENATION

Hydrogenation is a reaction in which an unsaturated substrate is reduced to a saturated substrate by addition of hydrogen. One of the most known reaction is the reduction of C=C double bond of an alkenes to form alkanes. This reaction is widely used in industry: for instance the food industry applies catalytic hydrogenation to convert liquid vegetable oils to semi-solid fats, also known as margarine. The main issue is that catalysts employed in hydrogenation can also lead to isomerization of some double bonds (which are naturally cis conformation in most of fatty acids); the consequences of this change in conformation is not well known yet, but some tests say that an high level of cholesterol in the blood has been found⁽¹⁾. In this work I will focus on the C=O polar double-bonds homogeneous hydrogenation of esters to alcohols.

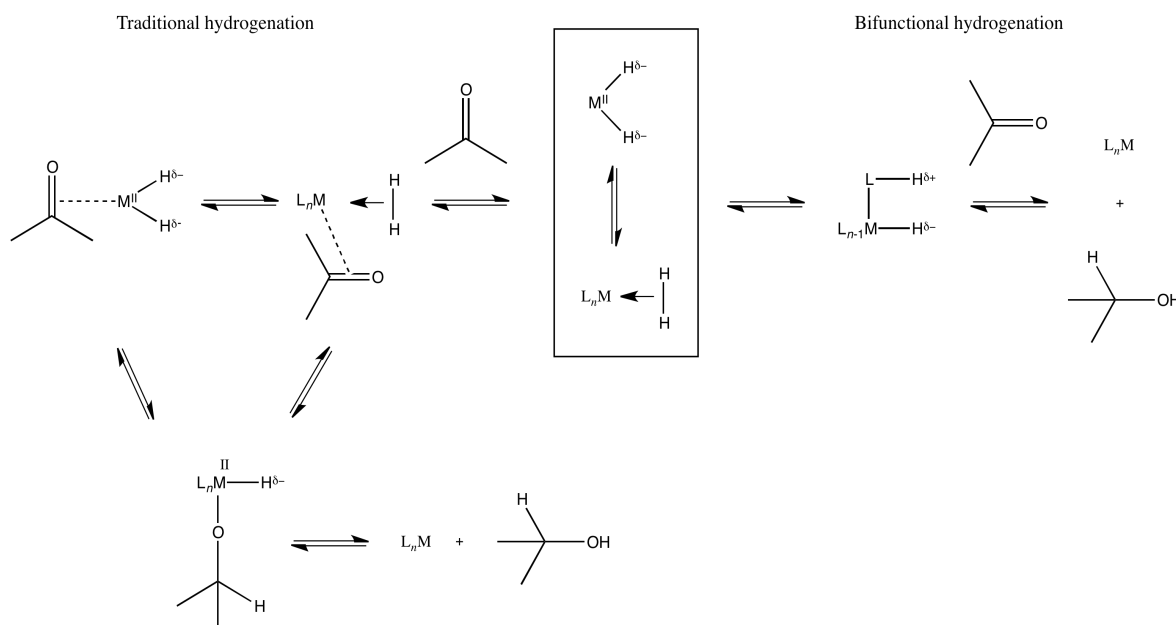
Reduction of ester to alcohol is one of the most important reactions in organic chemistry, indeed it is used in the field of pharmaceutical and fine chemistry, perfumes and agrochemicals. Classical methods in homogeneous hydrogenation rely on stoichiometric use of metal hydrides such as LiAlH₄ and NaBH₄, which are dangerous and lead to low atom efficiency and waste production⁽²⁾. New methods employ organometallic catalysts with molecular hydrogen H₂ as a reducing agent, which is far more advantageous due to high atom efficiency and the absence of side products.

On larger scale industry, heterogeneous catalysts are employed in hydrogenations of alkene, aldehydes and ketones, but less electrophilic carbonyl groups, such as carboxylic acids and their derivatives (Scheme 1), need more harsh conditions in order to get the desired products. On the other hand, homogeneous catalysts generally require milder conditions, which can lead to higher selectivity.



Scheme 1. Carboxylic acids derivatives with expected decrease C=O electrophilicity.

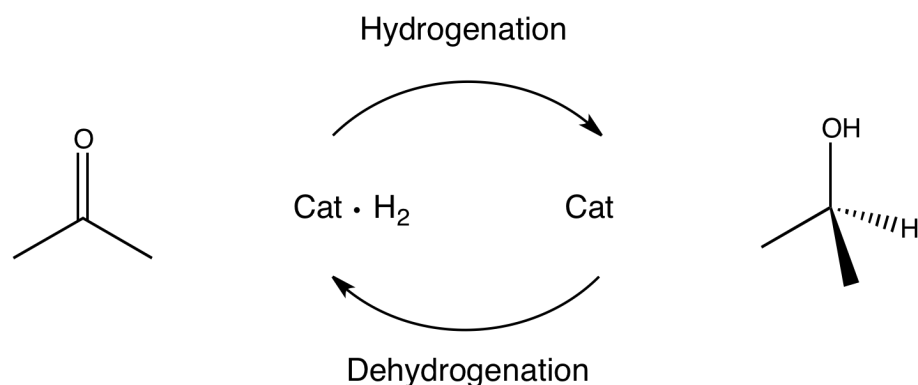
bounded to the metal⁽⁷⁾⁽⁸⁾. These functions (formally H⁺ and H⁻) are transferred to the substrate, which must be polarized. Thus, this mechanism can be usefully employed for hydrogenation of carbonyl groups, rather than alkenes. Advantages are associated to the lower activation energy required by heterolytic splitting compared to homolytic cleavage via oxidative addition.



Scheme 3. Hydrogen cleavage and type of hydrogenation: traditional on the left and bifunctional on the right.

1.2 DEHYDROGENATION

Reverse process of hydrogenation is called dehydrogenation (Scheme 4). Dehydrogenation involves loss of hydrogen from a molecule and converts a saturated substrate to an unsaturated one. An example of large-scale dehydrogenation is production of styrene from ethylbenzene⁽⁹⁾.

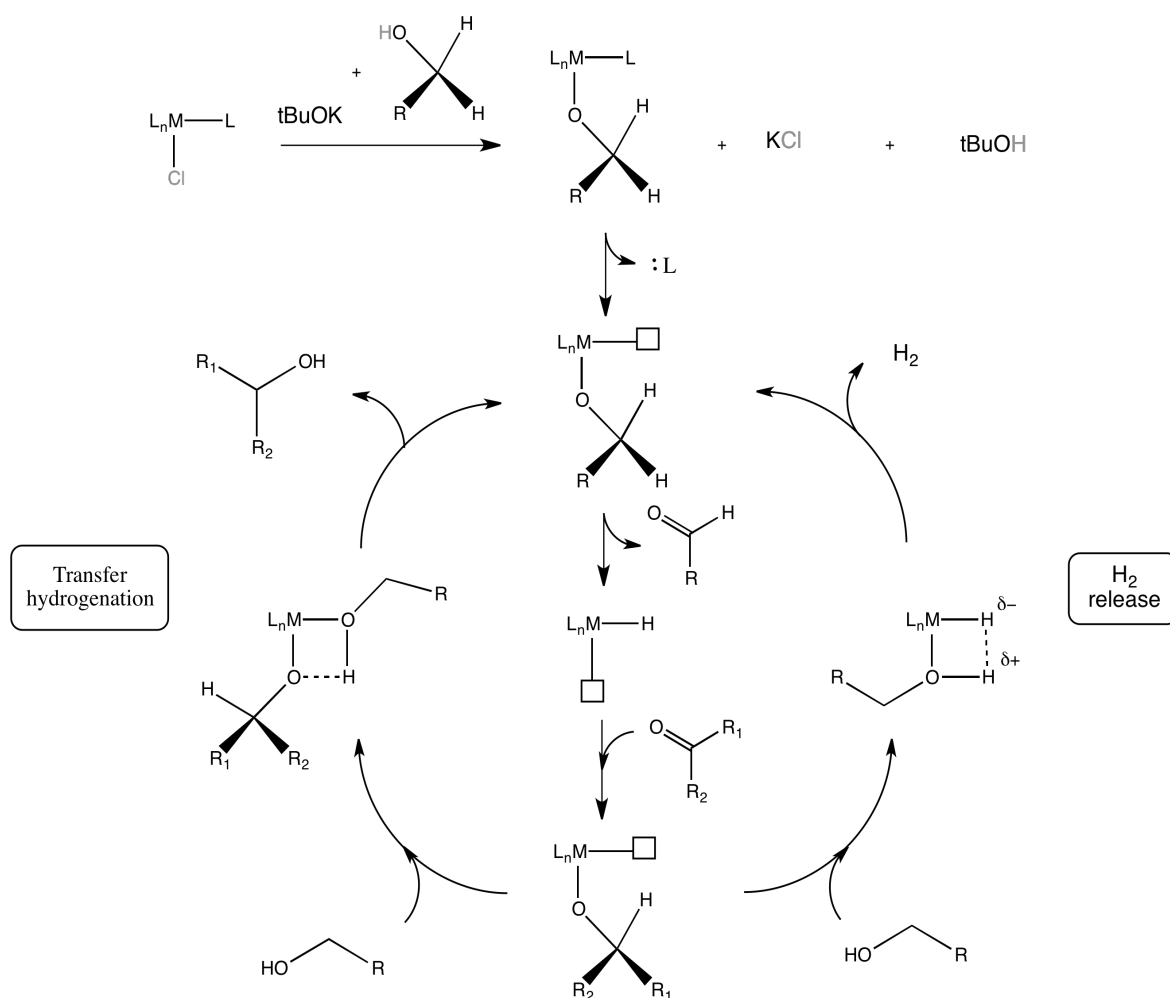


Scheme 4. Hydrogenation is the same reaction of dehydrogenation but on the other way around.

As for hydrogenation, also dehydrogenation mechanism can be divided into two:

- Inner-sphere or “classical” mechanism;
- Outer-sphere or bifunctional mechanism.

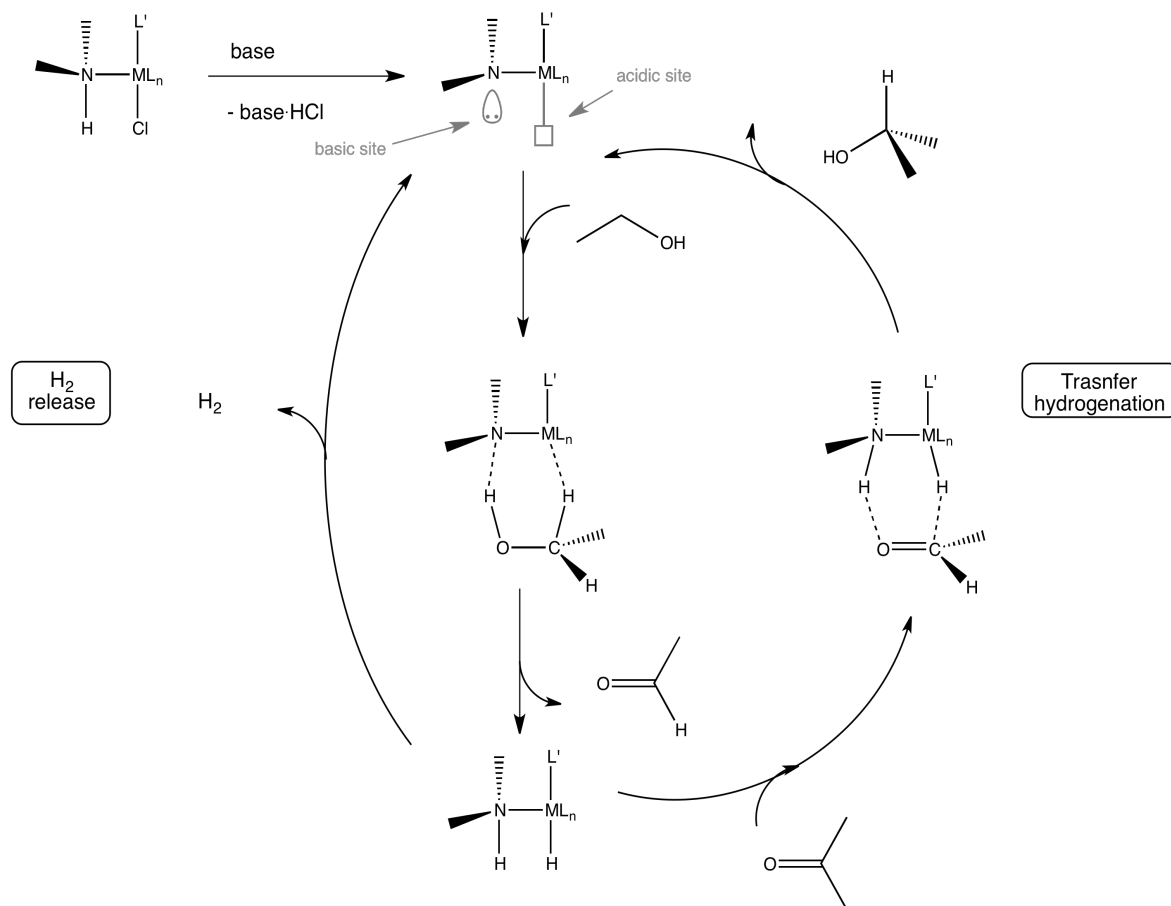
In inner-sphere mechanism, catalysts usually need a base for activation and heating for displacement of a labile ligand. The substrate is coordinated to the metal and a labile ligand is displaced in order to have a vacant site at metal center. By this way, a β -hydride elimination occurs and product can be released from the metal complex. An example of this mechanism is reported in Scheme 5. After dehydrogenation, the catalyst is regenerated via H_2 acceptorless release, or by hydrogen transfer to another molecule, which can be a sacrificial acceptor or substrate itself.



Scheme 5. A schematic example of a traditional dehydrogenation mechanism.

Outer-sphere catalysts are characterized by a basic site, usually a nitrogen in one ligand, and acidic site, on metal center. Also in this case dehydrogenation is typically performed using a base to obtain the active catalyst, but it is also possible to work without any base,

as in the case of the Shvo catalyst (*vide infra*). This reaction is usually described as a concerted transfer, where the transition state with H₂ transfer is shown as one single step. An example is described in Scheme 6, where the active catalyst is a 16 electron complex. After dehydrogenation the catalyst becomes an 18 electron complex. Catalyst needs to be recycled in the same way of inner-sphere catalyst, so by H₂ release or by hydrogen transfer to a other molecule.



Scheme 6. Example of outer-sphere mechanism.

1.3 PINCER LIGANDS

Pincer-type ligands are tridentate ligands with one neutral or anionic central donor atom (Y) surrounded by two neutral two-electron donor atoms (D) (See Figure 4). They coordinate the metal center forming a bicyclic structures due to their η^3 -mer coordination, and providing remarkable thermodynamic stability to the metal complex⁽¹⁰⁾⁽¹¹⁾. Furthermore, modifications of the structure can be easily achieved, allowing to change and tune both electronic properties and steric hindrance of the ligands⁽¹²⁾⁽¹³⁾⁽¹⁴⁾.

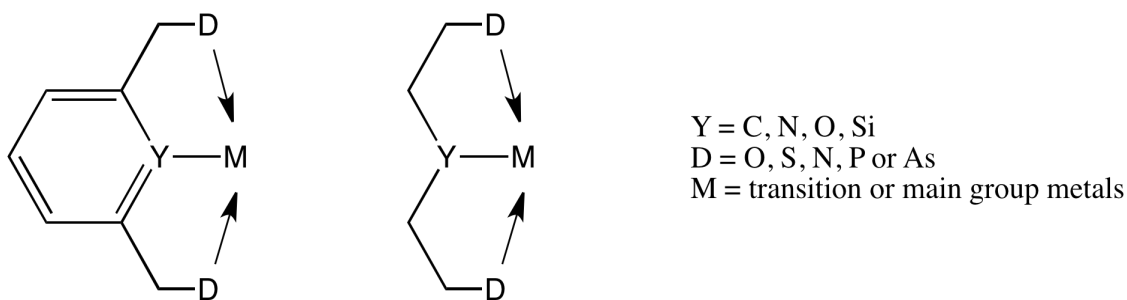


Figure 1. Structures of aromatic and aliphatic pincer-type complexes.

This type of pincer complexes was first described during the '70s and can be classified as:

- aromatic pincer complexes;
- aliphatic pincer complexes.

In general, pincer ligands based on an aromatic backbone are more robust of their aliphatic counterparts and their planar coordination allows to a better overlapping between the metal d_{xz} orbitals and the π orbitals of the aromatic backbone⁽¹⁵⁾. Moreover the manipulation of aromatic and hetero-aromatic rings was more simple, increasing the availability of different kind of DYD ligands.

Recently Milstein's group has developed a pyridine-based PNP and PNN pincer complexes of Ru(II), which have a completely new mode of ligand-metal cooperation.

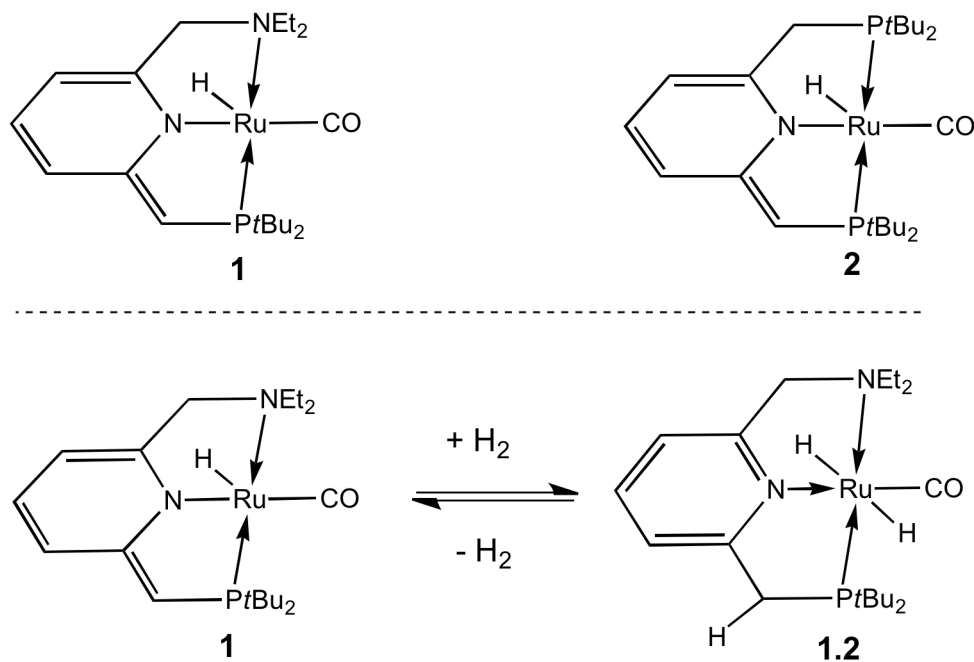
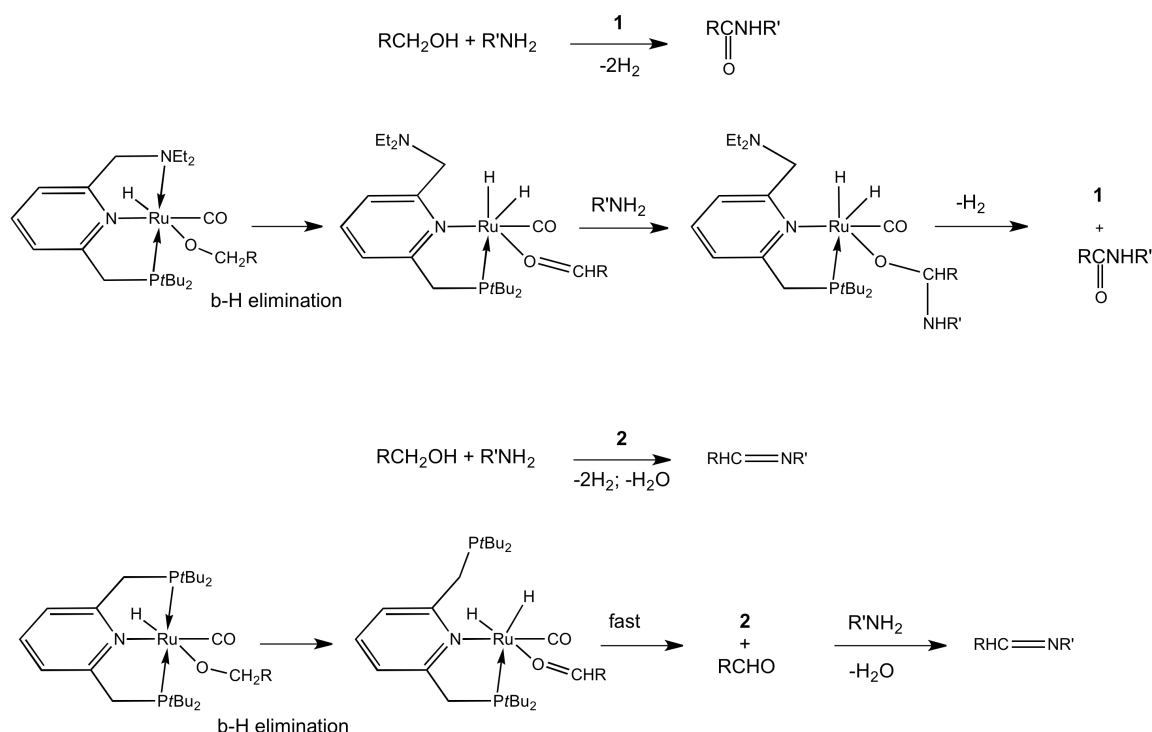


Figure 2. Ru(II) PNN **1** and PNP **2** complexes (top). Enamido **1** and imino **1.2** form (bottom).

These complexes can switch between an amido form (**1**, dearomatized) and imino form (**1.2**, aromatized), by changing the coordination of the N central atom. The switch involves a change in ligand coordination properties: in the enamido form the ligand is a π -donor, while in the imino form is a π -acceptor⁽¹⁶⁾. The PNN complex was used in the acceptorless dehydrogenative coupling of primary alcohols to obtain esters under mild conditions, and vice-versa in hydrogenation of esters to alcohols (*vide infra*).

A very interesting example of tuning of the ligand properties is the difference in reactivity of the two catalysts in a mixture of primary alcohols and amines. Complex **1** catalyzes the dehydrogenative formation of amides, whereas complex **2** brings to imines. This difference is likely due to the different lability of the ligand side arms (Scheme 7): phosphine arm is less labile than the amine one; this causes the displacement of the aldehyde intermediate and then imine as condensed product with the free amine; on the other hand, the amine arm allows the amide intermediates to form, that leads to amide product.



Scheme 7. Difference in reactivity of Ru-PNN and Ru-PNP catalysts brings to Imines or Amides.

More recently, a great interest has developed towards aliphatic pincer-type ligands due to reversible switching of the sp³ Y central atom, e.g. the interconversion between metal-amide/metal-amine form⁽¹⁷⁾ in PNP systems, which leads to heterolytic bond cleavage

(Figure 3). This metal-ligand coordination involves new non-oxidative formation and activation of polar and non-polar bonds.

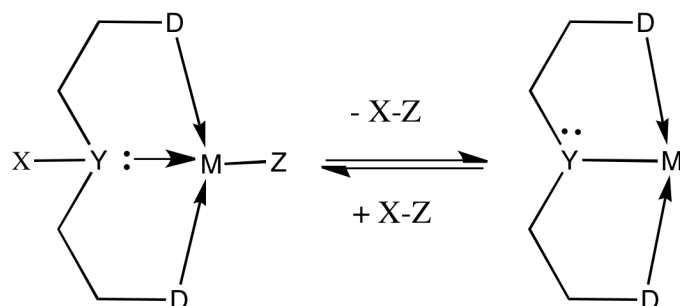


Figure 3. A schematic heterolytic bond cleavage.

Another advantage is the three dimensional steric environment due to the sp^3 hybridization, in that it this permits far more applications in stereoselective reactions.

Gusev et al. studied the activity of some iridium, osmium and ruthenium complexes in catalytic reactions such as acceptorless dehydrogenative coupling of alcohols, hydrogenation of esters and transfer hydrogenations of ketones. Beller et al., have described the synthesis of an iron-based complex bearing a PNP aliphatic ligand, which has been found active in dehydrogenation as well as hydrogenation catalytic reactions (*vide infra*).

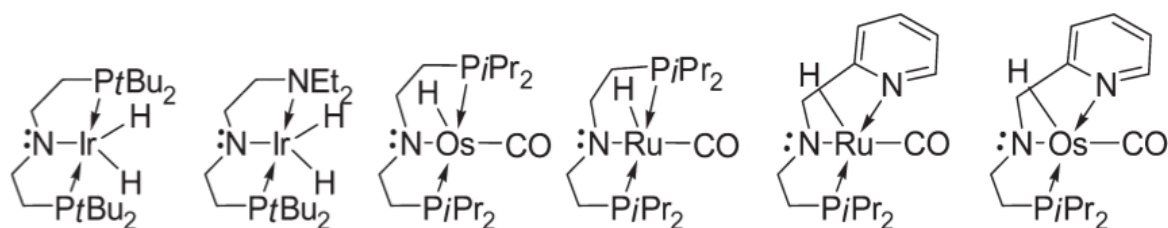


Figure 4. Different type DYD aliphatic complexes used by Gusev et al.

1.4 RUTHENIUM COMPLEXES FOR ESTERS HYDROGENATION

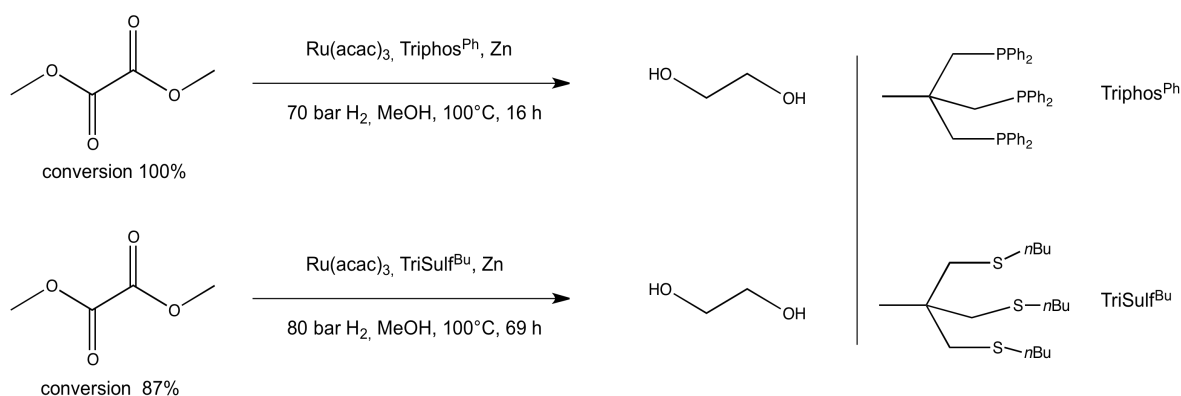
1.4.1 Triphos ligands

In 1997 Elsevier developed a new ruthenium system for esters hydrogenation starting from the study of Hara and Wada in the early 1990s. This new system consisted of $Ru(acac)_3$ /Triphos^{Ph} with addition of zinc as additive. The Triphos is tridentate phosphine, also known as 1,1,1-tris(diphenylphosphinomethyl)ethane, which confers a higher thermal stability to the corresponding complexes. In Scheme 8 the hydrogenation

of dimethyl oxalate is described. This reaction was tested to check the activity of different phosphine ligands⁽¹⁸⁾.

Also the analogue TriSulf^{Bu} has been tested to lead to the first ruthenium/sulphur catalytic system which demonstrated to be more active and selective, compared to the phosphine analogue.

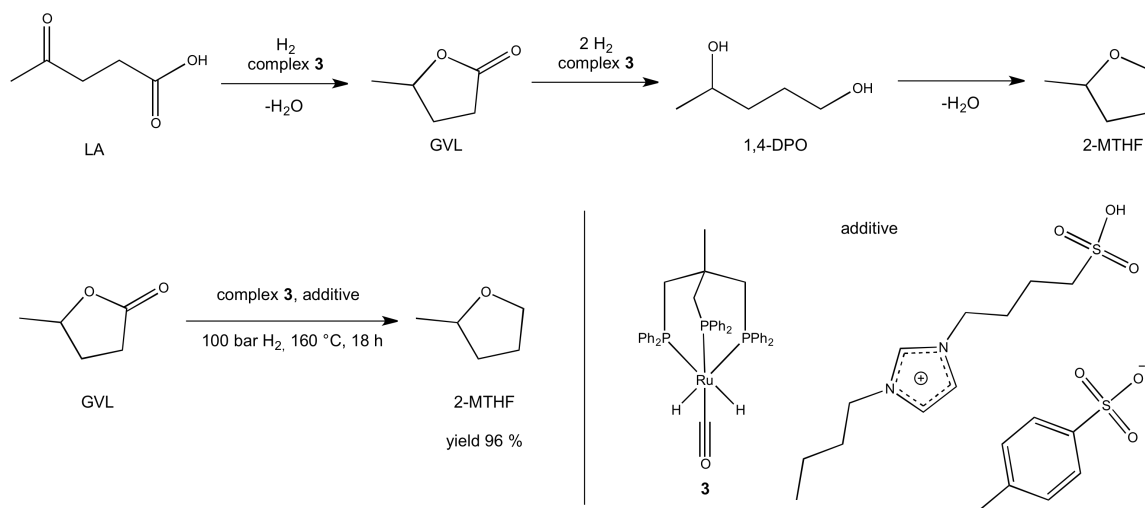
In 2011 the group of Hanton described two new ligands: N-Triphos^{Et} and N-Triphos^{Ph}⁽¹⁹⁾. Both were tested together with Ru(acac)₃ but gave lower rate of reaction. The lower activity was ascribed to decomposition of the more sensitive N-Triphos ligand. Furthermore, an array of additives was assessed by Hanton for the hydrogenation of dimethyl oxalate with Triphos, but with no change in activity.



Scheme 8. Hydrogenation of Dimethyl Oxalate with ruthenium/Triphos (up) and ruthenium/TriSulf (down) systems.

During 2011 also bio-based substrates were tested using the ruthenium/Triphos^{Ph} system (3), as described in Scheme 9, because of the interest in biomass resources. Leitner and Klankermayer focused on bio-based carboxylic acids such as levulinic acid (LA), which was hydrogenated to 2-methyltetrahydrofuran (2-MTHF, 3% yield)⁽²⁰⁾. Conversion to 2-MTHF proceeded through the formation of two intermediates: cyclic ester γ -valerolactone (GVL, 22% yield) and 1,4-pentanediol (1,4 PDO, 73% yield). In order to increase the overall yield, a catalytic amount of acidic additive was added to the reaction mixture, leading to a 96% final yield. The 2-MTHF can be used as a solvent in the pharmaceutical industry and as a fuel⁽²¹⁾⁽²²⁾⁽²³⁾⁽²⁴⁾.

The ruthenium system with Triphos ligands has been the first general catalytic system employed in homogeneous ester hydrogenations. The main issues of the catalyst concern reaction times and pressure.

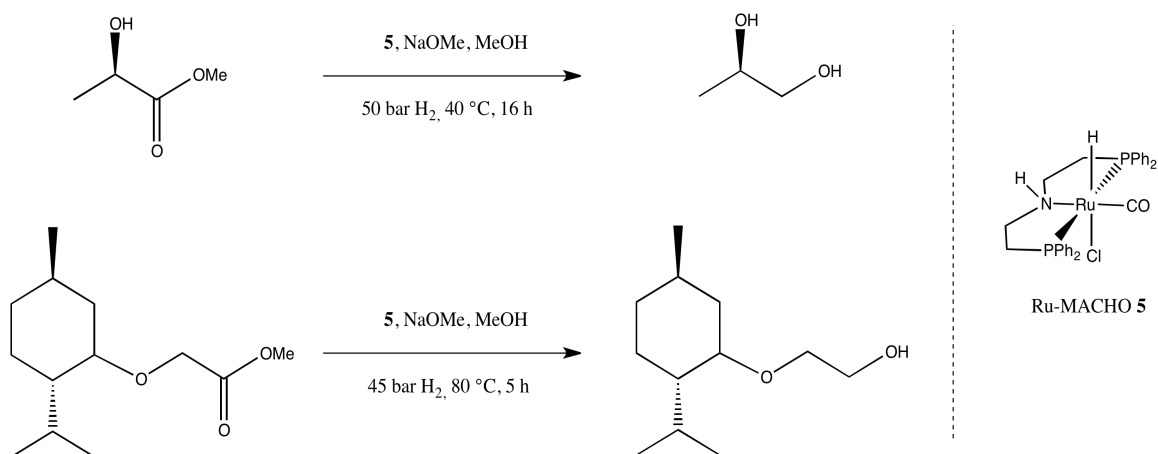


Scheme 9. Hydrogenation and corresponding yield of Levulinic Acid with complex **3** (up) and with acidic additives (down).

1.4.2 Polydentate ligands

Recently, new metal complexes bearing polydentate ligand (pincer ligands) have been discovered. In 2006 Milstein published a new ruthenium complex (**4.1**), which was able to hydrogenate non-activated esters without using any additives (e.g. fluorinated solvents, organic bases, salts, inorganic acids...) and under mild conditions⁽²⁵⁾. This homogeneous catalytic system, which was the first for hydrogenation of non-activated esters, largely contributed to rise new interest in PNN and PNP pincer-type ligands. I have already described the characteristic of these ligands in chapter 1.3.

Subsequently, new pincer-type complexes have been developed with the NNC modified ligands⁽²⁶⁾ (**4.2**, **4.3**). They bear a bipyridine-NHC carbene, which is more electron-rich and more firmly bound to the metal compared to the phosphine. Furthermore, the NHC can be easily modified with several functionalities in order to change hindrance and catalytic activity.



Scheme 11. Ru-MACHO complex (**5**) and hydrogenation of (R)-1,2-propanediol (up) and 2-(1-menthoxy)ethanol (down).

1.5 IRON PINCER COMPLEXES

In the last few years, interest toward new transition metal compounds has grown as consequence of an increased attention to sustainability. The need of replacing toxic and expensive precious metal complexes with more available and benign metals, has led to the development of new metal-based compounds, such as iron complexes. Research of reasonable iron mediated bond forming reactions involves also hydrogenations, which has been dominated by Ru and Pd. Recently, a remarkable progress has been made in the development of iron based catalyzed hydrogenations. The latest most interesting findings concern the use of pincer-type ligands.

In 2011 the group of Milstein has reported a pyridine based pincer-type ligand complex of iron (**6**, See Figure 6). These complexes involve a new mode of metal-ligand cooperation, which is dearomatization-aromatization of the pyridine ring. Complex **6** has appeared as one of the most efficient iron catalysts in ketone hydrogenation.

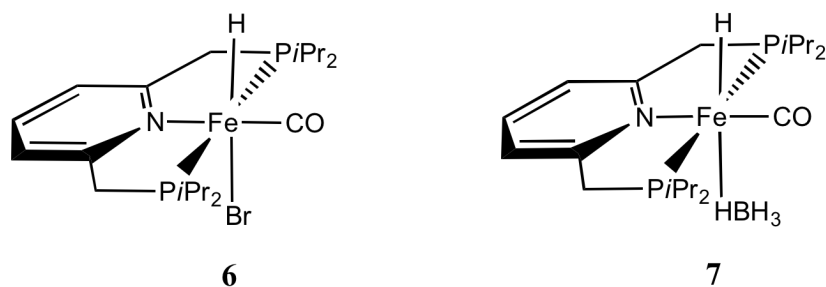
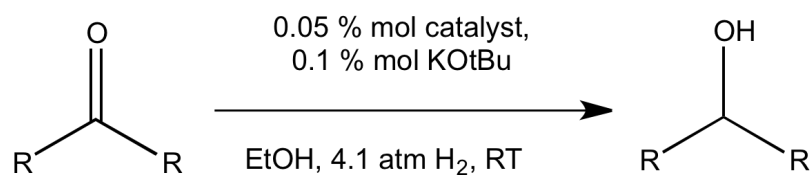


Figure 6. The two iron-based complexes bearing a bromide (**6**) and a η^1 -tetrahydroborate (**7**) ligands.

Milstein has also reported a tetrahydridoborate complex [(iPr-PNP)Fe(H)(CO)(η^1 -BH₄)] (**7**), which is able to catalyze the free-base hydrogenation of ketones under the same conditions (Scheme 12)⁽²⁸⁾.



Scheme 12. Hydrogenation of ketones by catalyst **6**.

These remarkable catalytic results have drawn the attention of the group of Beller, which started in 2013 the development of new iron catalysts for applications in the dehydrogenation of methanol in methanol reforming. As mentioned above, replacement of noble metal complexes (Ru) with non-noble ones (Fe) in alcohol dehydrogenation is an important matter due to the high prices and low availability of precious metals such as Ru.

Beller and co-workers started from their well-defined ruthenium catalyst [HN(CH₂CH₂PⁱPr₂)₂]RuH(CO)Cl (**a**), which is able to perform an aqueous phase methanol dehydrogenation in mild conditions⁽²⁹⁾. The pre-catalyst uses a “non-innocent” pincer-type PNP ligand, which is directly involved in the reaction.

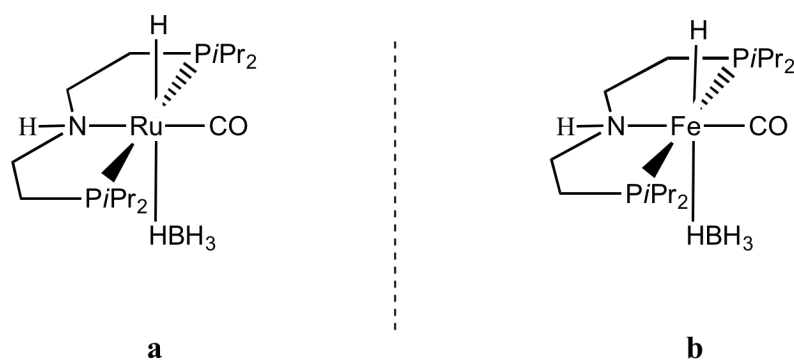
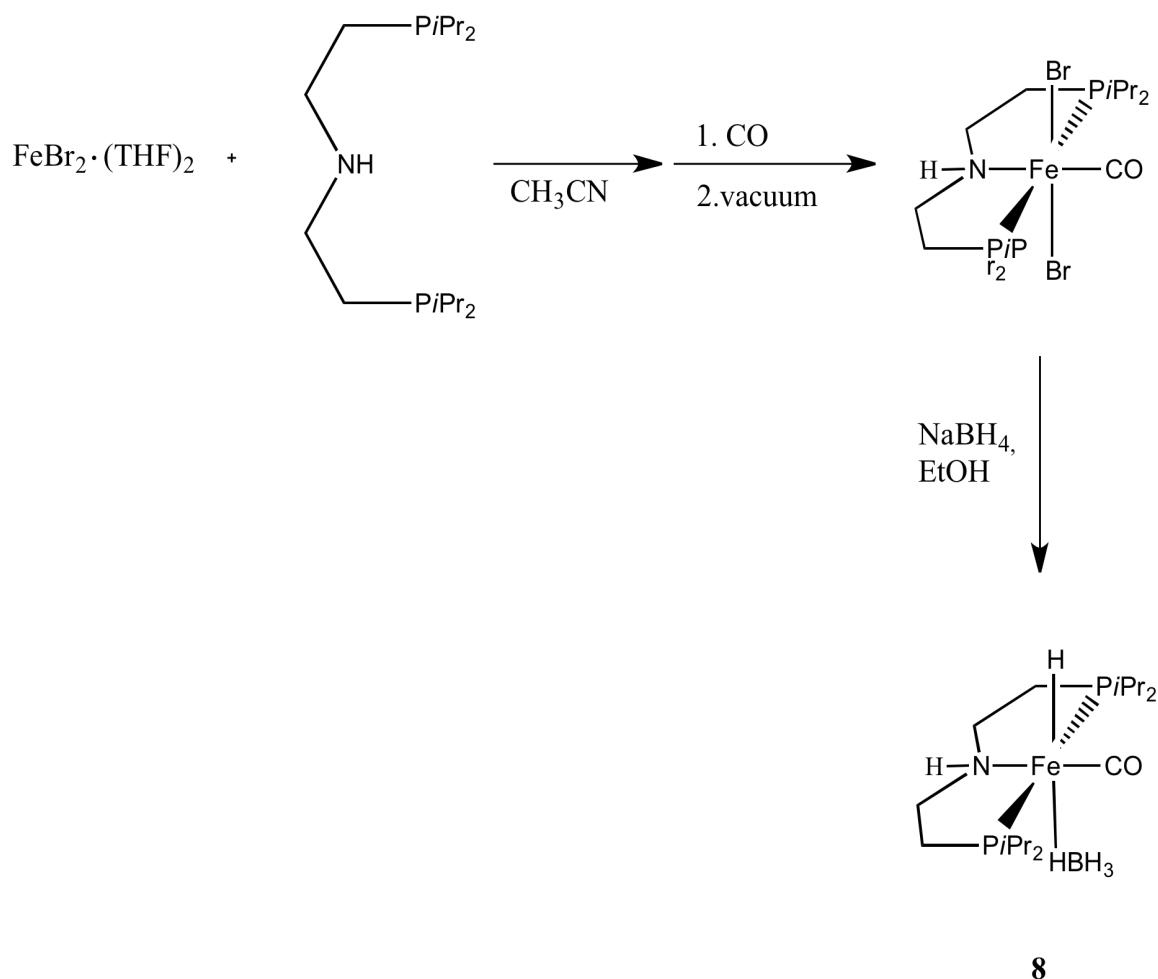


Figure 7. The Ru-complex (**a**) and the Fe-complex (**b**).

Inspired by the work of Milstein et al., Beller’s group has tried to develop a new non-noble metal catalytic system. First the precursor was prepared adding the amine ligand to a FeBr₂•(THF)₂ solution. The FeBr₂•(THF)₂ was freshly synthesized in order to avoid traces of Fe(III) inside the FeBr₂, besides any excess was easy to remove during the work-up step. Then the argon atmosphere was exchanged with a carbon monoxide atmosphere, as described in Scheme 13. Finally treatment of the precursor with an excess of sodium borohydride, led to the desired iron complex (**8**)⁽³⁰⁾.



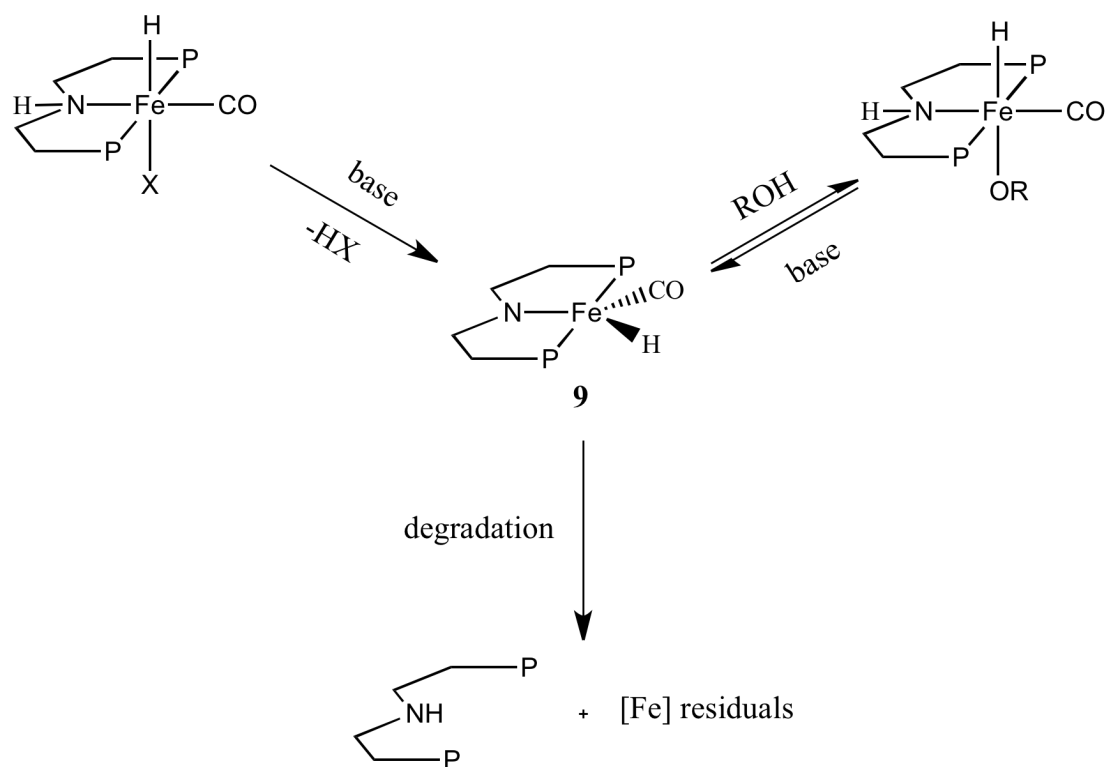
Scheme 13. Synthetic route of the iron complex **8** by Beller's group.

1.5.1 Methanol dehydrogenation

The new iron catalyst was tested in the dehydrogenation of MeOH and hydrogenation of esters.

Concerning MeOH, it is remarkable that hydrogen evolution was observed even in absence of base; this means that the iron complex directly forms the active species without any additives. However, when a base was added the activity boosted. Furthermore, several parameters were investigated: water content inside solvent, concentration and kind of base.

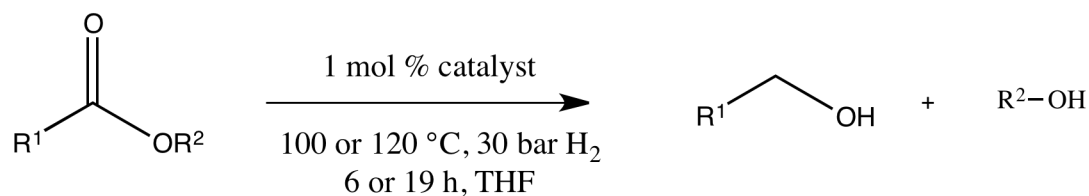
Concerning the reaction mechanism, it has been suggested an outer sphere mechanism, where the “non-innocent” ligand is involved (Scheme 14)⁽³⁰⁾. The active species should be the complex (**9**) and it should be able to release H₂ by abstracting hydrogen from the substrate (ROH).



Scheme 14. Possible active species involved in the reaction mechanism.

1.5.2 Esters hydrogenation

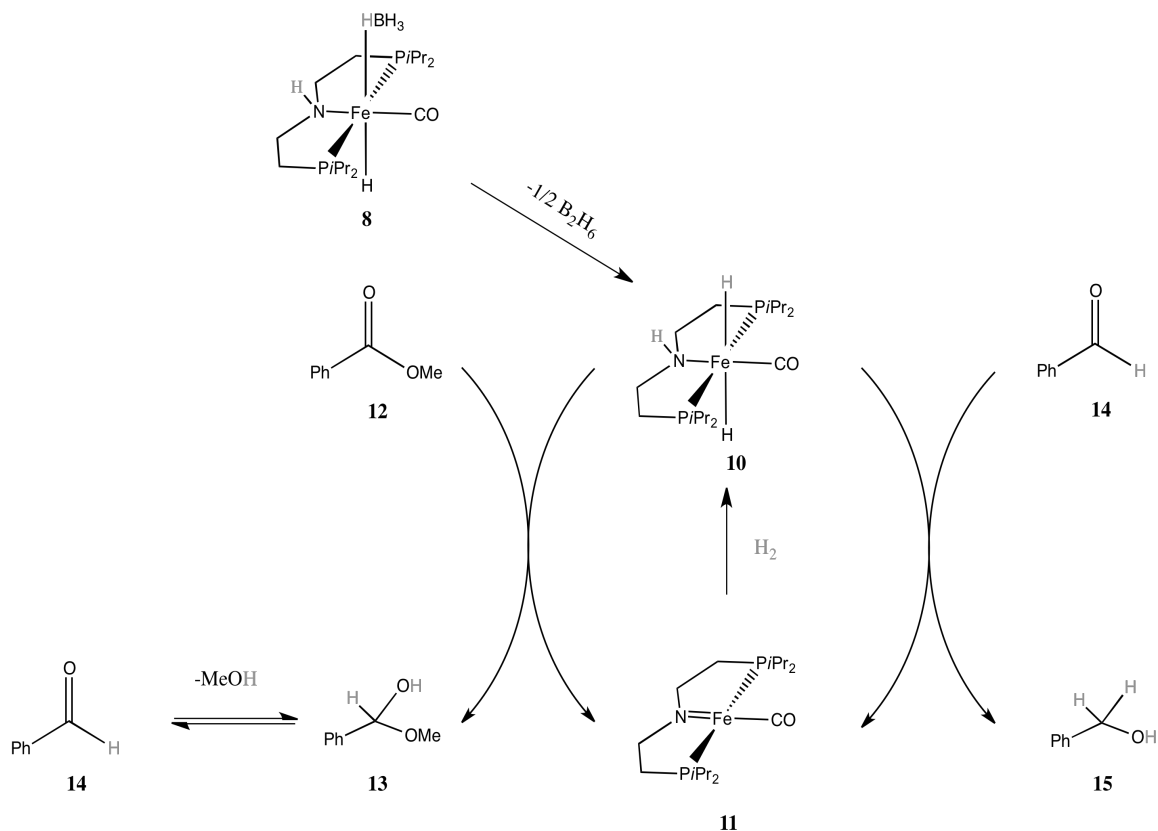
Complex **8** has also been tested in dehydrogenation of esters to form alcohols (Scheme 15)⁽³¹⁾. An array of different carboxylic acid esters and lactones was hydrogenated successfully with good to excellent yields. It should be emphasized that the reaction is base-free and when some additives have been added, the yield was lowered.



Scheme 15. Fe catalyzed hydrogenation of esters.

Finally, also in this case it is supposed an outer-sphere mechanism with contemporaneous transfer of the proton from nitrogen and hydride from iron center. This has been supported by computation and by replacing the proton bound to the nitrogen with a methyl group, which inhibited the reaction. In Scheme 16 the proposed mechanism for the hydrogenation of methyl benzoate **12** is reported. The benzoate **12** is reduced to the hemiacetal **13**, which loses methanol to give benzaldehyde **14**. The

precursor **8** generates the active species **10** by losing of $\frac{1}{2}$ BH_3 and goes through a metal-ligand cooperation, that is the transfer of a proton and a hydride to the $\text{C}=\text{O}$ bond. Complex **11** regenerates the active species by adding molecular H_2 by heterolytic cleavage. In the end, the benzaldehyde is hydrogenated to benzyl alcohol **15** by the same mechanism. All in all is a two-cycles hydrogenation.



Scheme 16. Example of the mechanism for the hydrogenation of methyl benzoate to benzyl alcohol.

1.6 COBALT PINCER COMPLEXES

In addition to iron pincer complexes, the group of Beller, in which I performed my internship, was also interested in cobalt complexes bearing PNP aliphatic pincer ligands, which are potentially valuable homogeneous catalysts. Just as iron, cobalt could be a good choice for replacement of more precious transition metals.

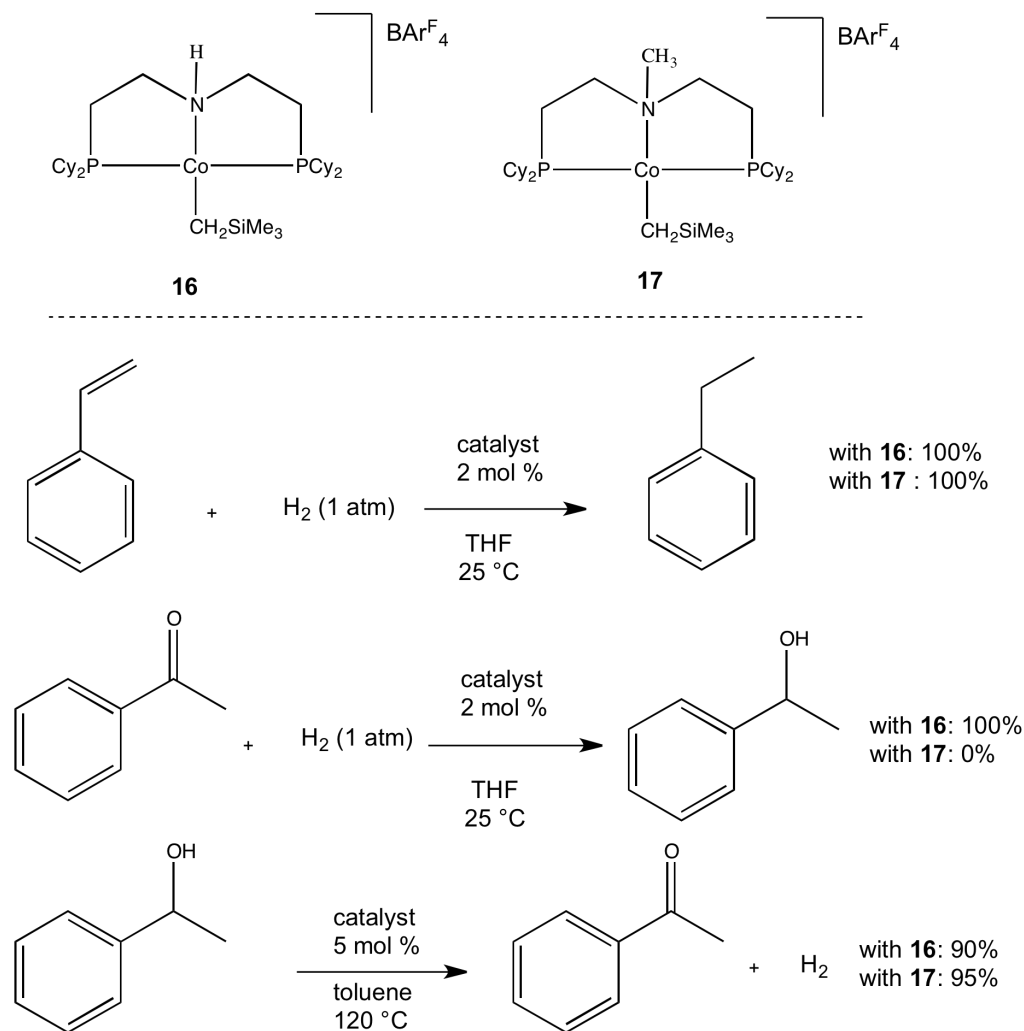
So far, cobalt complexes have displayed activity towards catalytic reactions as ethylene hydrogenation and hydrogenation of aldehydes, ketone and imine, as well as in 1,3-butadiene polymerization⁽³²⁾ and ethylene oligomerization⁽³³⁾.

Interesting is the work of Hanson's group, who focused on a cobalt-alkyl complex **16**, shown in Scheme 17. This complex is found to be active in alkene hydrogenation, $\text{C}=\text{O}$

(aldehydes and ketones) and C=N (imines) bonds hydrogenation under mild conditions, that is 1-4 atm of H₂ and 25-60°C, with good to excellent yields⁽³⁴⁾.

They also assessed the role of the ligand-metal cooperation in the reaction pathway, replacing the hydrogen on the nitrogen with a methyl group (complex **17**, Scheme 17), and testing the complexes in:

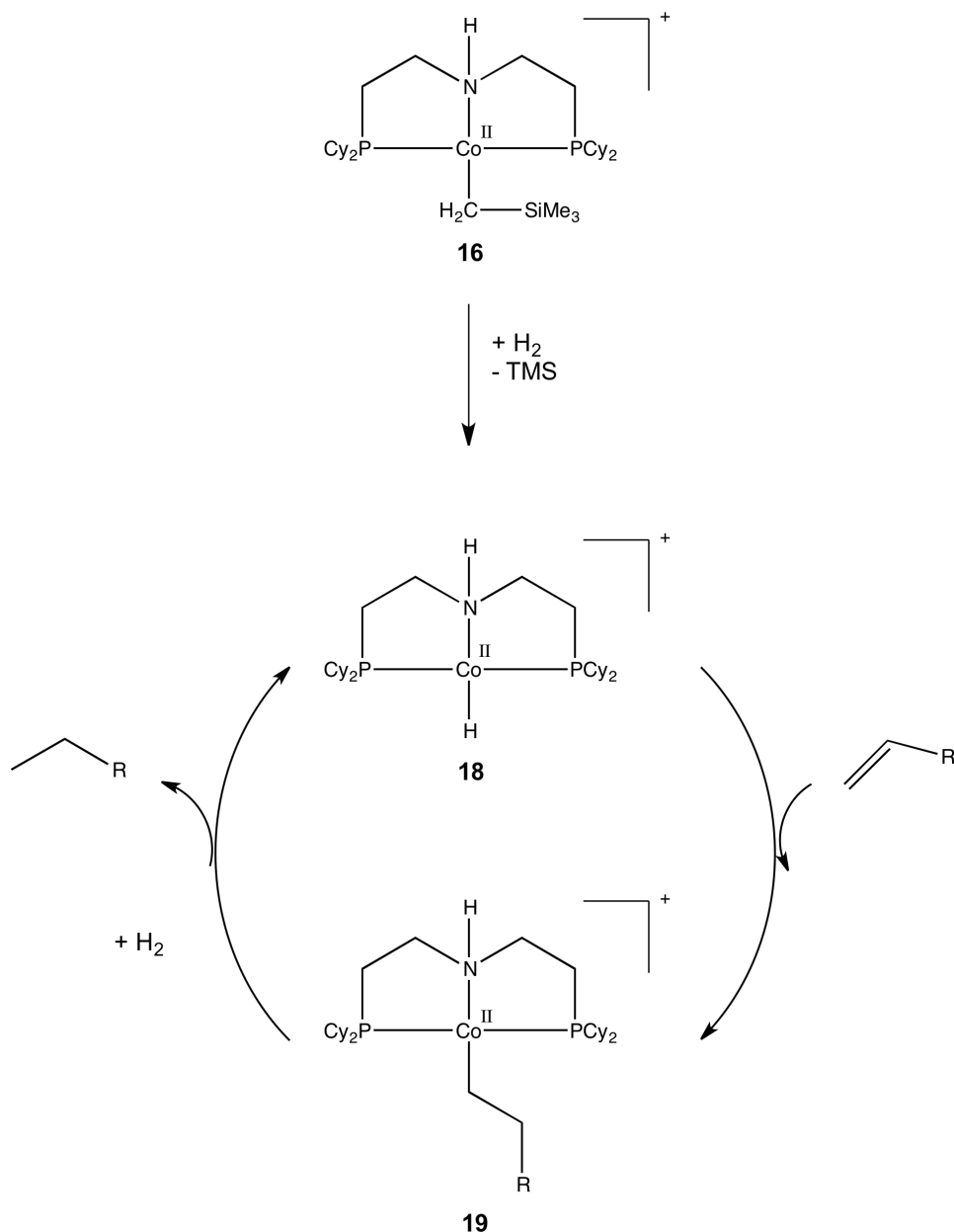
- hydrogenation of styrene and acetophenone;
- dehydrogenation of 1-phenylethanol.



Scheme 17. Hydrogenation of (a) styrene and (b) acetophenone. Dehydrogenation of (c) 1-phenylethanol.

Concerning the hydrogenation of acetophenone, the N-Me complex displayed no reaction and this supports a metal-ligand cooperation, in which the N-H bond is necessary in order to activate the polar C=O bond. On the other hand, in hydrogenation of styrene and in dehydrogenation of 1-phenylethanol both complexes are active, suggesting that in these reactions the expected cooperation is not necessary. Therefore, a catalytic cycle for olefin hydrogenation has been proposed without involving the PNP ligand: the active

species **18** is formed by hydrogenolysis of precatalyst **16**. Subsequent step is olefin insertion in the Co-H bond to originate the intermediate **19**, which finally reacts with H₂ to release the product and complete the cycle (Scheme 18).

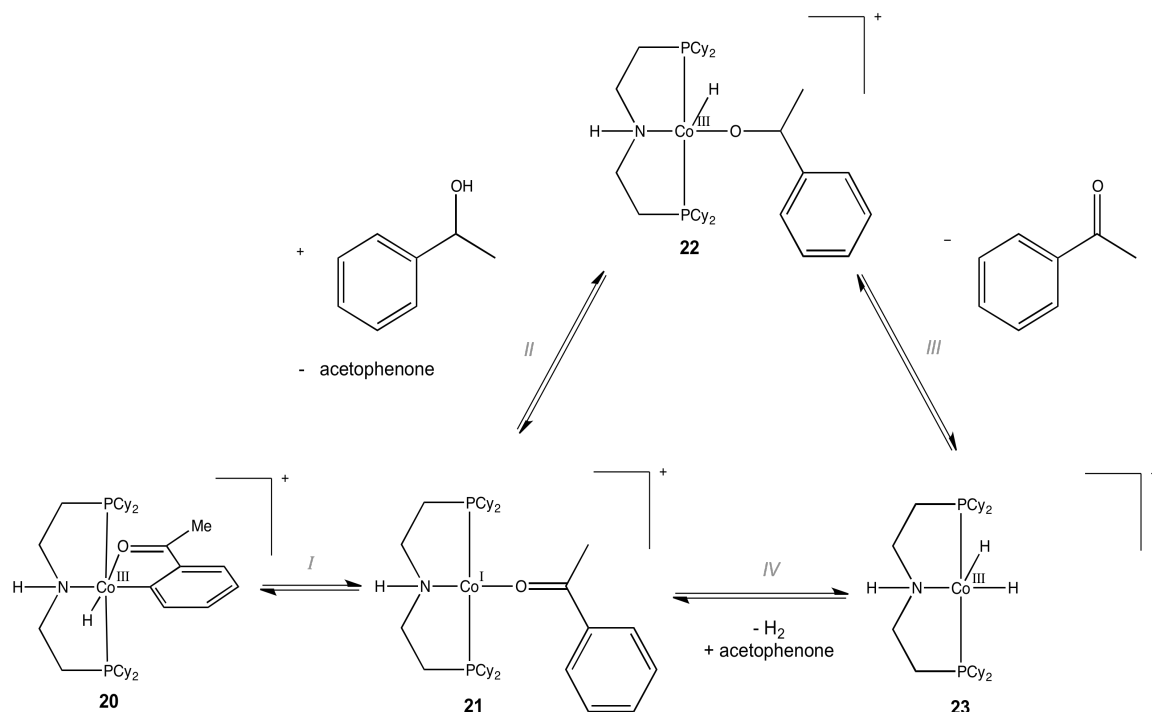


Scheme 18. Supposed mechanism for olefin hydrogenation with complex **16**.

Concerning the dehydrogenation of 1-phenylethanol, another mechanism is supposed (Scheme 19). During the reaction, the new cobalt (III) complex **20** was detected by ¹H-NMR spectrometry. Complex **20** was found to be inactive and his isolation suggested that the reaction goes through a redox cycle involving Co(I)/Co(III) oxidation states. The proposed cycle assumes **20** as a resting state and can be divided into several steps:

- I. reductive elimination of acetophenone leads to Co(I) complex (**21**);

- II. associative ligand substitution replaces acetophenone with 1-phenylethanol, through an oxidative addition of the O-H bond, which leads to a Co(III) (**22**);
 - III. β -hydride elimination of acetophenone leads to a dihydride Co(III) species (**23**);
 - IV. elimination both hydride as H_2 and adding of acetophenone closes catalytic cycle.
- The reductive elimination step is supported by exchange of bound acetophenone- d_8 with free one, which happens at $60^\circ C$.



Scheme 19. Proposed dehydrogenation mechanism of 1-Phenylethanol.

To my knowledge, that is what is known about catalytic activity of cobalt complexes bearing an aliphatic PNP ligand in homogeneous hydrogenation. It is a whole new field to explore in which Beller's group is involved, as previously stated, and in which falls the subject of the present thesis.

AIM OF THE THESIS WORK

During my training period I had the possibility to spend five months into the group of prof. Matthias Beller at Leibniz-Institut für Katalize (LIKAT) in Rostock (Germany), who has an outstanding experience in non-noble metal catalysis. I have worked in his redox group under supervision of dr. Kathrin Junge. Their main purpose is to explore new non-noble metal catalysts to be employed in redox reaction such is hydrogenation. I was involved in cobalt catalysis because is poorly present in literature, with following aims:

- Synthesis and characterization of a new cobalt complex bearing a PNP-type ligand to be use in hydrogenation reactions.
- Perform catalytic tests on cobalt complex to check its activity in some hydrogenation substrates such as esters to alcohols.
- Perform catalytic tests on cobalt complex activity against acceptorless dehydrogenative coupling (ADC) of ethanol to ethyl acetate.

Concerning time I have spent in Bologna in the group of my supervisor Prof. Zanotti, I focused on iron chemistry. In recent years, interest in sustainability and need of replacing precious and toxic metals, lead Zanotti's group to develop new iron-based complexes. Iron can be a good replacement due to high abundance and low toxicity. The project in which I was involved concerns the study and development of new iron complexes bearing cyclopentadienone and NHC ligands to be applied in redox reactions. The aims are:

- Synthesis and characterization of cyclopentadienone iron carbonyl based precursor with new reaction route based on microwave assisted method.
- Study on iron precursor to remove one carbonyl ligand in order to obtain a cyclopentadienone iron carbonyl complex bearing a NHC ligand.
- Study on iron precursor reactivity with silver complex.
- Study on iron precursor reactivity with imidazolium salt.

2. RESULTS AND DISCUSSION

2.1 COBALT COMPLEXES

As previously mentioned, during the period spent in Leibniz-Institut für Katalyse (LIKAT) in Rostock, I was involved in the synthesis of a new cobalt complex bearing a PNP-type ligand. Concerning the synthetic route, I was inspired by analogous iron complex **8** (see introduction) already synthesized by dr. Elisabetta Alberico in Beller's group⁽³⁰⁾.

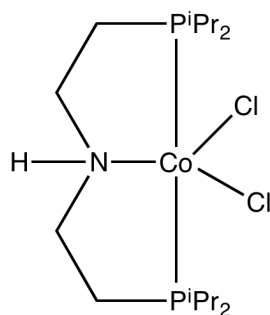
The synthesis was planned as a three-step route divided as follow: at first step ligand and cobalt precursor reacts together to lead to a dihalogen complex; at second step a carbonyl group is added to the complex; finally an hydride and a tetrahydroborate ligand should be added by reacting with sodium borohydride.

All detailed procedures can be found in experimental section.

2.1.1 Synthesis of dichloride-bis[(2-diisopropylphosphino)ethyl]amine-cobalt(II) (A)

Synthesis of complex (A) started from refluxing of isopropyl pincer ligand and cobalt chloride in THF overnight. Cobalt chloride has been chosen as a starting reagent because of its immediate availability in the laboratory. Furthermore, in 2011 J. Arnold⁽³⁵⁾ already described a synthetic route starting from cobalt chloride.

Cobalt chloride looks like small dark blue spheres, so it was decided to mash it inside the Schlenk tube before using, in order to favour dissolution in THF. At the end of reaction, the solid obtained by recrystallization was pink and crystals were needle, as described by Arnold.



A

Figure 8. Dichloride cobalt complex A.

Unfortunately, ^1H NMR and ^{31}P NMR analysis were useless due to high paramagnetism of sample. The complex was obtained in good yield and it was used immediately into the second step of route.

2.1.2 Synthesis of carbonyl-dichloride-bis[(2-diisopropylphosphino)ethyl]amine-cobalt(II) (B)

Second step was a carbonylation reaction, consisting in the addition of carbon monoxide to the cobalt complex.

In the corresponding synthesis of iron complexes iron, this step is achieved by replacing the atmosphere of argon with carbon monoxide. In order to obtain a complete replacement, it is necessary to degas the solution by freeze-pump-thaw technique. This method displays some weak points such as long times and hazard in carbon monoxide manipulation; indeed a special equipment was needed to avoid any carbon monoxide leaks during atmosphere exchange. For these reasons, it was decided to perform carbonylation by simply insertion of a cannula inside reaction solution to bubble carbon monoxide. A specific assemblage (Figure 9) was purpose-built.

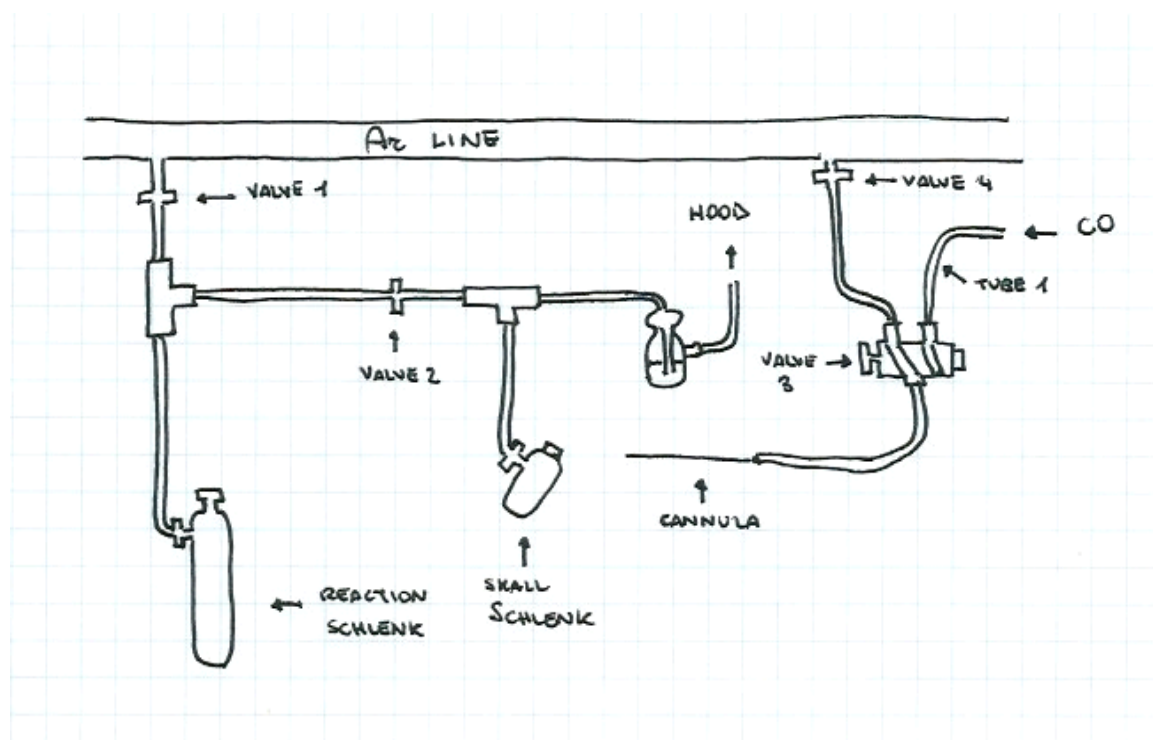


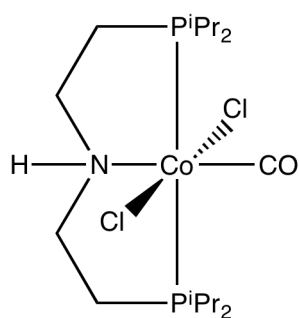
Figure 9. Assemblage for carbonylation reaction.

The cannula was connected to a special valve 3 with two way in: one link to argon line and the other to a small carbon monoxide tank. The cannula was inserted into the small

Schlenk through a septum, valve **2** closed and valve **3** turned to carbon monoxide line in order to flash the tube **1** connected to the tank. In this way CO went through the mineral oil bubbler to hood. About 5 bar CO was used for this purpose.

Then, valve **3** was turned to argon line in order to flash the cannula with argon and remove any traces of CO. After a few minutes, cannula was removed from the small Schlenk and inserted into reaction Schlenk (argon flow always open). Valve **1** was closed to avoid contamination of argon line, valve **2** opened to let gas flow through mineral oil bubbler and valve **3** turned to CO tank. About 30 bar CO was used for this step.

Reaction mixture turned almost immediately from purple to green. After work-up, it was obtained a light green solid.



B

Figure 10. Carbonyl-dichloride cobalt complex **B**.

NMR analysis was useless due to paramagnetism, but ATR was a useful tool to check the addition of a carbon monoxide. The IR spectrum evidenced new absorptions at 2009 cm^{-1} and 1986 cm^{-1} , typical of C=O stretching region. This was a proof that a carbonyl ligand was bounded to the complex.

Crystals suitable for a single X-ray diffraction were grown from a double-layered solutions, as shown in Table 1.

Table 1. Attempts of crystallization.

Solvents	Crystals suitable for X-ray
THF / Heptane	<i>x</i>
THF / Cyclohexane	<i>x</i>
Toluene / Heptane	<i>x</i>
Et ₂ O / Heptane	<i>x</i>
EtOH / Cyclohexane	<i>x</i>
CH ₂ Cl ₂ / Cyclohexane	<i>x</i>

All attempts were unsuccessful. Et₂O was found to be not a good solvent, thus it was replaced with ⁱPrOH, but together with EtOH, no crystals were found; besides, when dissolved in EtOH, solution turned to dark brown. CH₂Cl₂ destroyed complex **B**, leaving a light blue solid, which looked like reagent CoCl₂. THF and toluene led to twin and tiny crystals non suitable for X-ray diffraction, this was likely due to a too fast crystallization process. Nevertheless, toluene/heptane double-layer looked the best in crystal growing. To avoid this drawback, the cobalt complex was dissolved in toluene inside a small GC vial. The CG vial was dropped inside a large vial and surrounded by heptane; in this way solvents mixing occurred only via diffusion through gas phase (bp: toluene 110.6 °C, heptane 98 °C), which is a slow process.

Green needle-like crystals suitable for X-ray were obtained and crystal structure was confirmed (Figure 11).

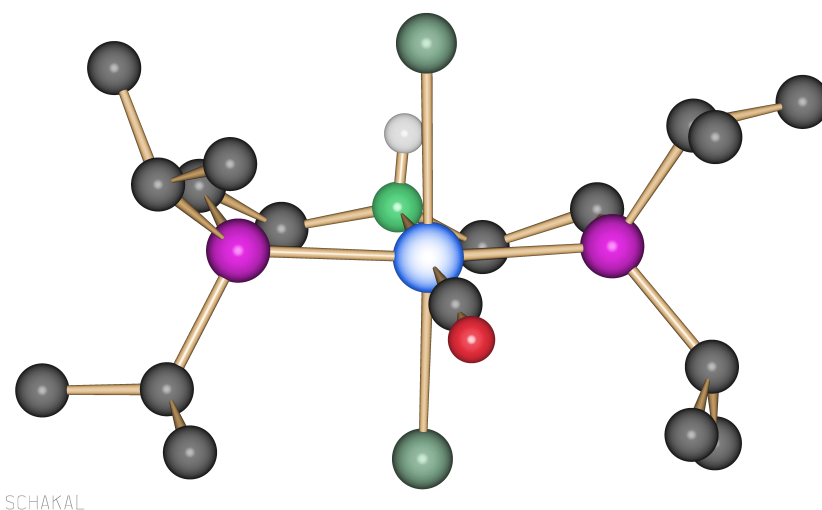


Figure 11. Crystal structure of carbonyl-dichloride cobalt complex.

ESI-MS analysis was not able to identify the molecular ion at 462. It is possible that carbonyl complex immediately eliminates CO. Indeed a 434.10824 was identified as a –CO loss and 398.13426 as a –HCl loss. Besides, a 414.12926 peak was identified as both –CO and –HCl loss together with O gain due to oxidation.

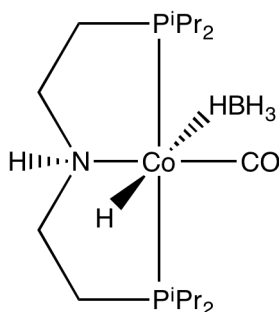
2.1.3 Synthesis of carbonyl-hydrido-tetrahydroborato-bis[(2-diisopropylphosphino)ethyl]amine-cobalt(II) (C)

Last step concerned addition of a hydride and a tetrahydroborate groups to cobalt center. In order to get this goal it was used sodium borohydride as reducing agent and a mixture of THF/EtOH (1:1) as solvent.

In previously crystallization attempts, complex **B** showed a brownish color in EtOH instead of green; this could be due to some unstability in solution. Hence, complex **B** was dissolved in THF and then EtOH was added dropwise. During reaction time, argon line was left open to oil bubbler because of hydrogen production from reaction mixture.

Solid obtained was re-dissolved in toluene and filtered; by this way, NaCl produced and excess of NaBH₄, which are not soluble, were removed. After solvent removal, a brownish solid with black spots was obtained.

Unfortunately it was not possible to identify the solid. ¹H-NMR analysis in toluene revealed a lot of superimposed signals, probably due to a mixture of compounds, and a very tiny triplet at about -23 ppm, in the region of metal hydrides, but it was not possible to make unequivocal attributions. Also ³¹P-NMR revealed more than one compound: at 51.85 ppm the oxidized ligand is visible, while not identified signals were observed at about 87 and 103 ppm. ATR spectrum showed a new band at 2313 cm⁻¹, which could prove that a tetrahydroborate was actually bound to cobalt center by comparison with a similar complex.



C

Figure 12. Expected cobalt complex **C** after last step of synthesis.

In one other attempt, the crude solid obtained after filtration was washed with heptane. Heptane dissolved part of the solid. Meanwhile, a crystallization attempt in toluene double-layered with heptane failed. Indeed solid turned out to be soluble in all organic solvents available in the laboratory.

It was decided to add more heptane to solid and to filter the resulting suspension. Two solids were obtained: one light brown above the filter; the other dark brown from the extract. NMR samples of both were recorded in benzene-*d*₆. It was tricky to take a sample of solid above the filter: it was very sensible to air and turned immediately black after air exposing, so it was dissolved with benzene-*d*₆ directly inside the filter. In both spectra, there were no hydride signals to confirm synthesis of expected product.

Last attempt with only EtOH as a solvent was made. Surprisingly, after EtOH removal not so much black spots were observed inside crude solid, but after filtration with toluene the black spots appeared again.

Since the solid was very unstable and was not possible to identify it, we decided to start again from another reagent: the cobalt bromide.

2.1.4 Synthesis of dibromide-bis[(2-diisopropylphosphino)ethyl]amine-cobalt(II) (**D**)

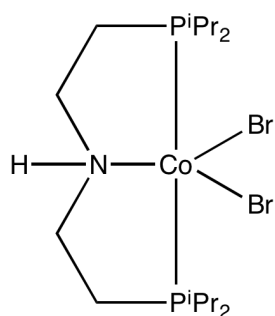
Synthesis of dibromide-bis[(2-diisopropylphosphino)ethyl]amine-cobalt(II) was the same as for dichloride complex **A**.

CoBr₂ looks like a green powder. Some solubility tests were taken (table 2) in order to assess right solvent in work-up.

Table 2. Solubility tests for CoBr₂.

Solvent	Solubility	Color
EtOH	✓	Dark blue
Et ₂ O	✓	Light blue
THF	✓	Blue
Toluene	✗	-
CH ₂ Cl ₂	✗	-
Heptane	✗	-
Water	✓	Pink

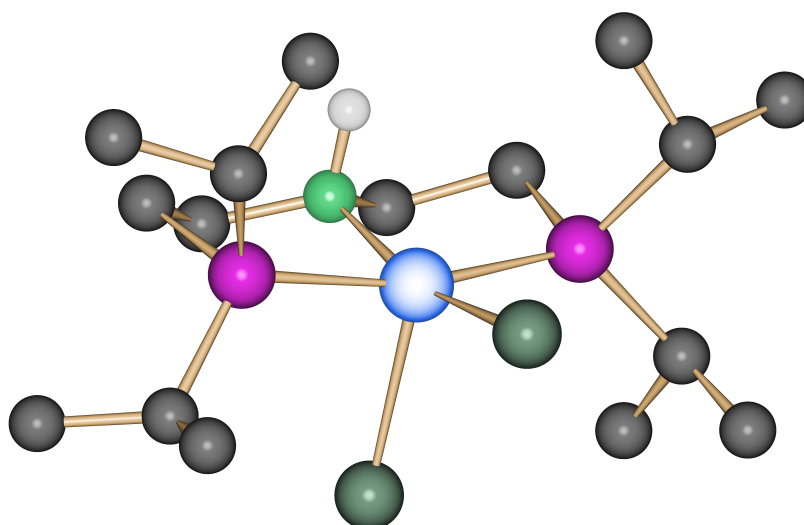
Toluene and CH₂Cl₂ were used for work-up procedure. At the end solid was washed with some EtOH to remove any traces of CoBr₂ unreacted, but also cobalt complex **D** was slightly soluble.



D

Figure 13. Bromide complex **D**.

Crystals were grown in CH_2Cl_2 double-layered with Et_2O . Unfortunately, crystals were very tiny and calculations were not accurate, nevertheless the expected crystal structure was found.



SCHAKAL

Figure 14. Crystal structure of complex **D**.

Like complex **A**, crystals were pink and needle like, and two halogen atoms are bound to the metal on the opposite side of nitrogen atom of PNP ligand.

^1H -NMR and ^{31}P -NMR analysis were useless. ATR spectrum reveals the same bands of dichloride complex **A**, this means that two complexes correspond one to each other.

Table 3. Comparison between complex **A** and **B** IR signals.

Complex	$\nu(\text{N-H}) \text{ cm}^{-1}$	$\nu(\text{C-H}) \text{ cm}^{-1}$
Dichloride (A)	3245	2952, 2921, 2866
Dibromide (D)	3101	2950, 2924, 2867

ESI-MS analysis identified molecular ion at 524.00798 (M+).

2.1.5 Synthesis of carbonyl-dibromide-bis[(2-diisopropylphosphino)ethyl]amine-cobalt(II) (E)

Synthesis of carbonyl-dibromide-bis[(2-diisopropylphosphino)ethyl]amine-cobalt(II) was performed in the same way of carbonyl-dichloride complex **B**. Interestingly, this complex did not change color when dissolved in EtOH and needed more quantity of solvent, probably because of different solubility.

This step was also tested in EtOH, but lower solubility let complex precipitate during reaction time. This phenomenon was a problem because precipitate stuck the cannula, which needed to be replaced by a new one. In later synthesis THF was used as a solvent to avoid this issue.

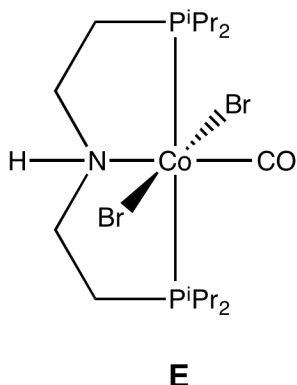


Figure 15. Cobalt complex E.

ATR spectrum showed the band of NH stretching at 3140 cm^{-1} and a new signal at 2010 cm^{-1} , which was related to CO stretching. $^1\text{H-NMR}$ analysis was useless due to paramagnetism of cobalt complex. A comparison with analogous chloride complex is reported in table 4.

Green prism-like crystals were grown in toluene solution double-layered with heptane inside a small GC vial as for complex **B**. Crystal structure confirmed the expected complex.

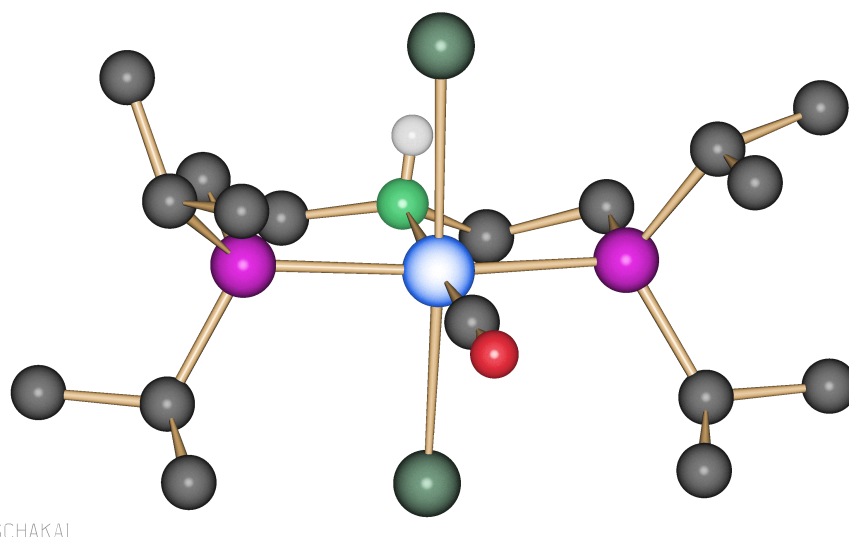


Figure 16. Crystal structure of complex **E**.

Bond lengths of complex **E** are similar with those of complex **B**. In complex **E** distances between cobalt and halogens are longer than in **B** due to more hindrance of bromide than chloride. There is a slight difference also in N-H bond: in complex **B** it is longer.

Table 4. Bond lengths in complex **B** and **E**.

	Dichloride B	Dibromide E
Crystal description	Green needle	Green prism
Crystal size	0.38x0.13x0.11 mm ³	0.315x0.261x0.251 mm ³
Co-C	1.7681(17) Å	1.759(2) Å
C-O	1.136(2) Å	1.132(2) Å
Co-N	2.0222(13) Å	2.0222(13) Å
N-H	0.878(19) Å	0.81(2) Å
Co-X ₁	2.5836(5) Å	2.6925(3) Å
Co-X ₂	2.5206(5) Å	2.7521(3) Å
Co-P ₁	2.2673(5) Å	2.2870(5) Å
Co-P ₂	2.2717(5) Å	2.2815(5) Å

ESI-MS analysis was able to identify the molecular ion at 552.00157 (M⁺). Other identified peaks were: at 524.00791 a -CO loss and a 442.08306 a Br⁷⁹/Br⁸¹ loss.

2.1.6 Synthesis of carbonyl-tetrahydroborato-bis[(2-diisopropylphosphino)ethyl]amine-cobalt (I) (F)

Last step of synthesis was performed in EtOH. NaBH₄ was added into reaction Schlenk in two different ways: as a solid before adding EtOH or as a solution in EtOH. It was important to use immediately the NaBH₄ solution because not very stable in EtOH. Both methods gave similar final results; main issue was to avoid moisture inside NaBH₄ because of high sensibility of cobalt complex.

In work-up procedures, Et₂O was used instead of toluene: Et₂O solution was dark red and did not dissolve NaBH₄ and HBr. Besides, it was easier to remove under vacuum. Et₂O was removed and residue washed with heptane. Heptane dissolved a part of solid. Removal of heptane left reddish solid with some black spots. Residue not dissolved by heptane was a brown and black solid. The yield of this last step was 91.8% after Et₂O filtration and dropped down to 45% after extraction with heptane.

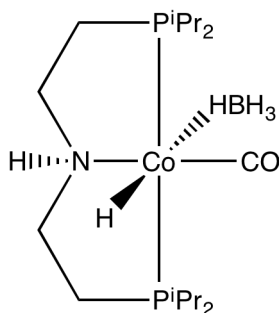


Figure 17. Expected structure of complex F.

Samples of both solids were taken for ¹H-NMR analysis and this time was possible to record useful spectra. Comparing these spectra with one taken before filtration step, led to a delightful discover. To simplify explanation, I will report spectra in Figure 18 and name them as follow: spectrum 1 (red), solid before filtration; spectrum 2 (green), solid soluble in heptane fraction; spectrum 3 (blue), solid not soluble in heptane.

Two solids were indeed two different species, which were separated after filtration. Full spectrum 1 was a sum of spectra 2 and 3. A superimposed picture of these spectra revealed clearly differences. At 0.85-1.55 ppm range signals related to isopropyl groups of PNP-ligand: isopropyl signals in spectrum 2 were better defined if compared with spectrum 3.

Hydride signals were never recorded, demonstrating that these cobalt complexes were different from the iron one **8**. So far it was not possible to identify exactly the structure of complex F.

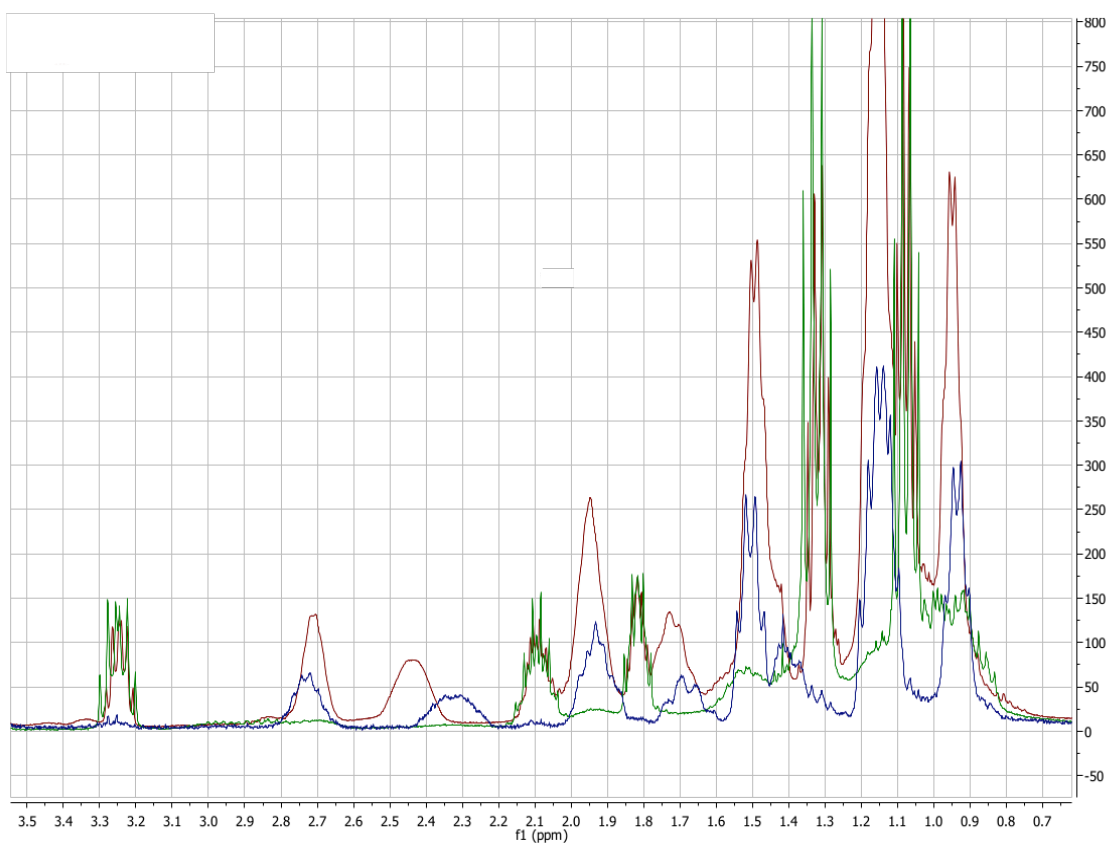
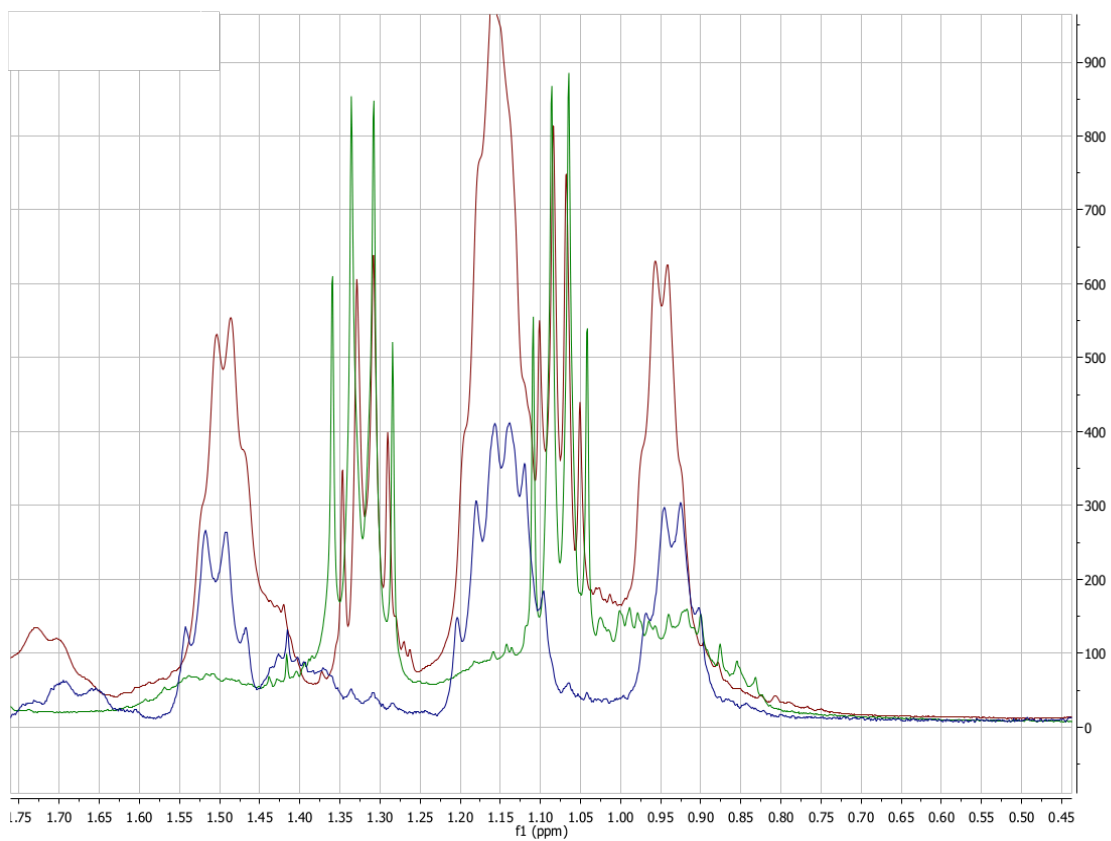


Figure 18. Superimposed NMR spectra: spectrum 1 (red), spectrum 2 (green) and spectrum 3 (blue). Full spectra (down) and focus on isopropyl range (up).

Attempts in crystallization were all but one unsuccessful. Crystals were grown from a solution of Et₂O, before filtration-step, double-layered with heptane and left in freezer for a weekend. At the end of time, some bright red crystals were recovered and crystal structure was obtained by X-ray diffraction. X-ray revealed the structure of **F** (Figure 19), which was different from that of the iron analogue and corresponding to spectrum 2 as demonstrated by ¹H-NMR.

Following signals were assigned: 3.58 (m, 2H, NH); 3.25 (m, 4H, CH₂), 2.1 (4H, CH(CH₃)₂); 1.8 (m, 4H, CH₂); 1.35 – 1.0 (m, 24H, PCH(CH₃)₂); -1.4 (broad, 4H, BH₄).

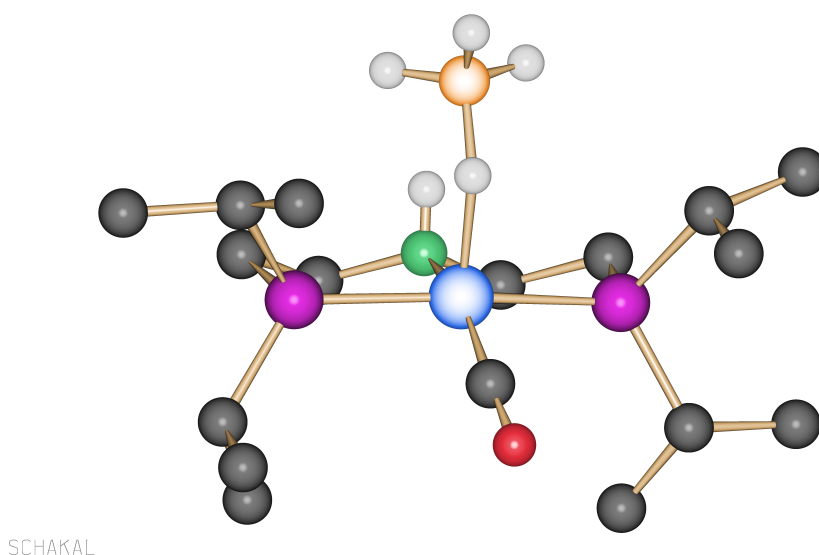


Figure 19. Crystal structure of complex **F**.

The structure shows a plane of symmetry, which cuts the molecule through N-Co-C bond. Therefore synthesis led to a new cobalt complex without a hydride, which means it is a Co(I) 18 electrons complex different if compared to Fe(II) complex **8**.

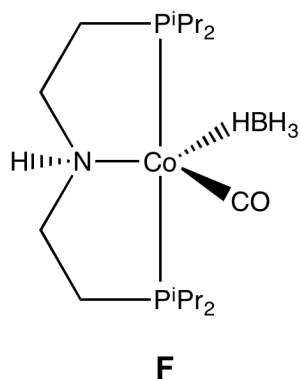


Figure 20. Cobalt(I) complex **F** synthesized.

Co-C bond length was slightly shorter than previous complex **E**, usually this means that metal center is more electron rich. Other bond lengths were comparable with complex **E** and Fe (II) complex **8** (See table 5).

ESI-MS was useless because analysis conditions produced decomposition of complex **F**.

Table 5. Comparison between cobalt complexes **F** and **E**, and iron (II) complex.

Distances	Complex F	Complex E	Fe (II) complex
Co-C	1.6949(17) Å	1.759(2) Å	1.7214(16) Å
C-O	1.163(2) Å	1.132(2) Å	1.161(2) Å
Co-N	2.0555(12) Å	2.0222(13) Å	2.0669(12) Å
N-H	0.823(19) Å	0.81(2) Å	0.81(2) Å
Co-H _{1-BH4}	1.66(2) Å	-	1.691(18)
Co-P ₁	2.1869(4) Å	2.2870(5) Å	2.2188(4)
Co-P ₂	2.1863(4) Å	2.2815(5) Å	2.2067(4)

2.1.7 Attempt of synthesis of carbonyl-dibromide-bis[(2-diisopropylphosphino)ethyl]amine-cobalt(II) *in situ*

In order to optimize overall synthesis, first two steps were tentatively combined in one-step reaction. This new route would be a valuable replacement because of less solvent consumption and lower reaction times.

The idea started from solubility tests of CoBr₂. CoBr₂ were very soluble in EtOH whereas carbonyl complex **E** was slightly soluble. CoBr₂ and PNP ligand were left under reflux in EtOH for one night and then carbon monoxide was bubbled in immediately without purification procedures. Main issue was to avoid cannula being stuck: a bigger cannula was used and reaction conditions were continuously checked. By this way, at the end of reaction product would be collected by simple filtration and washed with cold and fresh EtOH to remove excess of CoBr₂.

Unfortunately a very light and bright green solid precipitated immediately around cannula. At the end of reaction solvent was removed in vacuum to leave a bright green solid and an olive green solid. The only way to remove the bright solid was extraction with THF in which it was not soluble.

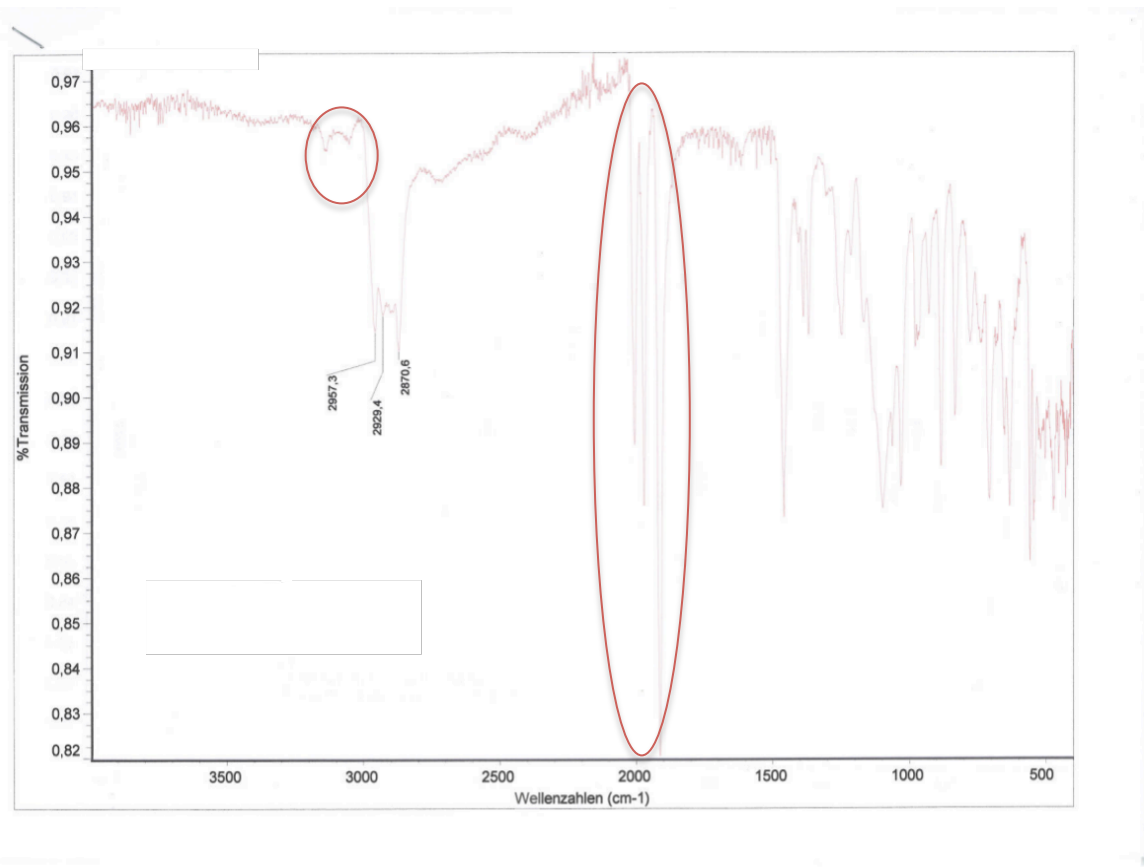
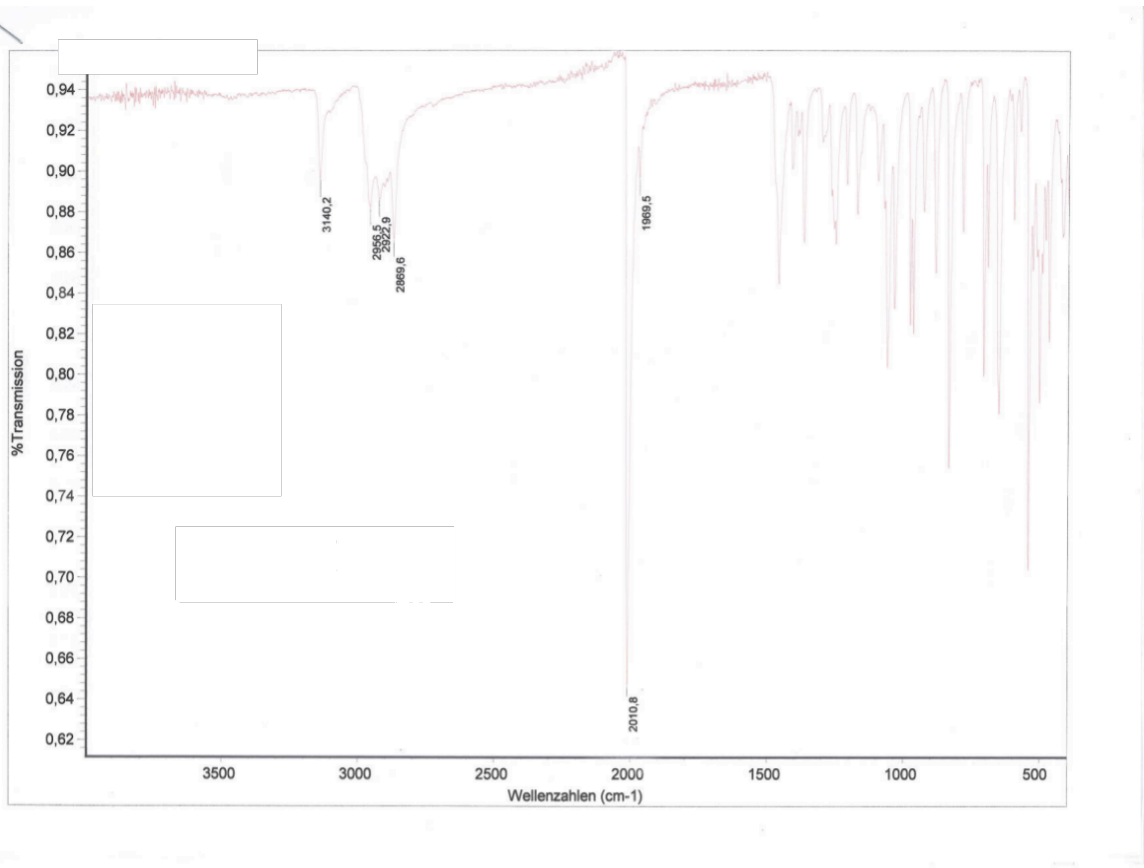


Figure 21. Comparison between IR spectra: already known carbonyl complex **E** (up) and new complex (down). Marked in red differences between the two.

The solid obtained was darker than previous carbonyl complexes. NMR analysis reveals superimposed signals at 0-2 ppm range in ^1H spectrum and a clear single signal at 98.8 ppm in ^{31}P spectrum revealing a single species. It was not possible to identify this new complex by NMR spectra only. ATR spectrum revealed a different pattern compared to previous carbonyl complexes (see figure 21). New set of three signals between 1800 and 2000 cm^{-1} was observed and no signal at about 3100 cm^{-1} , which revealed that there was no more N-H stretching. Also the fingerprint was distinctly different. Clearly it was not the carbonyl dibromide complex **E**.

ESI-HRMS analysis was useless and no crystals were obtained from repeated crystallization attempts.

Nevertheless an attempt of reduction with NaBH_4 was made, but with no success. For this reasons and lack of time further studies in two-step route were interrupted.

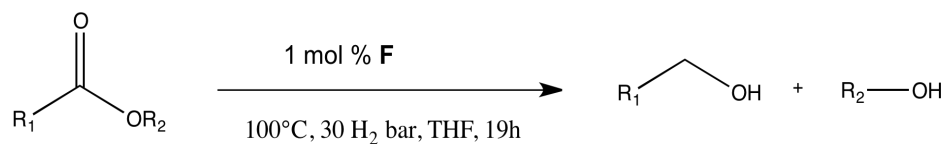
2.2 HYDROGENATION REACTIONS

Carbonyl-tetrahydroborato-bis[(2-diisopropylphosphino)ethyl]amine-cobalt (**I**) complex (**F**) has been checked in esters hydrogenation reactions under mild conditions. Complex **F** showed high sensibility to air and moisture either in solid state or in solution, so some preventive measures were taken to prevent decomposition.

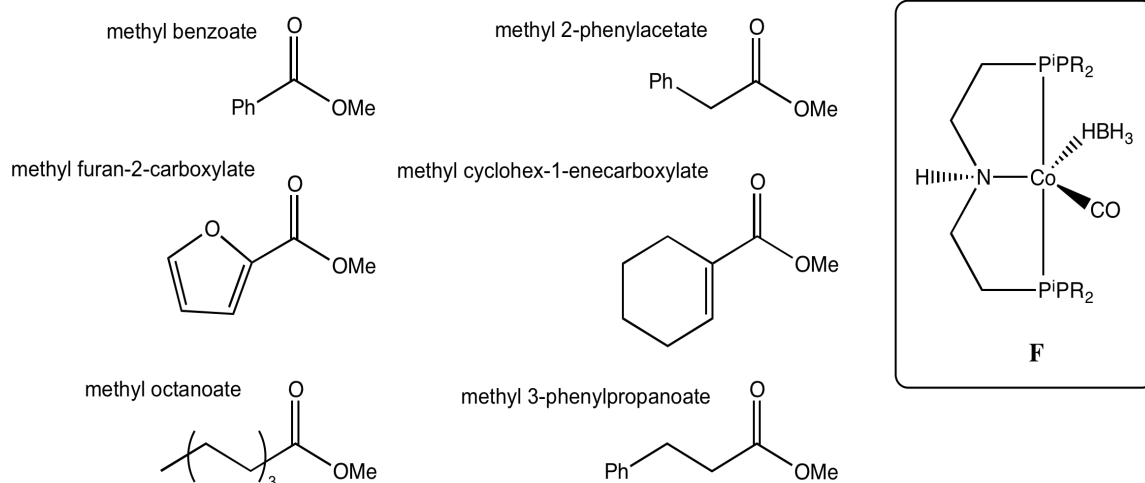
First, it was decided to use complex **F** as a solution in THF, since it was easier to handle, furthermore THF was used as a reaction solvent. Concentration of cobalt complex in THF solution was made in such a way that 2 mL was added to reaction vials under argon atmosphere as last step: in this way complex **F** and solvent of reaction were added at same time. Once reaction vials were charged with all reagents, they were dropped in a specifically assembled autoclave. For accurate description of procedure see experimental section.

Liquid esters were prepared before hydrogenation: they were stirred with CaH_2 then distilled in order to remove traces of moisture or other impurities, finally degassed by freeze-pump-thaw cycles. Reaction conditions such as temperature, H_2 pressure, solvent and reaction time were the same as iron catalyst **F**, which was already tested in esters hydrogenation⁽³¹⁾.

A first array of esters was tested as shown in Scheme 20.



Substrates



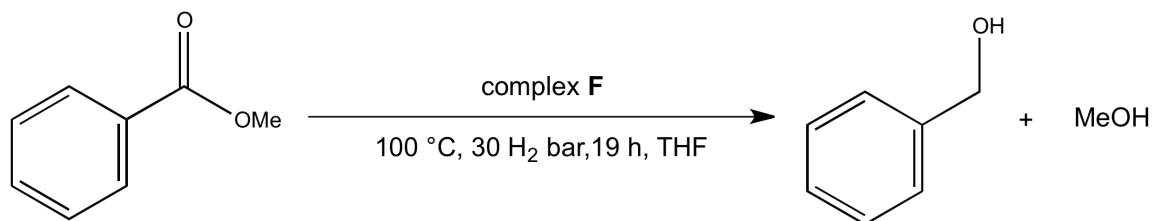
Scheme 20. Reaction conditions were 0.5 mmol of substrate, 0.0005 mmol complex **8**, 110°C temperature, 30 H₂ bar pressure, 19 hours reaction time.

At the end of reaction time, all solutions were red but methyl furan-2-carboxylate, which was olive green. Some minutes after the opening of reaction vials, breakage of cobalt complex **F** was clearly visible by changing in solution color from red to colorless, starting from top down to bottom (figure 22). GC analysis detected no conversion at all.



Figure 22. Reaction vials just after opening (up) and after few minutes (down).

At this point addition of base in reaction mixture was tried, as well as addition of different loading of complex **F** (Scheme 21). Methyl benzoate was used as a substrate. Reaction conditions were the same as previous test.



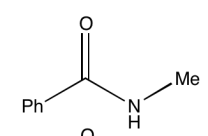
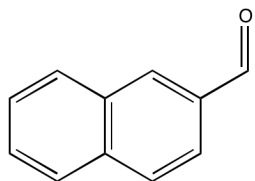
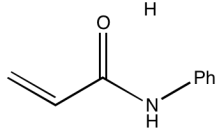
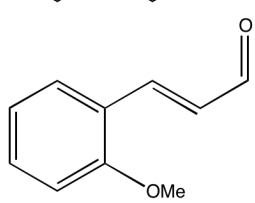
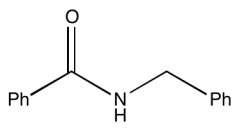
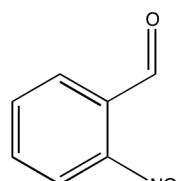
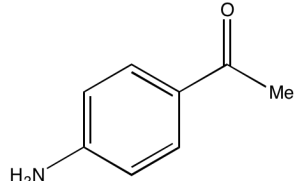
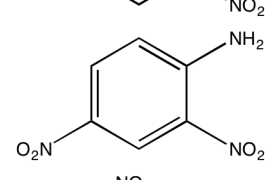
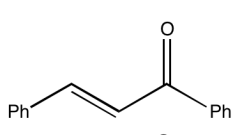
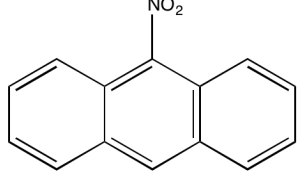
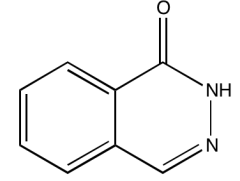
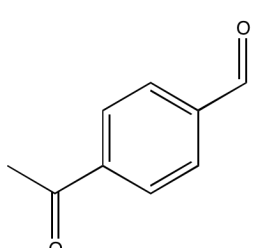
No. Test	KOtBu	Complex F
1	10%	2 mg (1%)
2	10%	4 mg (2%)
3	10%	8 mg (4%)
4	-	2 mg (1%)
5	-	4 mg (2%)
6	-	8 mg (4%)

Scheme 21. Methyl benzoate hydrogenation performed with 0.5 mmol of substrate at 110°C temperature, 30 H₂ bar pressure and 19 hours reaction time.

Even this time no products were detected by GC analysis. These results revealed that cobalt complex **F** is not active in hydrogenation of esters under tested conditions. This inactivity of cobalt complex was expected because of the differences compared to iron complex **8**, besides **F** is a 18 electron complex and electron-rich due to ligands, characteristics that make it unwilling to starting a catalytic cycle.

Nonetheless an array of different kind of substrate was tested in order to check any possible activity (Table 6).

Table 6. Substrates tested with complex **F**. Reaction conditions were 0.5 mmol substrate, 0.0005 mol complex **F** at 100 °C, 30 H₂ bar for 19 h.

No.	Substrate	No.	Substrate
1		8	
2		9	
3		10	
4		11	
5		12	
6			
7			

Only three of the twelve substrates reacted with cobalt complex and for all three there was full conversion. Samples for GC-MS analysis were taken. Unfortunately it was obtained a mixture of products for all of them.

In entry **8** (figure 23) a tiny signal at 27:45 was identified as the desired alcohol 2-naphthalene methanol (158 m/z). Other fragmentations were at 141 m/z, loss of water, and 129 m/z, loss of -CH₂OH. Main product of reaction was at 44:34 with m/z of 312, which was double compared to alcohol. This could be a condensation product of the alcohol just

synthesized, which led to a hydroxy-ketone. There were identified other main fragmentations at 155 m/z, at 141 m/z and 127 m/z.

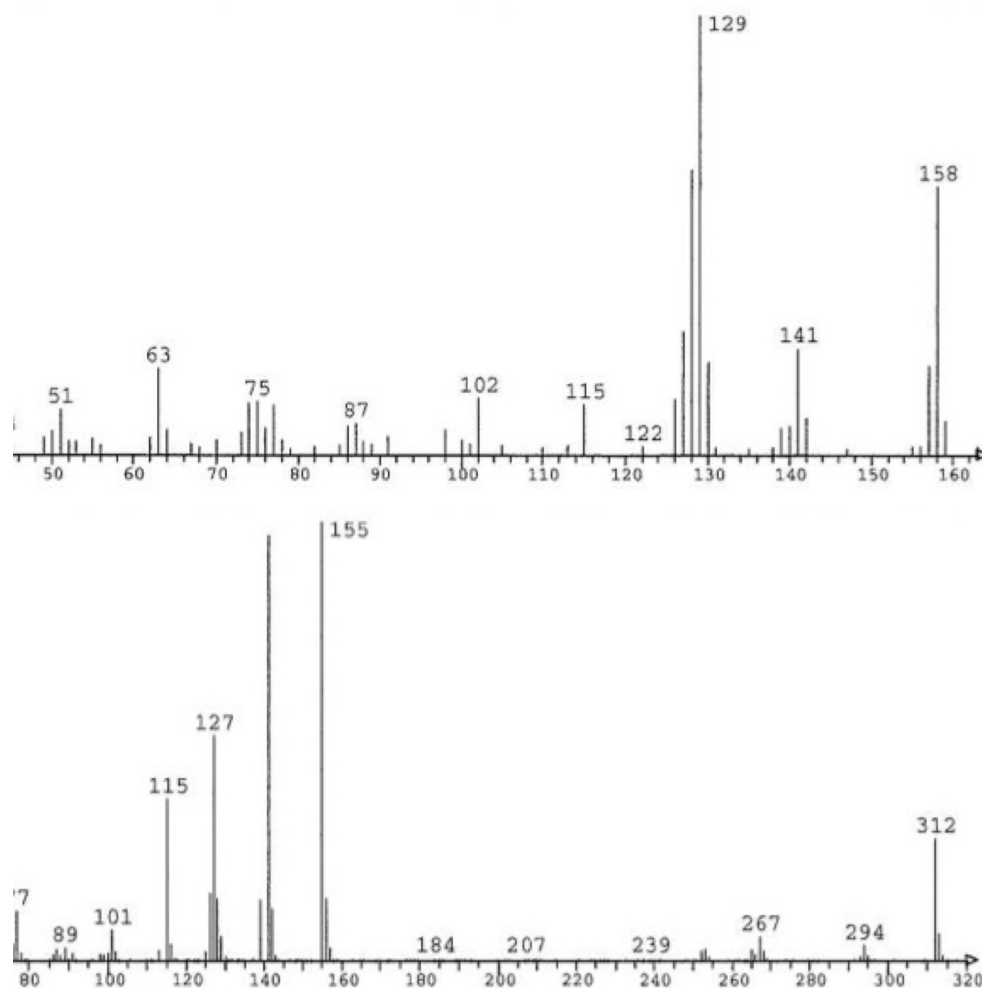


Figure 23. Mass spectrum of entry 8.

In entry 2 (figure 24), main signal at 12:44 was identified as expected product N-phenylpropionamide (149 m/z). Fragments resulted from cleavage of peptide bond were found at 93 m/z, amine side, and 57 m/z, carboxylic side. Similarly as in entry 8, other two products with high m/z were recorded at 18:58 and 21:08. These two compounds could be correlated to some condensation reaction of N-phenylpropionamide, but it was not possible to identify them.

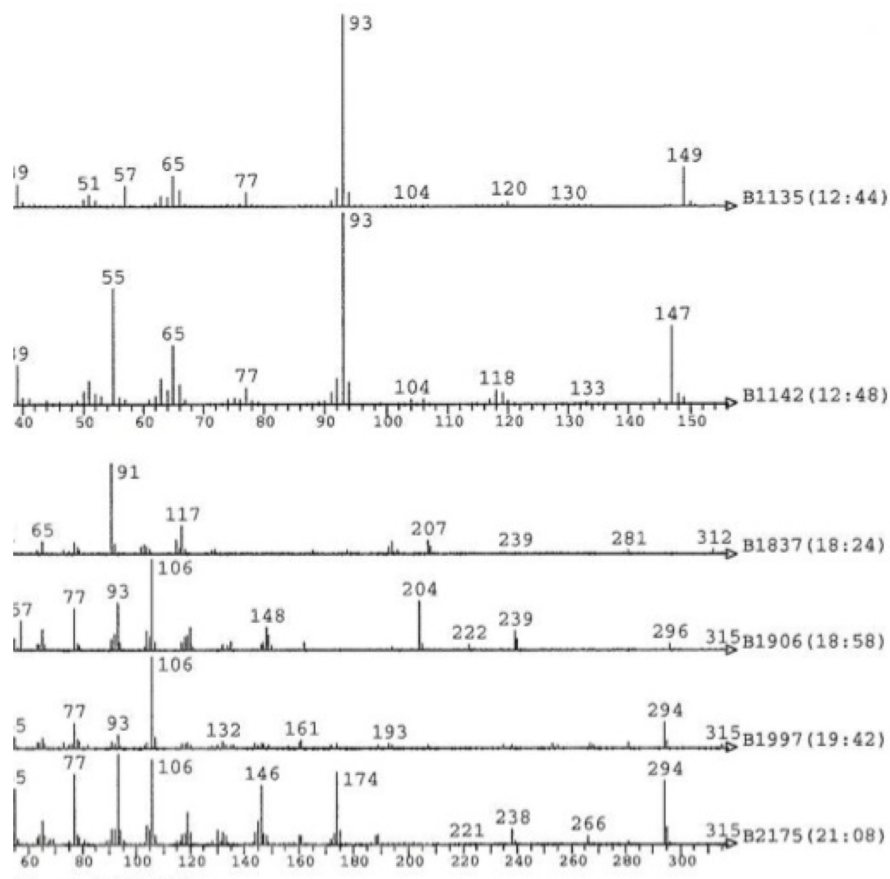
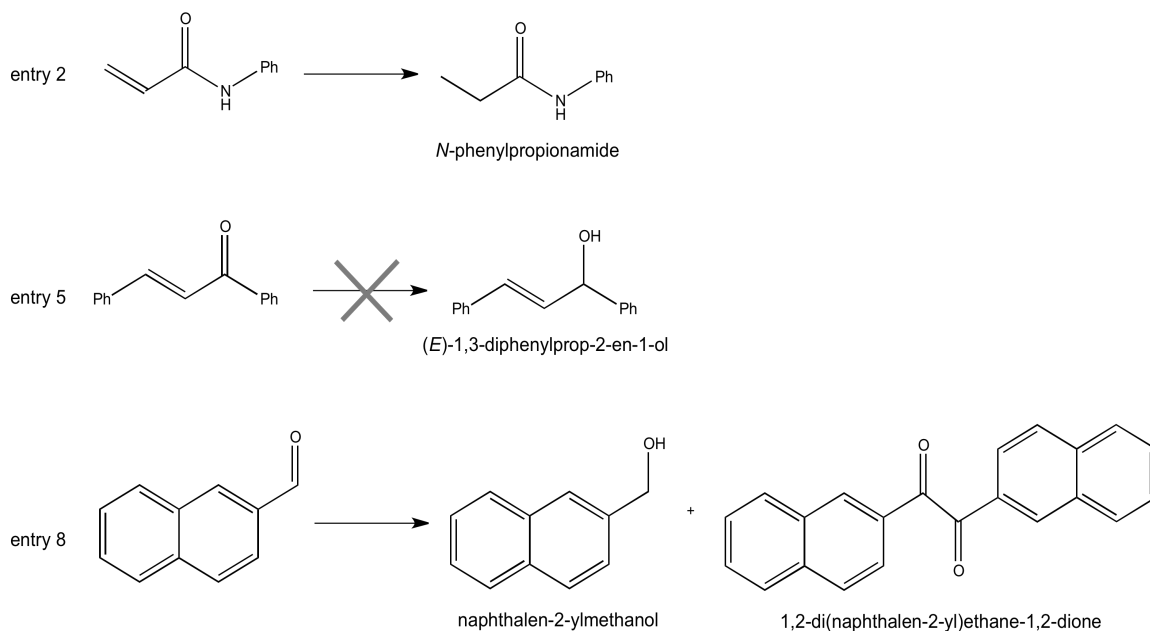


Figure 24. Mass spectra of entry 2: at 12:44 the desired product and at 12:48 starting reagent.

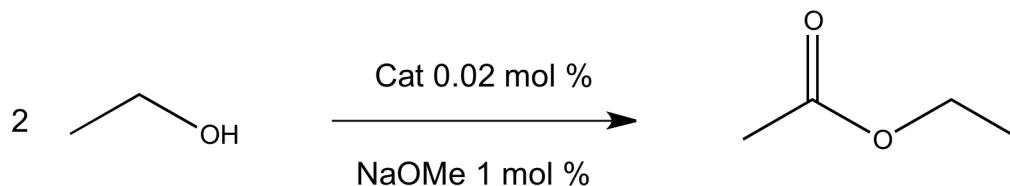
In entry 5 it was not obtained desired hydrogenated product, which was the corresponding alcohol (*E*)-1,3-diphenylprop-2-en-1-ol. Two signals were recorded at 20:08 and 24:24, but it was not possible to identify them by simple GC-MS analysis.



Scheme 22. Result of catalytic test with identified products.

2.3 ADC

New cobalt complex **F** was employed in Acceptorless Dehydrogenative Coupling (ADC) of EtOH, which is the reverse reaction of hydrogenation of corresponding symmetrical ester. It is a good catalytic approach to esters accompanied by hydrogen gas release.



Reactions were performed under argon and left under reflux for 1 day. A first attempt of ADC was run without base additive, in a second one NaOMe was added as base. Complex **F** was added as a solution in THF and then allowed to dry under vacuum to remove solvent.

The stopper of reaction Schlenk was replaced with a finger-type condenser connected to circulating fresh water. This was necessary to avoid any eventual vapor losses of ethyl acetate⁽³⁶⁾.

A septum was placed on the side-arm of Schlenk tube and EtOH was added by a syringe through the septum. The Schlenk vassel was connected to argon/vacuum line with a syringe pierced through septum: by this way vapor and gas could leave reaction vessel only through tiny needle of syringe, which is a very small exchange surface.

At the end of reaction time, reaction mixture was colorless, suggesting that complex **F** decomposed. Particular care was made to recover traces of solution on finger-type condenser. Cyclooctane was added as a standard and conversion to product was monitored by ¹H-NMR and GC analysis. In both cases no traces of acetyl acetate were found, revealing complex **F** inactivity for this kind of reaction. On ¹H-NMR spectrum reported in figure 25 as an example, the following signals were identified: 1.17 ppm quartet of CH₃ (EtOH), at 2.95 ppm singlet of –OH (EtOH), at 3.62 triplet of CH₂ (EtOH) and at 1.42 ppm singlet of standard.

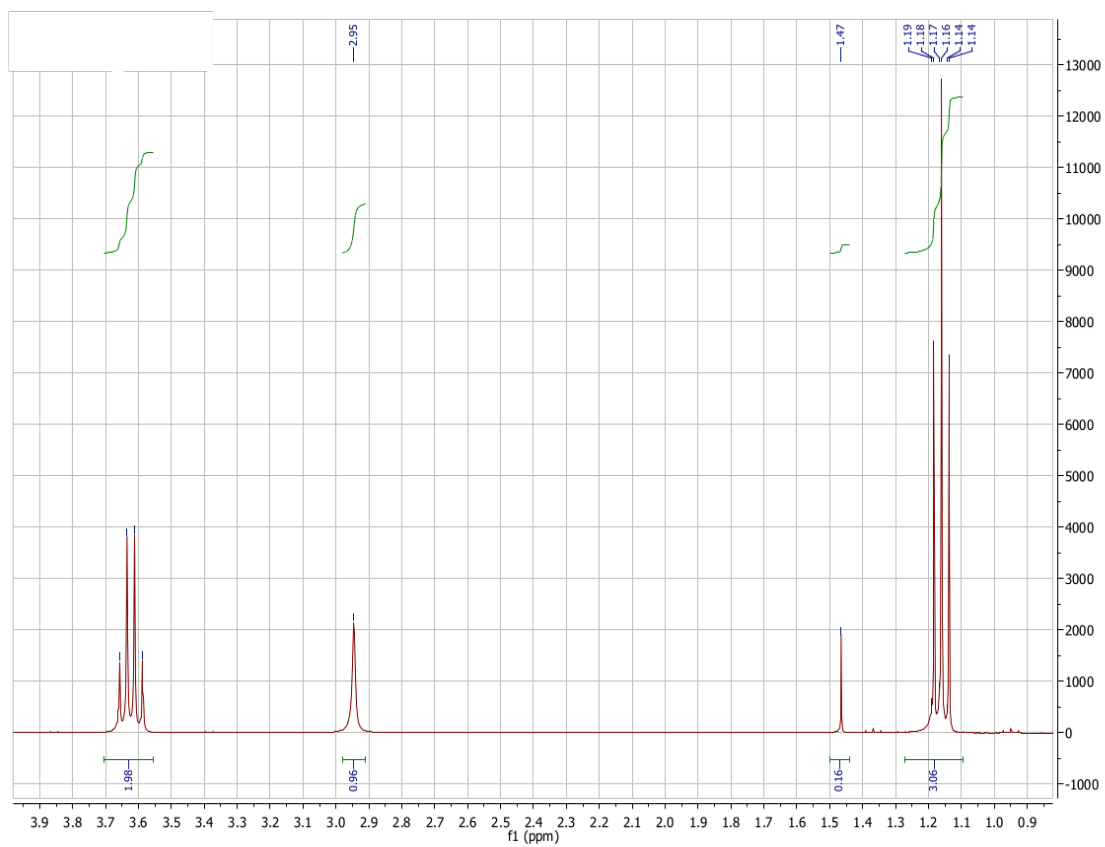


Figure 25. NMR spectrum of reaction mixture at end of reaction time.

2.4 SYNTHESIS OF A NOVEL IRON N-HETEROCYCLIC CARBENE COMPLEX

The thesis work performed in Bologna, also involved in the synthesis of a new non noble metal-based complex. The research group, in which I did my internship, deals with the development of new complexes, which can be involved in hydrogenation reactions by a metal-ligand cooperation.

Specifically, the group has recently used the Shvo catalyst (**24**) for the upgrading of bio-oil by homogeneous hydrogenation.

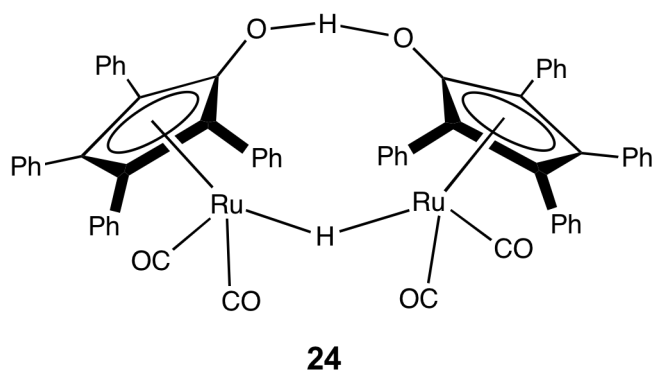


Figure 26. Shvo complex **24**.

2.4.1 SHVO'S CATALYST

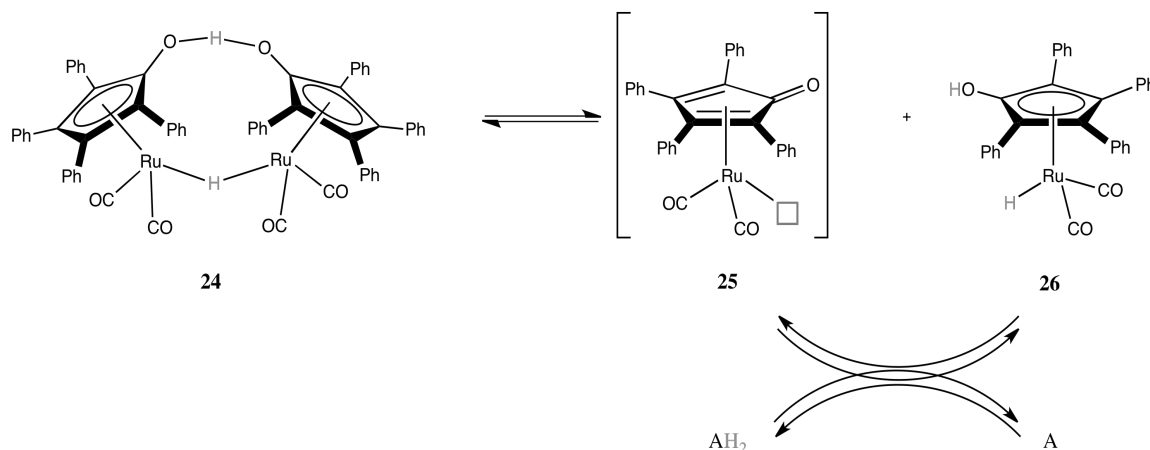
Shvo's catalyst is a cyclopentadienone ruthenium dimer $\{[\text{Ph}_4(\eta^5\text{-C}_4\text{CO})]_2\text{H}\}\text{Ru}_2(\text{CO})_4(\mu\text{-H})$ (**24**), which is air- and water-stable⁽³⁷⁾. Since its discovery in 1980s, has been used as a versatile catalyst in a variety of reactions such as hydrogenation of polar double bonds like carbonyls and imines, oxidation of alcohols and amines, dynamic kinetic resolutions, hydroboration reactions and ADC of primary alcohols.

2.4.1.1 Reactivity

Most of the properties of the Shvo's catalyst are due to the cyclopentadienone ligand, which is able to stabilize the metal in low oxidation states; furthermore it takes part in the catalytic cycle. The mechanism catalysed by complex **24** is an example of metal ligand cooperation: the redox activity depends both from the metal center and cyclopentadienone ligand. Indeed mechanistic studies by Casey et al., confirmed that H_2 transfer goes through a proton on the hydroxyl cyclopentadienyl ligand and a hydride on the metal center.

Complex **24** is the pre-catalyst, which dissociates in solution in an oxidizing (**25**) and a reducing (**26**) monomers. Concentration of the two species is an equilibrium depending on H₂ donors or acceptors as shown in Scheme 22.

Structures of both complexes have been established by NMR: complex **25** by use of trapping agents, **26** by NMR characterization.



Scheme 23- Shvo's precatalyst dimer (**24**) and two monomers: oxidizing agent (**25**) and reducing agent (**26**).

2.4.1.2 Structure

During dissociation of **24**, both hydrogen atoms are associated with just one monomer: this leads to one hydride ruthenium species in +2 oxidation state (**26**) and one unsaturated dicarbonyl species that is formally in zero oxidation state (**25**).

The latter one oxidizes substrates by extraction of one proton, added to cyclopentadienone ligand, and one hydride, added to its open site. The other one in the more oxidized form is the reducing agent. This behavior is unique because the species formally oxidized (2+) is the reducing agent, whilst the more reduced one (0) is the oxidizing agent. This is possible thanks to the ligand: a proton H⁺ is added to a formally neutral cyclopentadienone ligand, which transforms into a formally anionic hydroxycyclopentadienone ligand.

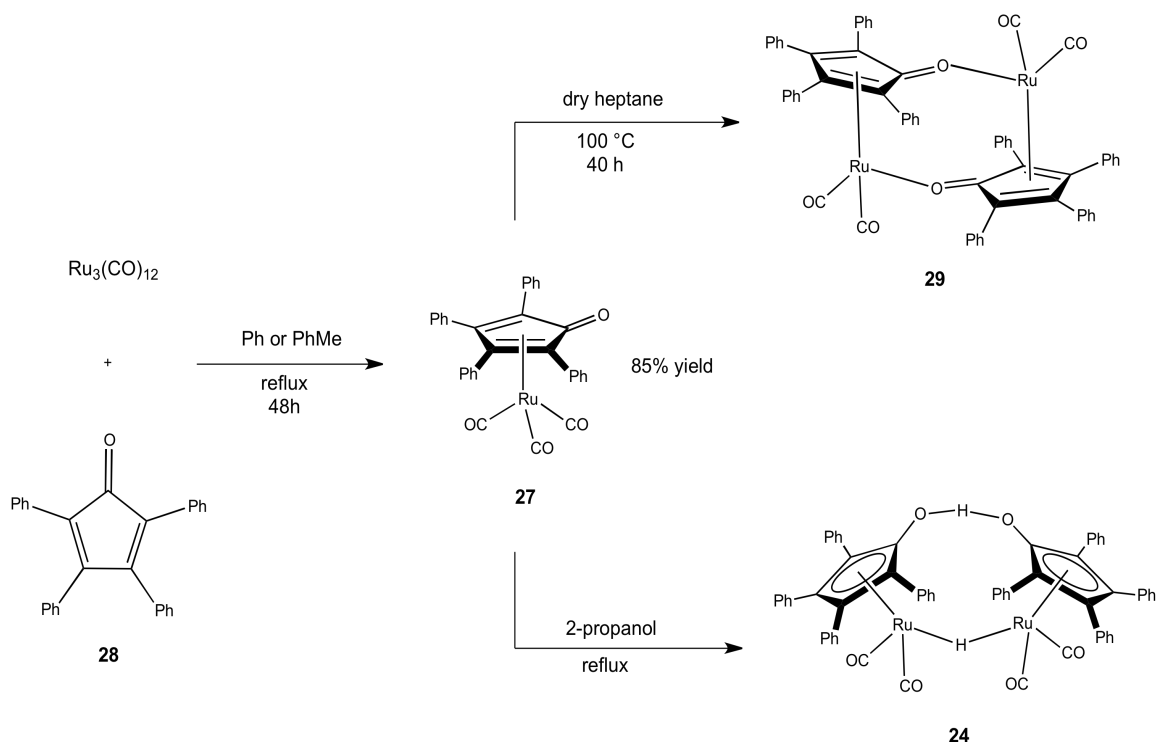
2.4.1.3 Discovery

The discovery of Shvo's catalyst **24** started from studies of dehydrogenation of alcohols to esters by Ru₃(CO)₁₂ in the presence of hydrogen acceptors like alkynes. When diphenylacetylene has been used as acceptor, Shvo found an increased activity of the ruthenium carbonyl catalyst and that the reaction solution kept the same yellow color and

homogeneity through all reaction times. These findings suggested that a ruthenium derivative was probably formed and that was stable and soluble in solution. In 1967, a refluxing $\text{Ru}_3(\text{CO})_{12}$ solution in an aromatic solvent with alkyne has been analyzed and found cyclopentadienone complexes such as $\{[\text{Ph}_4(\eta^5\text{-C}_4\text{CO})]_2\text{H}\}\text{Ru}_2(\text{CO})_4(\mu\text{-H})$ (**24**), $[\text{Ph}_4(\eta^4\text{-C}_4\text{CO})]\text{Ru}(\text{CO})_3$ (**27**) and free tetracyclone (**28**). These complexes have been formed by a [2+2+1] cycloaddition of one equivalent of metal-bound CO and two of diphenylacetylene.

2.4.1.4 Synthesis

Initially, Shvo's catalyst has been synthesized by a two-step route. $\text{Ru}_3(\text{CO})_{12}$ was refluxed together with **28** in aromatic solvent for a long time (>48 h) to form **27**. In this step a molecule of tetracyclone cleaves the ruthenium trimer and displaces one carbon monoxide. Then **27** is refluxed in 2-propanol to give Shvo's catalyst **24** (Scheme 18).

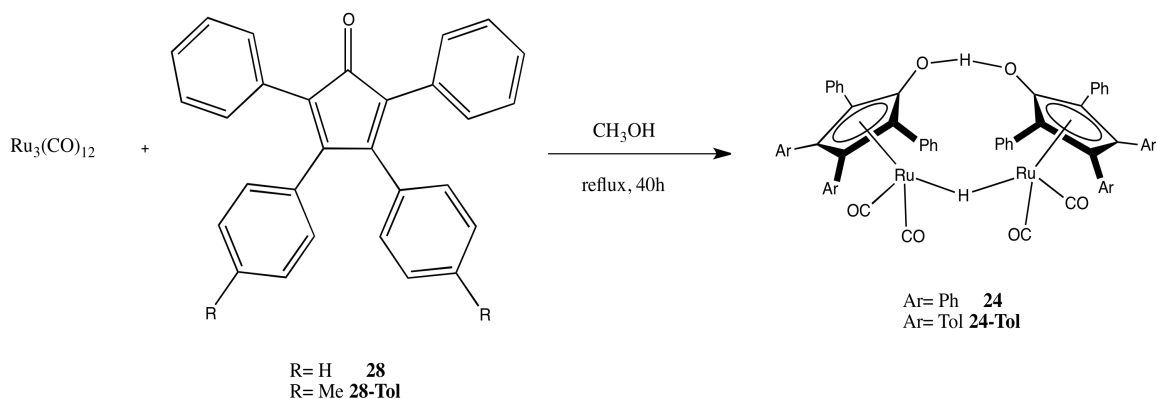


Scheme 24. First two-step synthesis of Shvo's catalyst.

First **24** was identified as $\{[\text{Ph}_4(\eta^5\text{-C}_4\text{CO})]\text{Ru}(\text{CO})_2\}$ (**29**) because of an analogy with an other iron complex already presented by Weiss. Later on, NMR analysis showed a proton signal at -18ppm in C_6D_6 , which was identified as a bridging hydride in structure **24**. Another hydrogen atom was added as a bridge between oxygen atoms of tetracyclone ligands. Therefore both ruthenium atoms are in +1 oxidation state due to the 2 electrons oxidation of 2-propanol solvent to acetone.

Other two synthesis are reported. Bäckvall refluxed $\text{Ru}_3(\text{CO})_{12}$ and **28** in mesitylene, then isolated monomer **27** by purification on silica gel.

Casey et al found a more straightforward approach: a one-step synthesis of a Shvo's catalyst derivative (**24-Tol**). $\text{Ru}_3(\text{CO})_{12}$ and **27** are refluxed in methanol for 40h. This procedure leads directly to complex **24-Tol** by filtration and washing with water in a moderate yield (59%). This procedure it is also used to get Shvo's catalyst (Scheme 25).

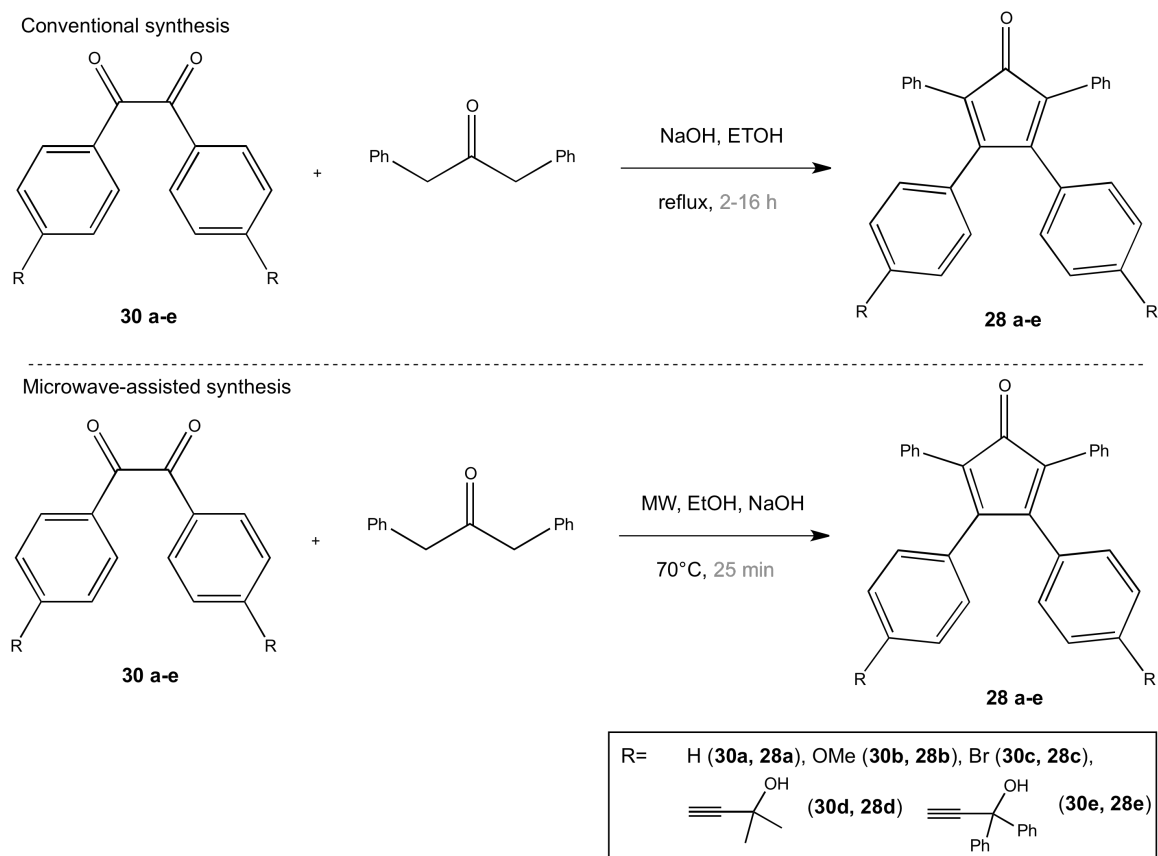


Scheme 25. One-step synthesis of Shvo's catalyst and derivatives.

2.4.1.5 Microwave assisted synthesis

Due to the harshness of reaction conditions reported in the literature⁽³⁸⁾ (long reaction times and high temperatures) a more efficient procedure was developed exploiting microwave irradiation.

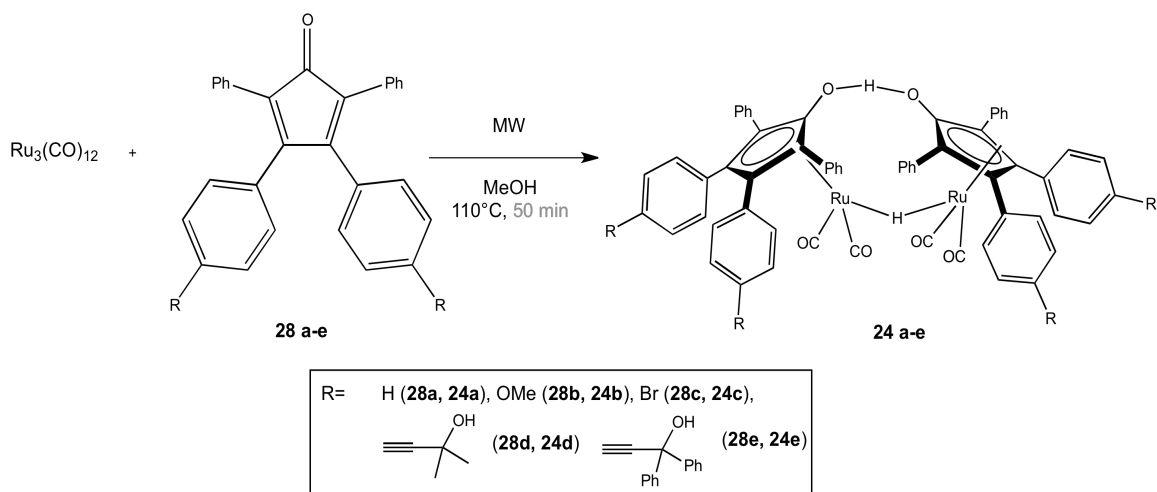
First, a new synthesis of the cyclopentadienone ligands (**28 a-e**) and its derivatives has been investigated (Scheme 26). Classical routes are bis-aldol condensation of 1,3-diphenylacetone with several aromatic diketones (**30 a-e**) in refluxing EtOH for variable reaction times (2-16 h). Best conditions under microwave heating were found at 70°C temperature for 25 min time⁽³⁹⁾. In general yields with microwave irradiation were comparable with the classical reflux method and were influenced by the aryl functionalization (20-91 % yields).



Scheme 26. Comparison between conventional (up) vs microwaved-assisted (down) methods.

In consideration of these results, it has been decided to apply this new route to organometallic synthesis of Shvo catalyst.

Concerning Shvo complexes (**24 a-e**), best reaction conditions were found at 110°C temperature and 50 min time⁽³⁹⁾. Remarkably, in all cases, yields were comparable or higher with respect to classical methods. By this way, Shvo catalyst synthesis goes from 40 h to 50 min without affecting reaction yield. So a new efficient procedure that leads to variously functionalized Shvo-type complexes with reduction of reaction time has been established (Scheme 27).



Scheme 27. Microwave-assisted synthesis of Shvo-type complexes.

2.4.1.6 Applications

Shvo's catalyst is a very versatile compound that has been used in several homogeneous redox reactions: oxidation reactions such as coupling of primary alcohols to esters, oxidation of alcohols to ketones and amine to imine; reduction reactions such as hydrogenations of ketones, alkenes and imine.

Furthermore, the catalyst is a very robust and shows remarkable air- and water-stability. For this reason the research group in which I did my internship in Bologna, tried to test it in upgrading of bio-oil obtained from flash pyrolysis of biomass and hydrogenation of renewable building blocks.

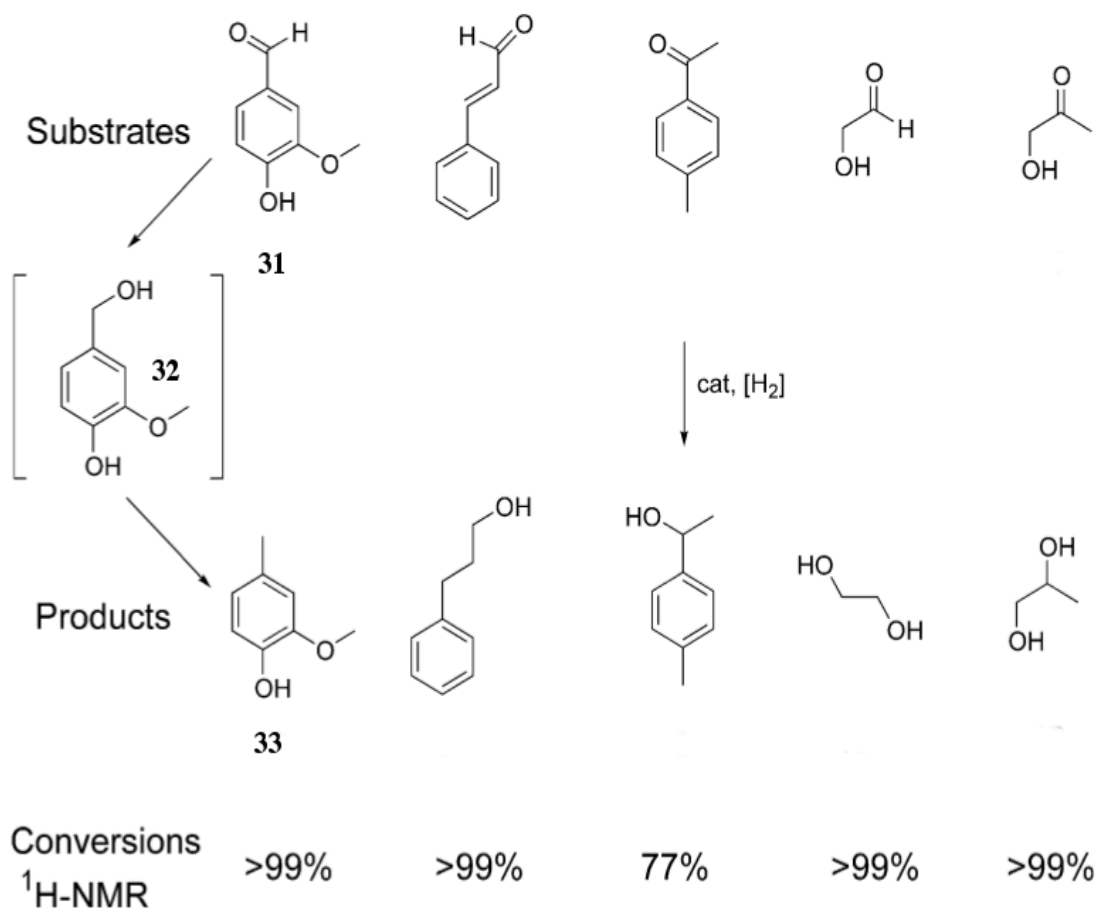
2.4.1.7 Upgrading of bio-oil

Bio-oils derived from pyrolysis have some typical characteristics that need to be improved: higher oxygen and moisture content, high acidity (pH about 2.5), low volatility, high viscosity, corrosiveness and high organic compounds content. One of the major consequences is chemical instability of the oil, which needs upgrading.

Shvo's catalyst is a good candidate for upgrading by hydrogenation due to its stability, and its selectivity in polar double bonds because of his metal-ligand cooperative mechanism.

In a previously reported work, hydrogenation of single model compounds has been tested in order to determine the best reaction conditions. Then hydrogenation experiments have been performed on a biphasic mixture (water/toluene) containing model compounds and acetic acid to reproduce typical bio-oil conditions. Best conditions were found at 10 bar H_2 pressure, 145°C temperature, 1 h reaction time and 200:1 substrate to catalyst ratio⁽⁴⁰⁾. In model mixture, Shvo's catalyst was able to reduce polar double bonds without

hydrogenate aromatic double bonds. In addition, an unexpected deoxygenation of vanillin (**31**) to 2-methoxy-4-methylphenol (**33**) has been obtained, maybe due to an *in situ* acid effect by water at reaction temperature (Scheme 28).



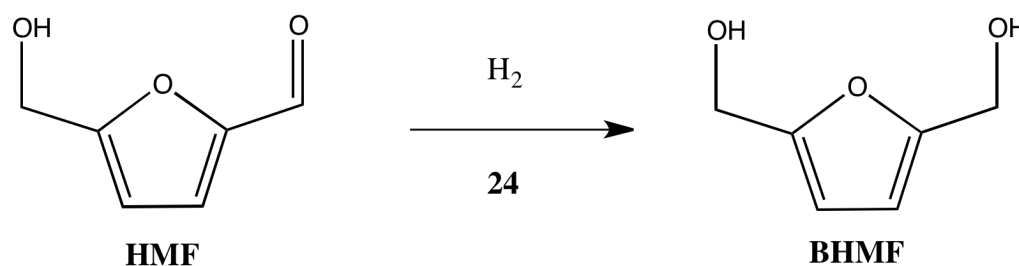
Scheme 28. Compounds hydrogenated by Shvo's catalyst in biphasic mixture. Unexpected deoxygenation of vanillin **31** to compound **33**, instead of getting the vanillin alcohol **32**.

Finally, it has been reported the result of catalytic hydrogenation of a real matrix: a bio-oil derived by pyrolysis of white poplar. Shvo's catalyst was completely soluble and hydrogenated successfully aldehyde, ketones and non-aromatic double bonds. Sugar oligomers were also split into monomers. All these modifications improved the stability of the bio-oil, showing that Shvo's catalyst is an effective homogeneous catalyst for upgrading processes.

2.4.1.8 Hydrogenation of HMF

The Shvo's catalyst has been also employed by R. Mazzoni and co-workers in hydrogenation of biomass derived building blocks such as 5-hydroxymethylfurfural⁽⁴¹⁾ (HMF) (Scheme 29).

HMF is reduced to diol 2,5-bishydroxymethylfurfuran (BHMF), another building block that can be used as monomer in polymer industries or to obtain polyol derivatives. Best conditions were found at 10 bar H₂ pressure, 90 °C temperature, 1 h reaction time, toluene as solvent and 1000:1 substrate to catalyst ratio.



Scheme 29. HMF hydrogenation to BHMF performed by Shvo's catalyst.

The catalyst was also recycled by two methods:

- Product extraction with water. BHMF was recovered in water, whilst the catalyst remained in toluene phase
- Product removal by filtration. Cooling down the autoclave lead to BHMF precipitation: catalyst is collected by simple filtration.

The latter method revealed to be the most convenient in that the catalyst undergoes some decomposition upon treatment with water.

2.4.1.9 Iron analogous

Iron-based analogue of Shvo catalyst for hydrogenation of polar double bonds can be of interest as a non noble metal center.

In 2007, while studying a tolyl Shvo analogue, Casey was inspired by nature hydrogenase (**34**), which is an iron-based catalyst used in reductions⁽⁴²⁾. The diiron co-factor has a hydride and an acidic proton that can be both easily transfer to a substrate: this mechanism is called metal-ligand cooperation, as previously mentioned. These considerations lead him to test Knölker's iron complex (**35**) as a catalyst for hydrogenation of ketones.

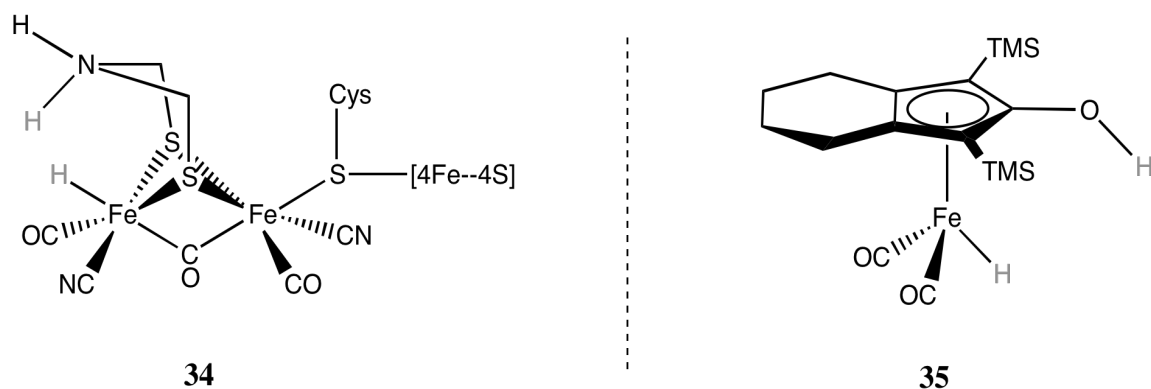
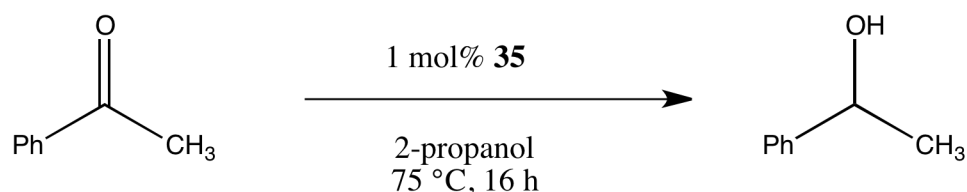


Figure 27. Diiron co-factor of hydrogenase (**34**) and Knölker's complex (**35**). Acidic and hydridic hydrogens in grey.

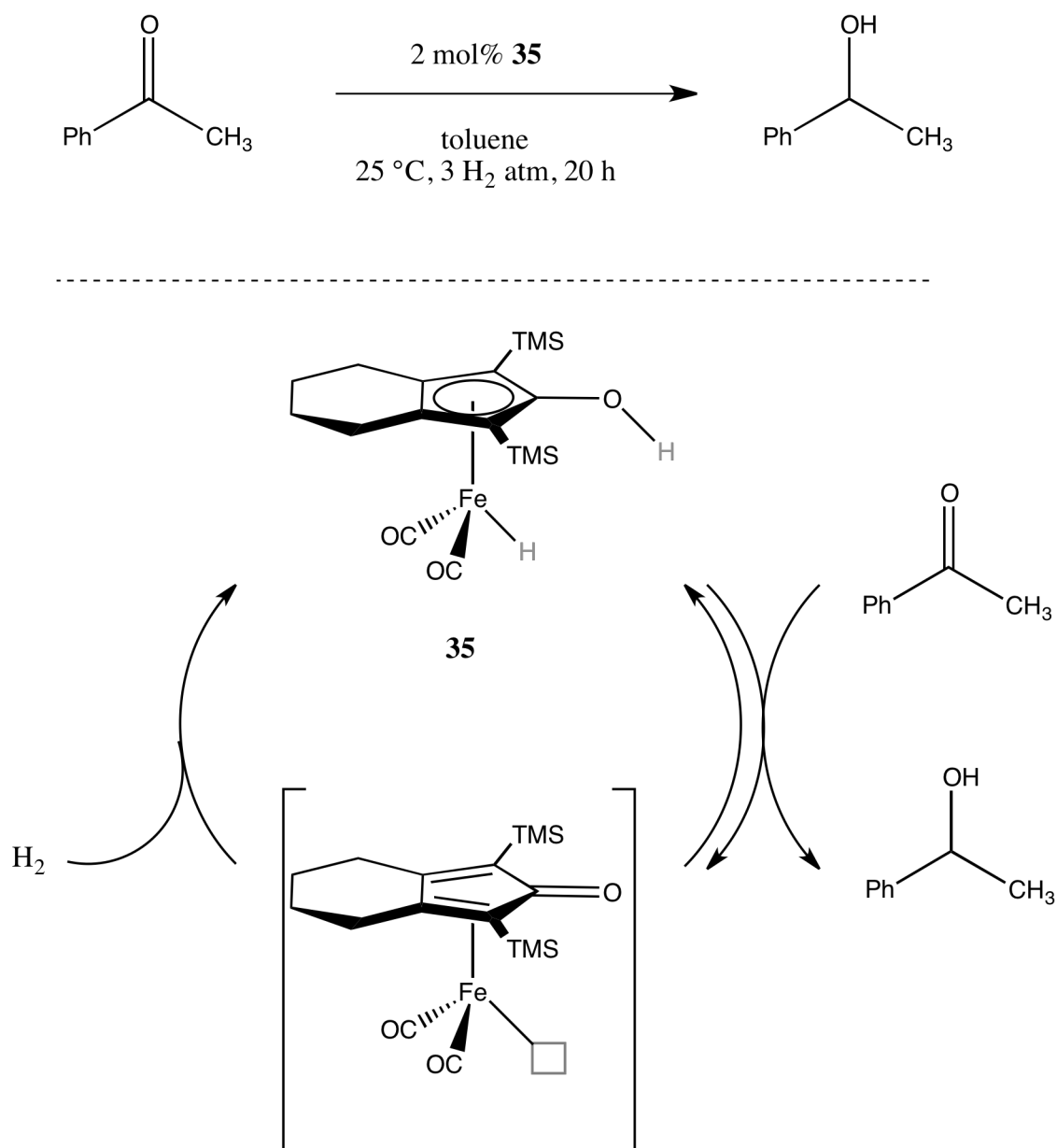
Starting from a simple reduction of acetophenone in toluene- d_8 , he established a catalytic cycle for hydrogenation of acetophenone and then other ketones, involving the use of H_2 as a reducing agent (Scheme 31, see next page). Hydrogenation occurs under mild conditions: 25°C temperature and 3 H_2 atm pressure for 20 h reaction time⁽⁴³⁾.

Moreover, the iron complex catalyzes also the transfer hydrogenation of ketones to alcohols as described in Scheme 30.



Scheme 30. Transfer hydrogenation of acetophenone with 2-propanol as hydrogen donor.

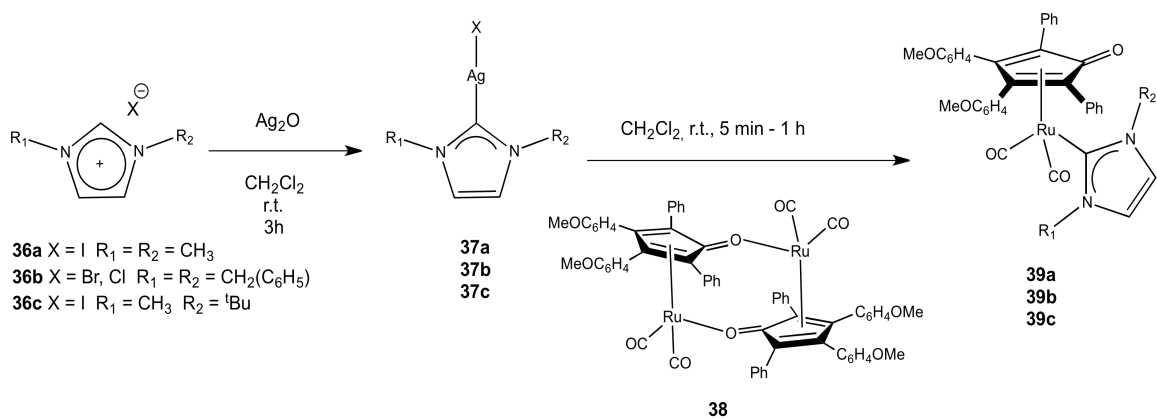
On the basis of what previously described the research group of Zanotti and Mazzoni has been recently interested in the development of new ruthenium complexes bearing both tetraarylcyclopentadienones and N-heterocyclic carbenes, aimed at possible applications in metal-ligand bifunctional catalysis.



Scheme 31. Hydrogenation of acetophenone and related mechanism. The key step is the hydrogen transfer to acetophenone.

Several imidazolium salts have been employed in order to obtain, by means of transmetalation of the corresponding silver complexes, the neutral species **39** reported in Scheme 32⁽⁴⁴⁾.

The internship work in the Prof. Zanotti's group was aimed at the synthesis of new iron analogue to type **39** complexes.



Scheme 32. Transmetalation reaction involving silver complex **37** and Shvo-type ruthenium complex **38**.

2.4.2 SYNTHESIS OF IRON COMPLEX

2.4.2.1 Synthesis of triscarbonyl-(η^4 -3,4-bis(4-methoxyphenyl)-2,5-diphenylcyclopenta-2,4-dienone)iron (**G**)

Synthesis of triscarbonyl-(η^4 -3,4-bis(4-methoxyphenyl)-2,5-diphenylcyclopenta-2,4-dienone)iron (**G**) was performed in a Teflon tube under microwave irradiation. A first attempt was carried on at 80°C for 50 min, but with no product formation. Optimization tests were made under following conditions: 140°C for 50min, 140°C for 90 min, 140 °C for 120 min and 140 °C for 70 min. Best conditions were determined by ¹H-NMR analysis of the crude. Free ligand / product ratio was estimated and best conditions were found at 140°C for 70 min with a free ligand / product ratio of 6:1. Free ligand / product ratio was based on O-CH₃ peaks at 3.78 ppm (cyclopentadienone ligand) and at 3.76 ppm (triscarbonyl product). Longer reaction times resulted in decomposition of product **G**, due to longer exposure to microwave irradiation. Lower temperatures were not able to activate reagents.

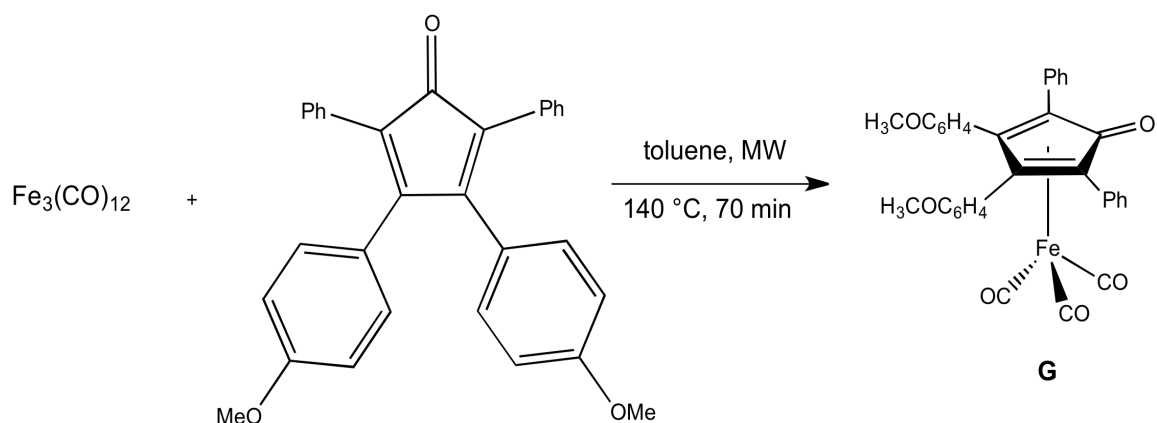


Figure 28. Iron complex **G**.

In order to purify the product different ways have been tried.

Based on solubility tests (Table 7), it was decided to separate the ligand by extraction of triscarbonyl-(η^4 -3,4-bis(4-methoxyphenyl)-2,5-diphenylcyclopenta-2,4-dienone)iron **G** with hexane. Even though the concentration of **G** vs. **28b** was increased by subsequent extractions, it was not possible to obtain complete purification of **G** by means of this method.

Table 7. Solubility tests of complex **G**.

Solvents	Soluble	Not soluble
Hexane	✓	
Toluene	✓	
Dichloromethane	✓	
Ethyl Ether	✓	
Petroleum Ether	Partially	
Isopropanol	✓	
Tetrahydrofuran	✓	
Acetonitrile	✓	

Crude was then dissolved in CH_2Cl_2 double-layered with petroleum ether, considering that it was the only solvent in which triscarbonyl-(η^4 -3,4-bis(4-methoxyphenyl)-2,5-diphenylcyclopenta-2,4-dienone)iron was slightly soluble. By IR and $^1\text{H-NMR}$ analysis, crystals obtained were identified as the ligand 3,4-bis(4-methoxyphenyl)-2,5-diphenylcyclopenta-2,4-dienone (**28b**).

Purification was finally attempted by chromatographic column. First attempt was made on flash silica: hexane / ethyl acetate ratio (5:2), leading to total decomposition of the product triscarbonyl iron, likely due to acidity of silica. Detachment of cyclopentadienone **28b** was observed. Hence in a second attempt alumina was used as a fixed phase and mixture of dichloromethane / ethyl ether (10:1) as mobile phase, given previously TLC tests. In this case, the ligand was completely eluted by dichloromethane, while the product remained adsorbed at top of column, even with just ethyl ether as eluent. By this way, column chromatography could be viewed as a simple filtration, and then it was built just a 3 cm high. Solid was recovered as a yellow fraction by elution with ethyl acetate. A second fraction was recovered by increasing polarity with ethyl

acetate / methanol (10:1) mixture. Both fractions were identified as tricarbonyl iron product **G** by IR and ¹H-NMR analysis (see experimental).

In IR spectrum bands were identified in typical carbonyl range at 2067 cm⁻¹, 2013 cm⁻¹, 1998 cm⁻¹, and C=C bond of cyclopentadienone ligand at 1609 cm⁻¹ and 1518 cm⁻¹. In NMR spectrum were identified signals due to methoxy group on ligand at 3.76 ppm.

2.4.2.2 Synthesis of dicarbonyl-(η⁴-3,4-bis(4-methoxyphenyl)-2,5-diphenylcyclopenta-2,4-dienone)(acetonitrile)iron (**H**)

The reaction was run in acetonitrile, which is a coordinating solvent. If a carbonyl is removed, acetonitrile is expected to coordinate to the iron centre, changing frequencies in IR spectrum. Triethylamine-N-oxide was chosen as reagent to promote CO loss⁽⁴⁵⁾. Spectrum of tricarbonyl iron was recorded in acetonitrile in order to follow reaction by direct sample taking.

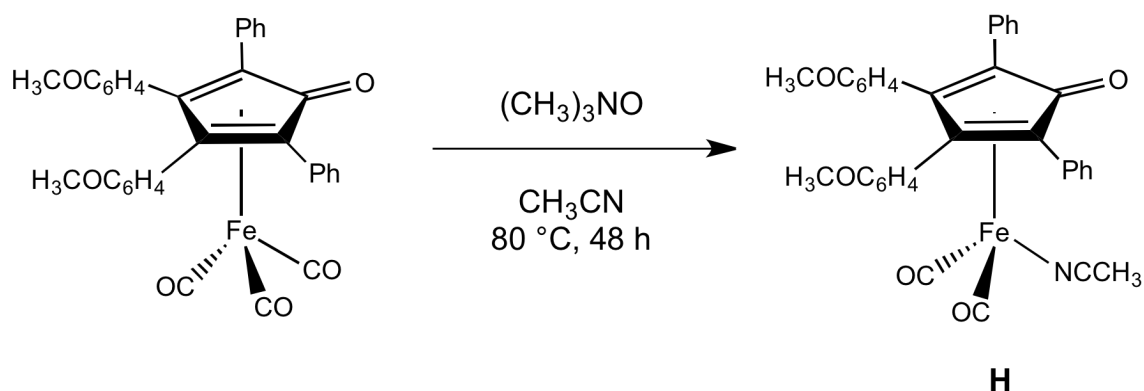


Figure 29. Dicarbonyl iron complex **H**.

Terminal carbonyl bands moved to lower frequency from 2068 and 2012 cm⁻¹ to 2008 and 1953 cm⁻¹ (Figure 30). By ¹H-NMR analysis was identified the desired product: at 7.64-6.63 (m, 18H, CH aromatics), at 3.74 (s, 6H, -OCH₃) and at 2.01 (s, 3H, -NCCH₃).

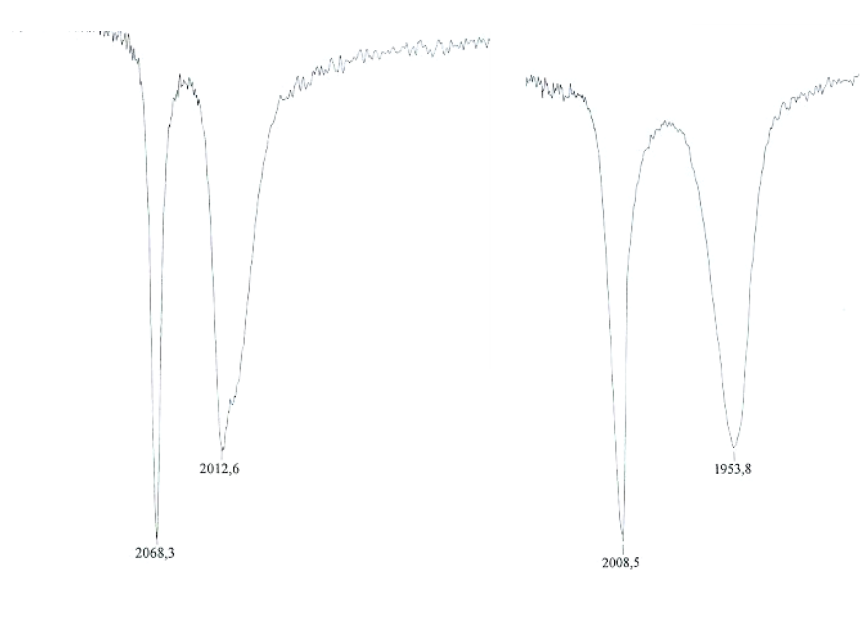


Figure 30. IR CO frequency of iron precursor **G** (left) and iron complex **H** (right).

2.4.2.3 Synthesis of dicarbonyl-(η^4 -3,4-bis(4-methoxyphenyl)-2,5-diphenylcyclopenta-2,4-dienone)(1,3-dimethyl-ilidene)iron (**I**)

In order to obtain a cyclopentadienone iron carbonyl complex bearing a NHC ligand, it was assessed the reactivity of dicarbonyl iron precursor **H**, obtained in previous syntheses, toward silver complex (**37a**, see Scheme 32).

Silver complex was synthesized following a known method: imidazolium salt reacted with silver oxide in dichloromethane⁽⁴⁴⁾.

Solution of silver complex in dichloromethane was added to a reaction vessel together with solid iron precursor **H** and was kept under stirring at room temperature for one night. The day after it was take a sample for IR analysis, which revealed a tiny new band at 1988 cm⁻¹. Solution was left under stirring for a weekend and a IR spectrum revealed a new set of bands at 1987 and 1930 cm⁻¹, which was growing up (Figure 31). The old set of bands related to iron precursor was still there, but with lower intensity. Reaction mixture was left under stirring for 15 days.

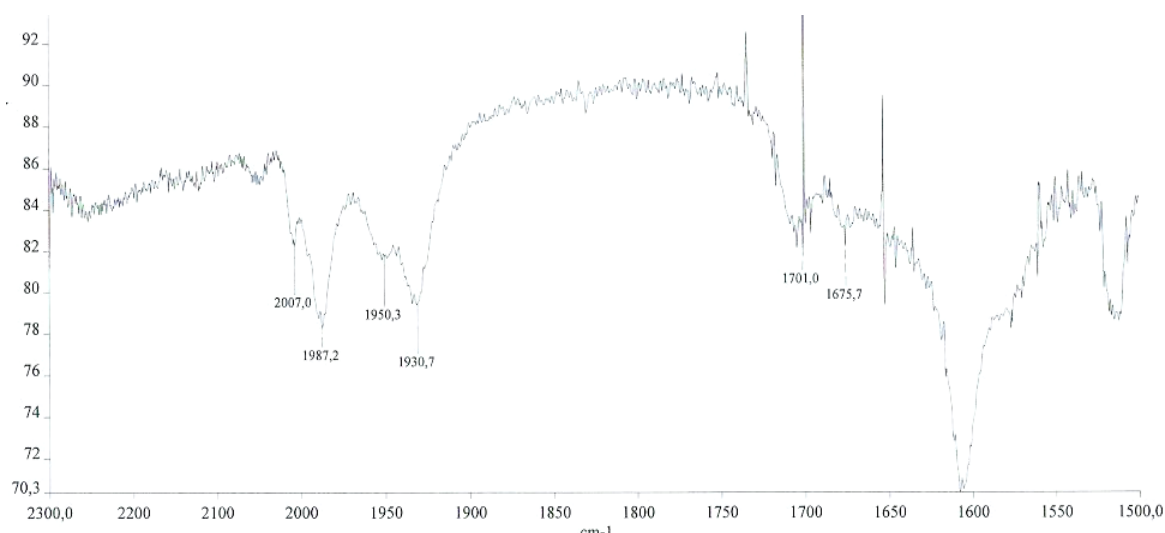


Figure 31. IR spectrum recorded after one weekend of reaction: the set of bands at 2007 cm^{-1} and 1950 cm^{-1} related to iron complex **H** were decreasing, while the new set at 1987 cm^{-1} and 1930 cm^{-1} related to iron complex **I** were growing up.

IR analysis revealed a full conversion with just the new set of bands at 1986 and 1931 cm^{-1} . At 3.18 ppm in $^1\text{H-NMR}$ spectrum was visible peak related to $-\text{NCH}_3$ of the carbene ligand. ESI-MS (+) evidenced peaks at 653 [M+H]^+ , 675 [M + Na]^+ and 691 [M + K]^+ , proving formation of complex **I** by transmetalation reaction from silver to iron.

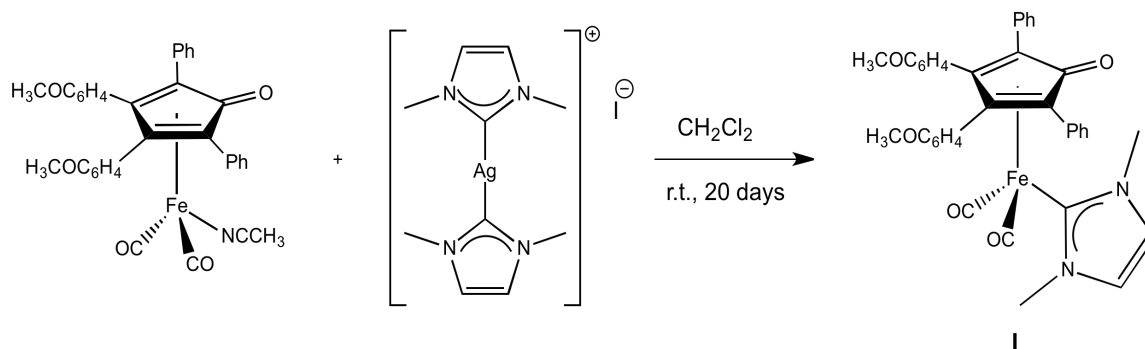


Figure 32. NHC dicarbonyl iron complex **I**.

2.4.2.4 Attempts of synthesis of dicarbonyl-(η^4 -3,4-bis(4-methoxyphenyl)-2,5-diphenylcyclopenta-2,4-dienone)(1,3-dimethyl-imidene)iron *in situ*

In a new attempt of *in situ* synthesis of iron complex **I**, silver complex **37a** were synthesized in acetonitrile and added directly to tricarbonyl iron precursor with triethylamine-N-oxide. Solution mixture was left under reflux.

After 2 hours of reaction, a IR sample was taken and the spectrum showed bands associated to iron complex bearing acetonitrile at 2008 and 1953 cm^{-1} . After one night IR

spectrum revealed a new set of bands growing up at 1989 and 1932 cm^{-1} , which could be related to successful transmetallation reaction from silver complex to iron complex **I**.

After 5 days, reaction was stopped and IR spectrum showed just one set of bands very broad at 1992 and 1938 cm^{-1} . Solution is filtered through a pad of Celite and crude re-dissolved in toluene double-layered with hexane. IR analysis of solution showed the only presence of cyclopentadienone ligand, while analysis of precipitate, a mixed of yellow and violet solid, revealed a set of bands at 2000 and 1945 cm^{-1} and one new band at 2098 cm^{-1} . It was not clear what was recovered at the end of work-up, but probably NHC iron complex decomposed during work up procedure.

Another attempt of *in situ* synthesis was made in toluene, which is a non-coordinative solvent, hence carbonyl could be directly removed and NHC ligand could coordinate easily. Silver complex was synthesized in dichloromethane because imidazolium salt resulted not soluble in toluene. Dichloromethane was removed, solid re-dissolved in toluene and added to triscarbonyl iron precursor with triethylamine-N-oxide. After one night IR spectrum showed the appearance of a row of bands related to NHC iron complex **I** at 1988 and 1930 cm^{-1} , but from $^1\text{H-NMR}$ (Figure 33) analysis an array of peaks in $-\text{OCH}_3$ range were recorded.

Reaction mixture was left under reflux for a weekend. IR and $^1\text{H-NMR}$ sample were taken, but spectra were the same as before, revealing that reaction in toluene lead to the formation of a complex mixture.

Solvent was removed and crude purified by chromatographic column on alumina. At first free cyclopentadienone ligand **28b** was recovered by dichloromethane in the same way as triscarbonyl precursor **G**. Polarity of eluent was increased by means of dichloromethane / ethyl ether mixture with increasing ratio (10:1 to 2:1), but without any success. After addition of ethyl acetate, a yellow fraction was recovered. IR and $^1\text{H-NMR}$ analysis of latter fraction identified triscarbonyl iron precursor. No product was recovered.

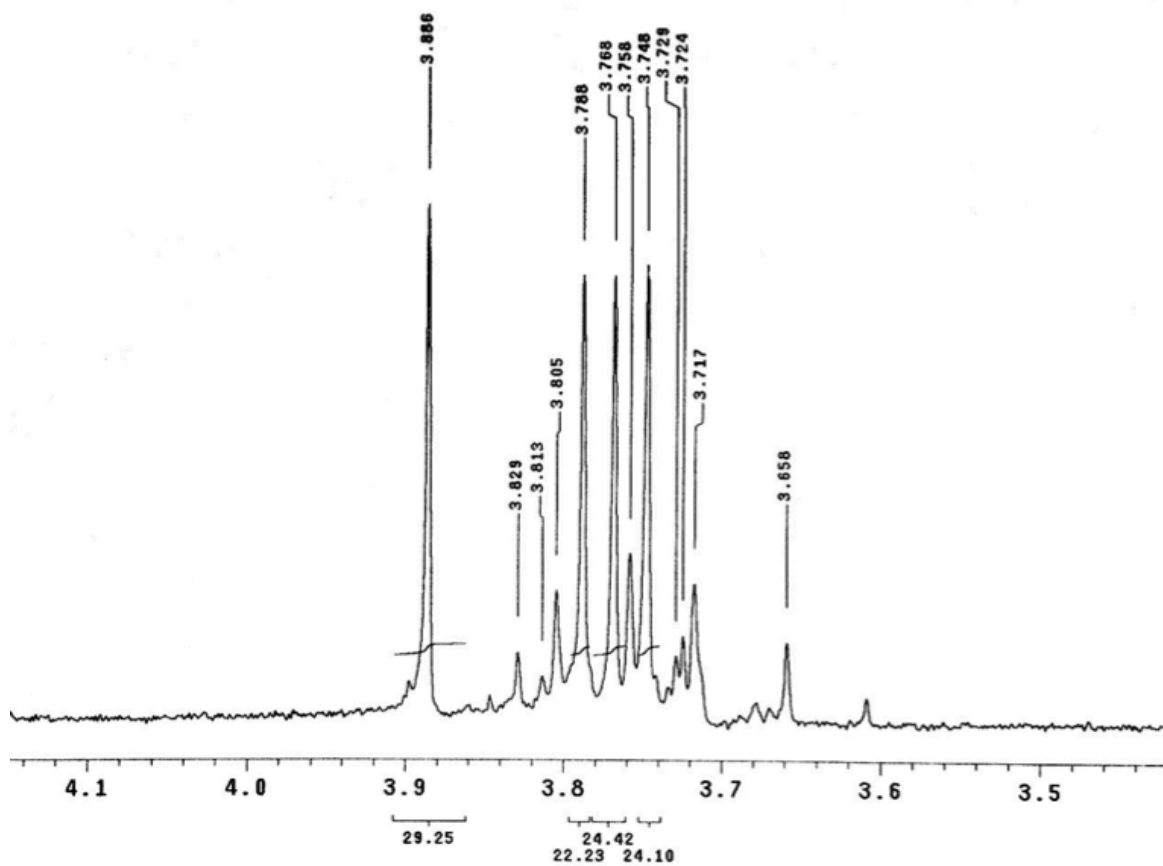


Figure 33. Enlargement of $-OCH_3$ range in 1H -NMR spectrum.

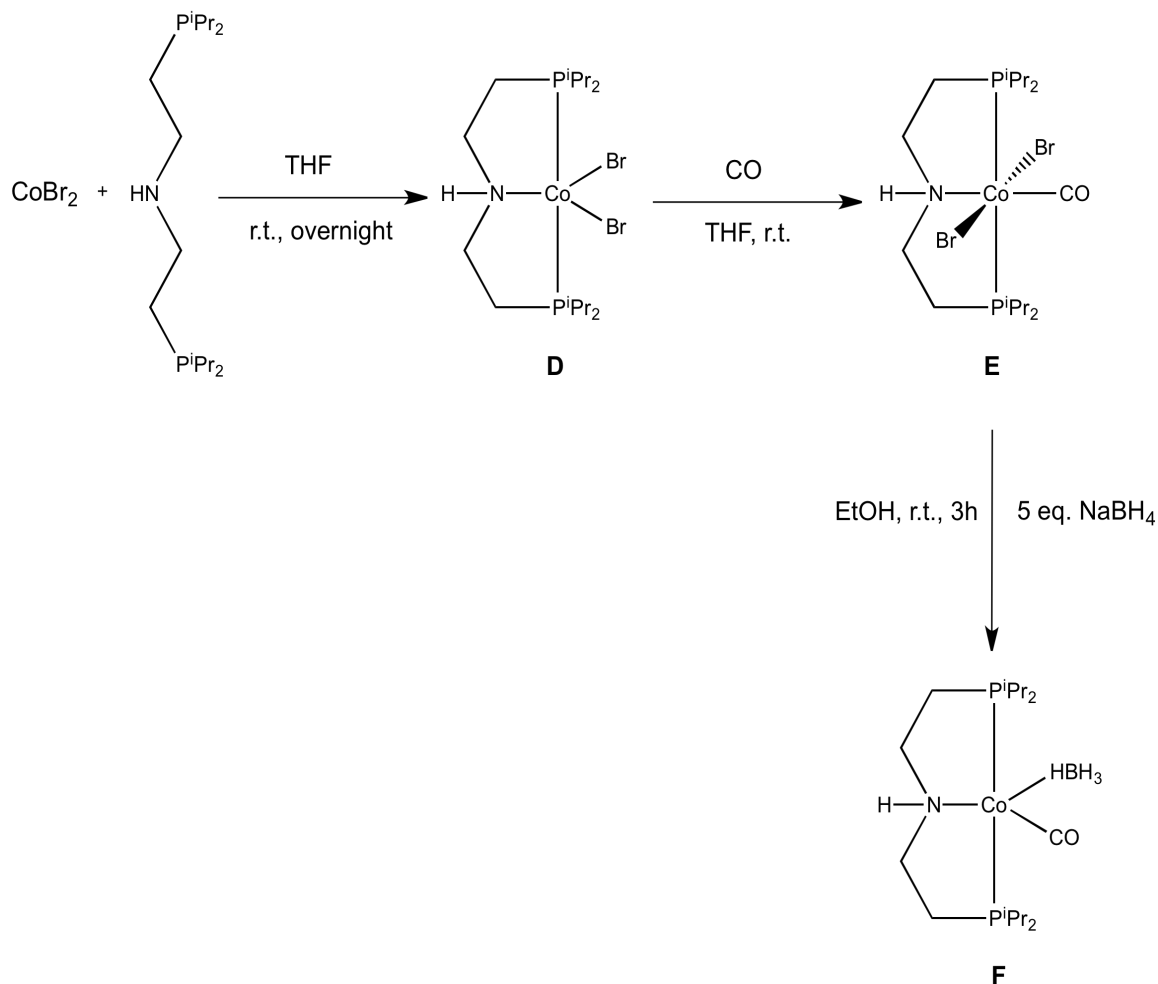
3. CONCLUSIONS

This work of thesis has focused on study and synthesis of new metal-based complexes in a perspective of replacement toxic and expensive precious metals. At the end of my training period two new non-noble metal based complexes were synthesized successfully: a cobalt and an iron complex. Both complexes could be employed in redox reactions.

Synthesis of carbonyl-tetrahydroborato-bis[(2-diisopropylphosphino)ethyl] amine-cobalt (**F**) was based on iron analogous **8** and was divided in 3 steps:

1. Bis[(2-diisopropylphosphino)ethyl]amine (PNP) insertion.
2. Carbonylation reaction.
3. Sodium borohydride insertion.

Characterization was tricky due to paramagnetism and high sensitivity to air and moisture of cobalt complex. A well-defined structure was obtained by X-ray diffraction, revealing the cobalt in +1 oxidation state.



Scheme 33. Full synthetic route of cobalt complex **F**.

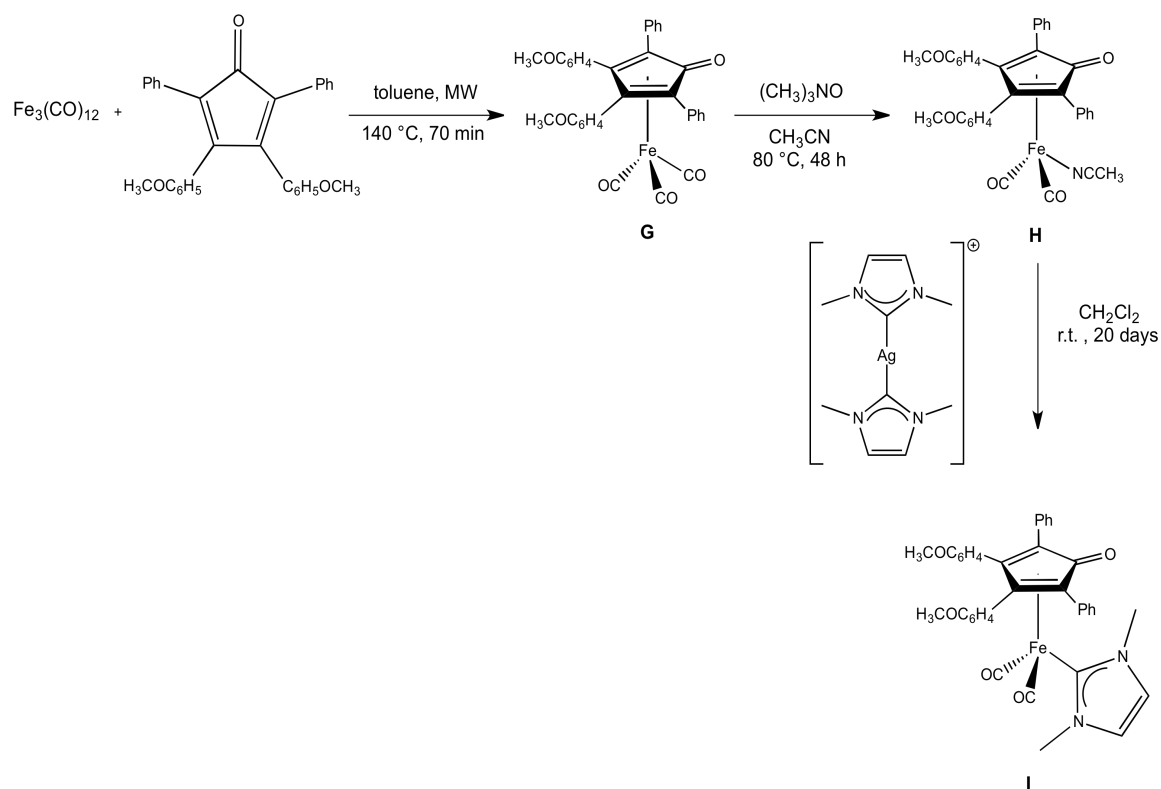
Optimization of reaction route was assessed in order to lowering reaction times and waste of solvent. Step 1 and 2 were joined in one single step, but without success.

Preliminary catalytic tests on esters hydrogenation revealed no activity of cobalt complex and so did ADC tests of ethanol. These results were expected because of differences between cobalt complex **F** and already known iron complex **8**, concerning the absence of hydride group and the electron properties of the metal center (cobalt being more electron rich than the iron analogue) An array of substrates was tested to assess any possible activity of cobalt complex: two were fully converted to desired product and by-products, while one was converted to a mixture of not-identified products.

Future studies will concern the assessment of activity of cobalt complex in order to evaluate future applications.

Synthesis of dicarbonyl-(η^4 -3,4-bis(4-methoxyphenyl)-2,5-diphenylcyclopenta-2,4-dienone)(1,3-dimethyl-imidene)iron (**I**) was based on a three steps route:

1. Synthesis of tricarbonyl precursor (**G**) by microwave assisted method.
2. Removal of carbonyl ligand.
3. Transmetalation of NHC ligand by means of silver complex, derived by an imidazolium salt.



Scheme 34. Full synthetic route of NHC iron complex **I**.

Attempts are under study in order to get a crystal structure of dicarbonyl-(η^4 -3,4-bis(4-methoxyphenyl)-2,5-diphenylcyclopenta-2,4-dienone)(1,3-dimethyl-ilidene)iron (**I**) and a better insight in reactivity against silver complex.

4. EXPERIMENTAL SECTION

4.1 GENERAL PROCEDURE

All reactions were performed under inert atmosphere (argon or nitrogen) with exclusion of moisture from reagents and glassware using standard techniques for manipulating air-sensitive compounds. All Schlenk flasks were flame dried with heat gun and argon flushed.

4.1.1 LIKAT (Rostock)

Solvents

Tetrahydrofuran (THF), toluene, dichloromethane (CH_2Cl_2), diethyl ether (Et_2O), heptane, cyclohexane, ethanol (EtOH), isopropanol ($^i\text{PrOH}$) and methanol (MeOH) were refluxed over suitable anhydrication agent (sodium/benzophenone alkyl for THF, Et_2O , hexane and toluene; calcium hydride for CH_2Cl_2 , magnesium for MeOH , EtOH and $^i\text{PrOH}$), distilled, stored under argon and used as anhydrous solvent. Deuterated solvent were distilled over sodium/benzophenoneketyl (benzene) or calcium hydride (dichloromethane) and stored under argon.

Reagents

Bis[(2-diisopropylphosphino)ethyl]amine solution 10 wt. % in THF (Sigma-Aldrich), cobalt chloride (CoCl_2), cobalt bromide (CoBr_2), sodium borohydride (NaBH_4) and calcium hydride (CaH_2) were purchased, stored under argon and used as received.

Methyl benzoate, methyl 2-phenylacetate, ethyl furan-2-carboxylate, methyl cyclohex-1-enecarboxylate, methyl octanoate, methyl 3-phenylpropanoate were refluxed over calcium hydride, distilled, degas and stored under argon.

N-methylbenzamide, N-phenylacrilamide, N-benzylbanzamide, 1-(4-aminophenyl)ethanone, (E)-2-methylpenta-1,3-diene, phtalazin-1(2H)-one, 4-acetylbenzaldehyde, 2-naphthaldehyde, (E)-3-(2-methoxyphenyl)acrylaldehyde, 2-nitrobenzaldehyde, 2,4-dinitroaniline, 9-nitroanthracene, hexadecane and cyclooctane were purchased and used as received.

Instrumentation

Catalytic hydrogenation experiments were carried out in Parr Instruments autoclave (300 mL) with alloy plate with well for 4 mL vials equipped with a needle through the septum. ^1H -NMR and ^{31}P -NMR spectroscopy were obtained at 300 MHz (Bruker AV-300) or 400 MHz (Bruker AV-400).

IR spectra were recorded on a Bruker Alpha P FT-IR spectrometer.

Mass spectra were recorded on a MAT 95XP (Termo Electron) Mass spectrometer or on a 6210 Time-of-Flight LC/MS (Agilent). Gas chromatography was performed on a HP 6890 with a HP5 column (Agilent).

X-ray structures were determined with a Bruker Kappa APEX II DUO CCD diffractometer and data processed with APEX2 (Bruker 2012).

4.1.2 Bologna

Solvents

Dichloromethane (CH_2Cl_2), petroleum ether (Etp), ethyl ether (Et_2O), acetonitrile (CH_3CN) and tetrahydrofuran (THF) were reflux over suitable anhydric agent (sodium/benzophenone alkyl for THF and Et_2O ; calcium hydride for CH_2Cl_2 and CH_3CN , sodium-potassium alloy for Etp), distilled and stored under inert atmosphere with molecular sieves. Ethyl acetate (EtOAc), methanol (MeOH), ethanol (EtOH), isopropanol ($^i\text{PrOH}$), toluene, hexane and deuterated chloroform (CDCl_3 , Sigma-Aldrich) were used without further purifications.

Reagents

Anisole, benzophenone, potassium hydroxide (KOH), triiron dodecarbonyl ($\text{Fe}_3(\text{CO})_{12}$), silver oxide (Ag_2O), triethylamine-N-oxide ($(\text{Me})_3\text{NO}$), alumina (Al_2O_3) and silica flash were purchased and used as received.

Instrumentation

All reactions were followed by IR spectroscopy and products were characterized by spectroscopy methods (IR, NMR, ESI-MS).

IR spectra were recorded at 298K on a Perkin Elmer Spectrum 2000 FT-IT spectrometer using a NaCl cell (1 mm width) for solutions.

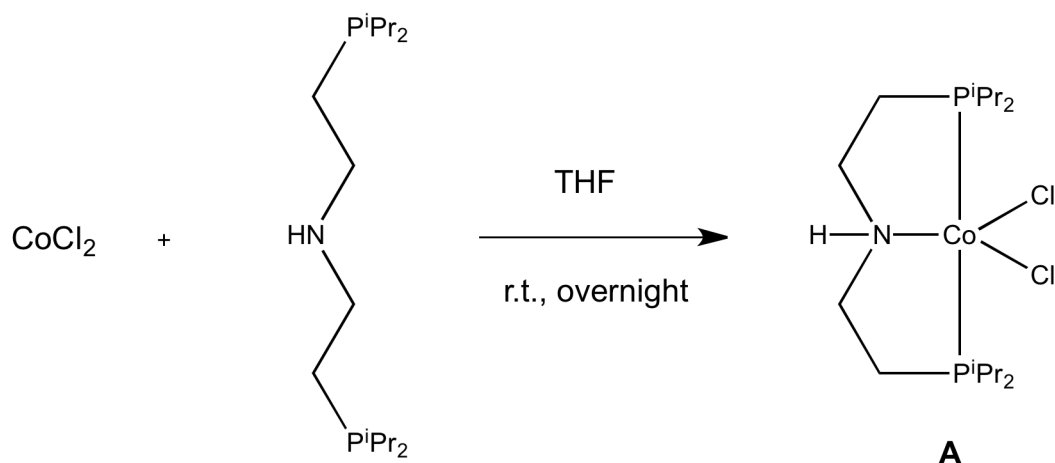
NMR spectra were obtained at 300 MHz (Varian Inova 300) or at 400 MHz (Varian Mercury Plus VX 400). All chemical shift are reported in parts per million (ppm) downfield from tetramethylsilane and were referenced to the residual proton resonance and natural abundance of ^{13}C resonance of the solvent chloroform- d_3 (7.26 (^1H), 77.1 (^{13}C)).

ESI-MS analyses were performed on Waters ZQ-4000 spectrometer by injection of product in ethanol.

Microwave reactions were performed on a Milestone PRO 16/24 “High throughputrotor” instrument using Teflon vials equipped with temperature and pressure sensors. Power of instrument was set to 600 W. Temperature program provides a ramp of 5 minutes until reaching of desired reaction temperature. At the end samples were cooled down to room temperature. All reactions were monitored through temperature and pressure sensors, while microwave power was set automatically by instrument itself between 0-100 W ranges, in order to keep constant the reaction temperature.

4.2 COBALT COMPLEXES

4.2.1 Synthesis of dichloride-bis[(2-diisopropylphosphino)ethyl]amine-cobalt(II) (A)



Procedure

In a 50 ml Schlenk tube, CoCl_2 (0.127 g, 0.98 mmol, 1 equivalent) was dissolved in 10 ml of absolute THF and a solution of bis[(2-diisopropylphosphino)ethyl]amine (0.314 g, 1.03 mmol, 1.05 equivalent) was added dropwise. The resulting violet solution was stirred overnight at room temperature.

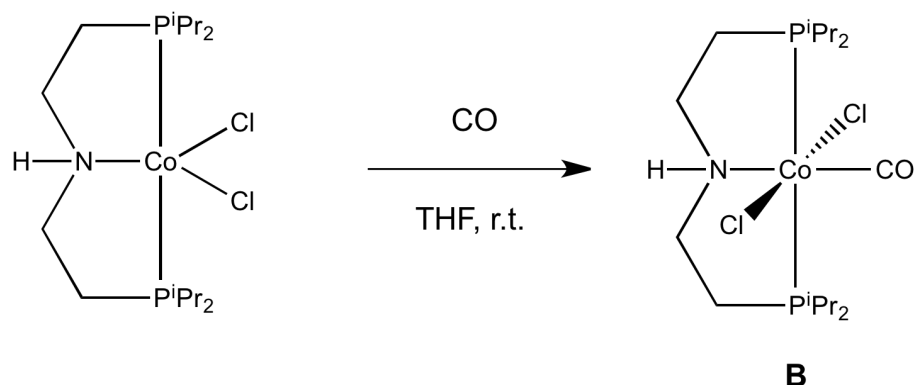
The solvent was removed under vacuum and the solid suspended in 10 mL of toluene and filtered. The solid was washed repeatedly with toluene to remove unreacted reagents. The residue was re-dissolved in the minimum amount of CH_2Cl_2 and recrystallized from dichloromethane and diethyl ether.

The solvent was removed and the resulting pink solid was washed several times with diethyl ether. Yield: 0.306 g (71.4%).

Characterization

IR (ATR) $\nu(\text{N-H})$: 3245 cm^{-1} ; $\nu(\text{C-H})$: 2952 cm^{-1} ; 2921 cm^{-1} ; 2866 cm^{-1} .

4.2.2 Synthesis of carbonyl-dichloride-bis[(2-diisopropylphosphino)ethyl]amine-cobalt(II) (B)



Procedure

In a 50 mL Schlenk tube, $\text{CoCl}_2[\text{HN}((\text{CH}_2\text{CH}_2)\text{P}(\text{CH}(\text{CH}_3)_2)_2)]$ (0.277 g, 0.64 mmol) was dissolved in 20 mL of absolute THF and the CO was bubbled into the solution by cannula. The solution turned green.

The solvent was removed under vacuum and the residue washed several times with EtOH and heptane. The resulting green solid is dried under vacuum. Yield: 0.283 g (95.3%).

Characterization

IR (ATR) ν (CO): 2009 cm^{-1} ; 1986 cm^{-1} ; ν (NH): 3162 cm^{-1} , ν (CH): 2956 cm^{-1} ; 2927 cm^{-1} ; 2867 cm^{-1} .

ESI-HRMS (m/z) (+) = 434.10824 $[\text{M-CO}]^+$; 414.12926 $[\text{M-HCl-CO+O}]^+$; 398.13426 $[\text{M-HCl}]^+$.

Pure green crystals suitable for a single X-Ray diffraction were grown from a solution of toluene layered with heptane.

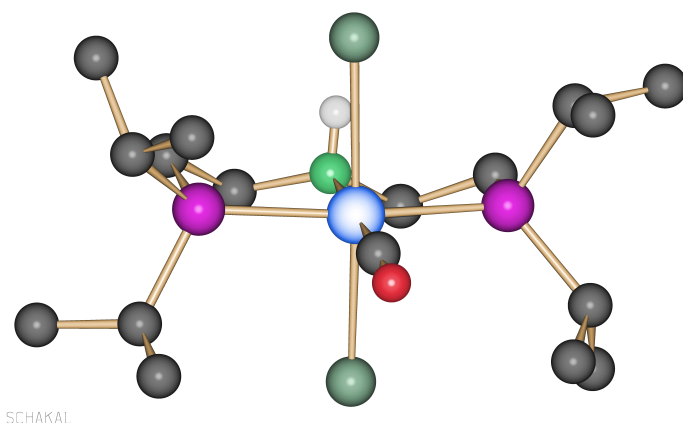


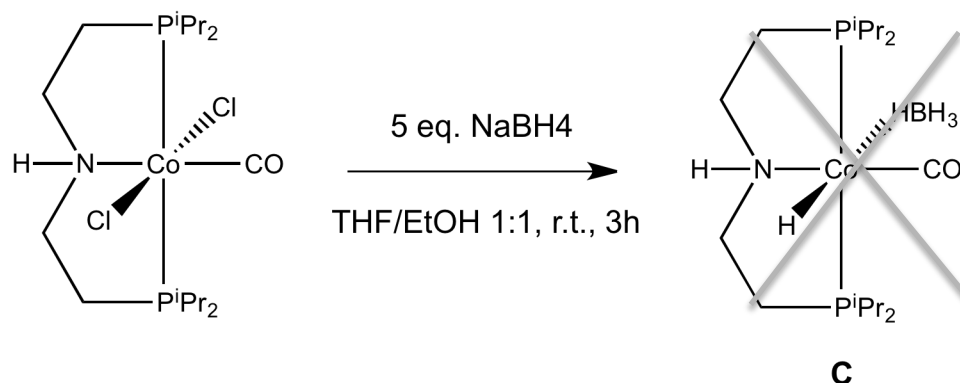
Figure 34. Crystal structure of complex B.

Table 8. Crystal data of compound **B**.

Identification code	
Crystal description	Green needle
Empirical formula	C ₁₇ H ₃₇ Cl ₂ CoNO ₂ P ₂
Formula weight	463.25 g·mol ⁻¹
Temperature	150(2) K
Wavelength	0.71073 Å
Crystal system	Triclinic
Space group	P-1
Unit cell dimensions	a=11.4916(3) α= 86.366(1)° b=12.0608(3) β= 84.722(1)° c=16.5530(4) γ= 79.004(1)°
Volume	2240.07(10) Å ³
Z	4
Density (calculated)	1.374 mg/m ³
Absorption coefficient	1.153 mm ⁻¹
F(000)	980
Crystal size	0.38x0.13x0.11 mm ³
Distances	
Co-C	1.7681(17) Å
C-O	1.136(2) Å
Co-N	2.0222(13) Å
N-H	0.878(19) Å
Co-Cl ₁	2.5836(5) Å
Co-Cl ₂	2.5206(5) Å
Co-P ₁	2.2673(5) Å
Co-P ₂	2.2717(5) Å
Angles	
C-Co-N	178.85(7) °

Co-N-H	102.3(12) °
C-Co-P ₁	95.47(6) °
C-Co-P ₂	94.41(6) °
C-Co-Cl ₁	97.57(6) °
C-Co-Cl ₂	90.43(6) °

4.2.3 Attempt of synthesis of carbonyl-hydrido-tetrahydroborato-bis[(2-diisopropylphosphino)ethyl]amine-cobalt(II) (C)



Procedure

In a 25 mL Schlenk tube, CoCl₂(CO)[HN((CH₂CH₂)P(CH(CH₃)₂)₂)] (0.277 g, 0.64 mmol) and NaBH₄ (20.6 mg, 0.55 mmol) were suspended in 5 mL of absolute THF. A 5 ml of EtOH was added dropwise. The solution turned dark brown.

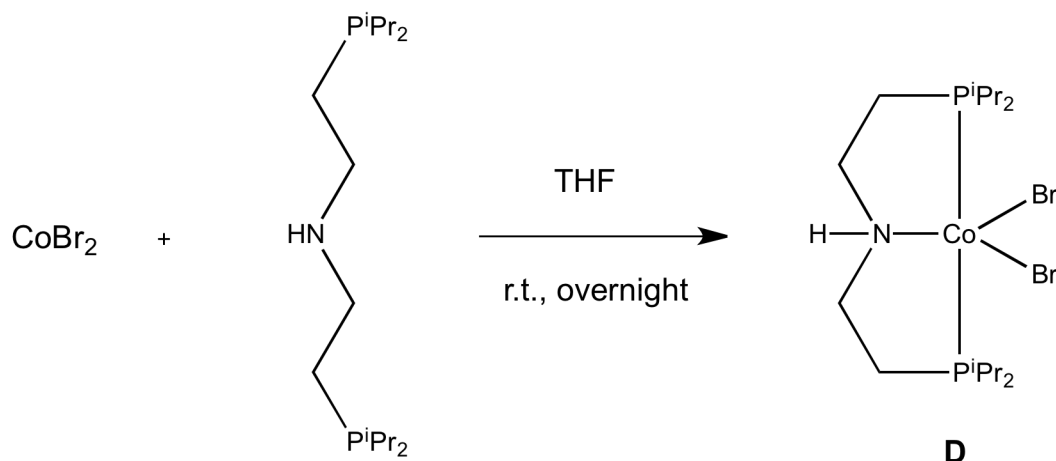
The solvent was removed under vacuum. The residue was dissolved in toluene and filtered. The solvent was removed in vacuo.

The resulting brown and oily solid is dried under vacuum.

Characterization

IR ATR ν (CO): 1880 cm⁻¹; ν (NH): 3178 cm⁻¹, ν (CH): 2954 cm⁻¹; 2929 cm⁻¹; 2869 cm⁻¹; ν (BH): 2313 cm⁻¹.

4.2.4 Synthesis of dibromide-bis[(2-diisopropylphosphino)ethyl]amine-cobalt(II) (D)



Procedure

In a 50 ml Schlenk tube, CoBr₂ (0.209 g, 0.96 mmol, 1 equivalent) was dissolved in 10 ml of absolute THF and a solution of Bis[(2-diisopropylphosphino)ethyl]amine (0.321 g, 1.05 mmol, 1.05 equivalent) was added dropwise. The resulting violet solution was stirred overnight at room temperature.

The solvent was removed under vacuum and the solid suspended in 10 mL of toluene and filtered. The solid was washed repeatedly with toluene to remove unreacted reagents. The residue was re-dissolved in the minimum amount of CH₂Cl₂. The solvent was removed and the resulting pink solid was washed several times with ethanol. Yield: 0.405 g (80.2%).

Characterization

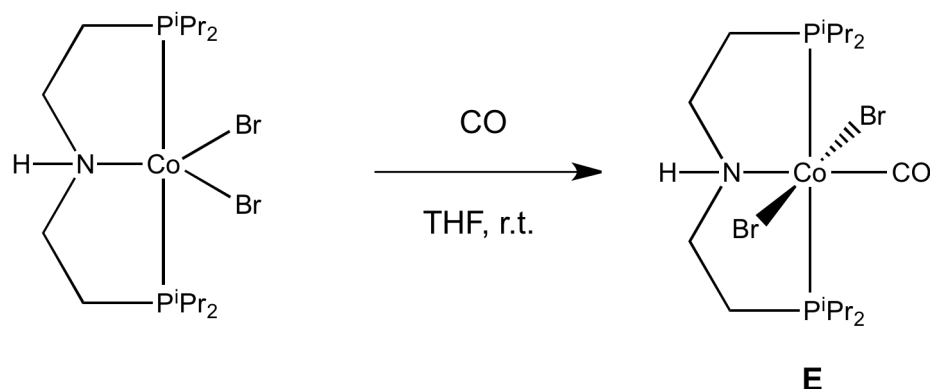
IR (ATR) $\nu(\text{N-H})$: 3101 cm⁻¹; $\nu(\text{C-H})$: 2950 cm⁻¹; 2924 cm⁻¹; 2867 cm⁻¹

ESI-HRMS (m/z) (+) = 524.00798 [M⁺]; 442.0834 [M-Br]⁺

EA: C=36.44, H=7.045, N=2.936, Br=28.503

Pure pink crystals suitable for a single X-Ray diffraction were grown from a solution of dichloromethane layered with ether. Unfortunately, the crystals were too small and calculations were not enough accurate to report here, even though a crystal structure has been found.

4.2.5 Synthesis of carbonyl-dibromide-bis[(2-diisopropylphosphino)ethyl]amine-cobalt(II) (E)



Procedure

In a 50 mL Schlenk tube, $\text{CoBr}_2[\text{HN}((\text{CH}_2\text{CH}_2)\text{P}(\text{CH}(\text{CH}_3)_2)_2)$ (0.255 g, 0.49 mmol) was dissolved in 15 mL of absolute THF and the CO was bubbled into the solution by cannula. The solution turned green.

The solvent was removed under vacuum and the residue washed several times with EtOH and heptane. The resulting green solid is dried under vacuum. Yield: 0.275 g (99.9%).

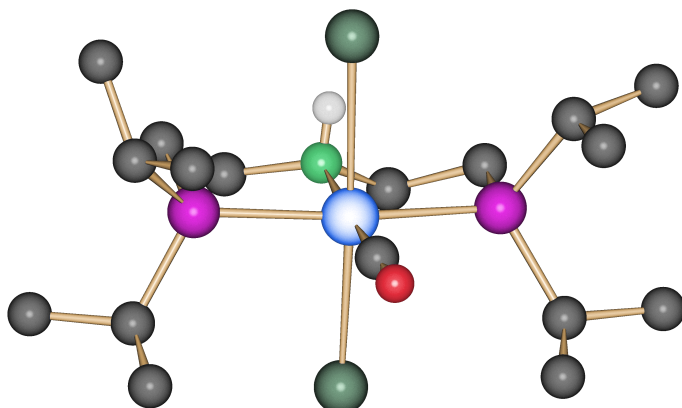
Characterization

IR ATR ν (CO): 2010 cm^{-1} ; ν (NH): 3140 cm^{-1} , ν (CH): 2957 cm^{-1} ; 2923 cm^{-1} ; 2867 cm^{-1} .

ESI-HRMS (m/z) (+) = 552.00157 [M]^+ ; $524.00791\text{ [M-CO]}^+$; $442.08306\text{ [M-Br}^{79}\text{/Br}^{81}]^+$.

EA: C=36.55; H=6.687; N=2.711; Br=28.385; Co=10.53.

Pure green crystals suitable for a single X-Ray diffraction were grown from a solution of toluene layered with heptane.



SCHAKAL

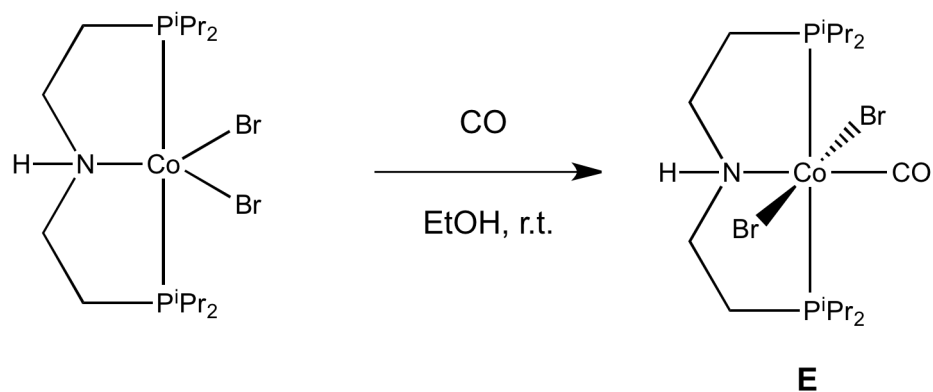
Figure 35. Crystal structure of complex **E**.

Table 9. Crystal data of complex **F**.

Identification code	
Crystal description	Green prism
Empirical formula	$C_{17}H_{37}Cl_2CoNO P_2$
Formula weight	$600.25 \text{ g}\cdot\text{mol}^{-1}$
Temperature	150(2) K
Wavelength	0.71073 \AA
Crystal system	Triclinic
Space group	P-1
Unit cell dimensions	$a=11.6637(5)$ $\alpha= 77.000(1)^\circ$ $b=11.8226(5)$ $\beta= 88.166(1)^\circ$ $c=19.8862(8)$ $\gamma= 81.733(1)^\circ$
Volume	$2644.17(19) \text{ \AA}^3$
Z	4
Density (calculated)	$1.508 \text{ mg}/\text{m}^3$
Absorption coefficient	3.804 mm^{-1}
F(000)	91232
Crystal size	$0.315 \times 0.261 \times 0.251 \text{ mm}^3$
Distances	
Co-C	$1.759(2) \text{ \AA}$

C-O	1.132(2) Å
Co-N	2.0222(13) Å
N-H	0.81(2) Å
Co-Br ₁	2.6925(3) Å
Co-Br ₂	2.7521(3) Å
Co-P ₁	2.2870(5) Å
Co-P ₂	2.2815(5) Å
Angles	
C-Co-N	177.04(8) °
Co-N-H	103.2(15) °
C-Co-P ₁	95.41(6) °
C-Co-P ₂	94.65(6) °
C-Co-Br ₁	93.83(6) °
C-Co-Br ₂	91.45(6) °

4.2.6 Synthesis of Carbonyl-dibromide-Bis[(2-diisopropylphosphino)ethyl]amine-Cobalt(II) (E)

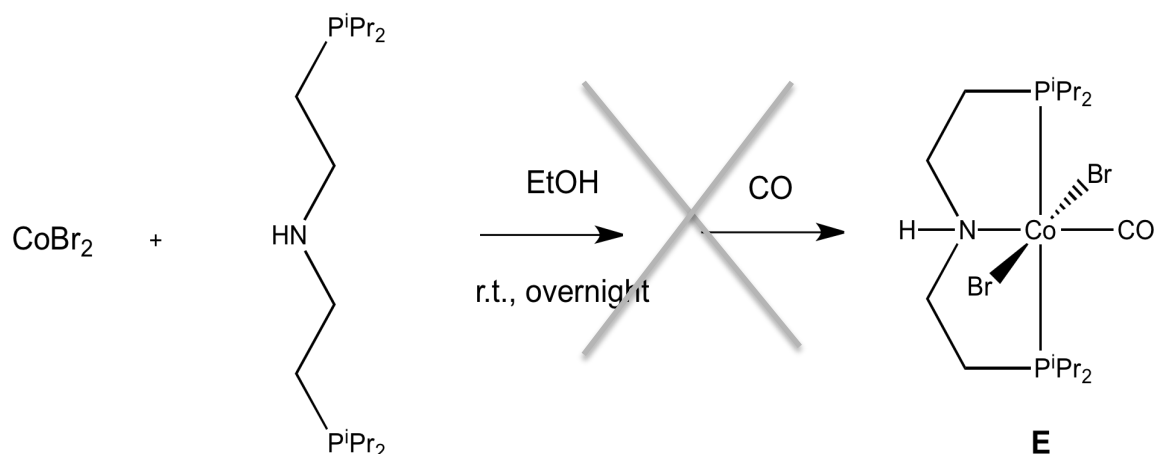


Procedure

In a 50 mL Schlenk tube, $\text{CoBr}_2[\text{HN}((\text{CH}_2\text{CH}_2)\text{P}(\text{CH}(\text{CH}_3)_2)_2)]$ (0.396 g, 0.76 mmol) was dissolved in 20 mL of absolute EtOH and the CO was bubbled into the solution by cannula. The solution turned green.

The solvent was removed under vacuum and the residue washed several times with heptane. The resulting green solid is dried under vacuum. Yield: 0.396 g (94.7%).

4.2.7 Attempt of synthesis of carbonyl-dibromide-bis[(2-diisopropylphosphino)ethyl]amine-cobalt(II) (E) *in situ*



Procedure

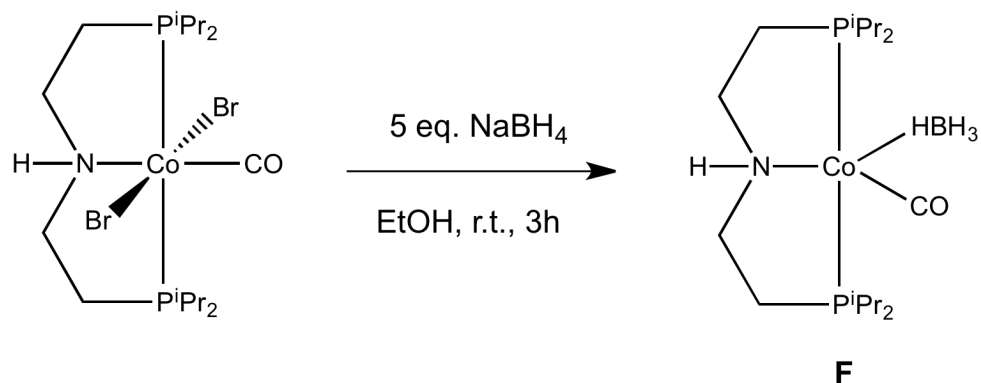
A solution of Bis[(2-diisopropylphosphino)ethyl]amine (0.321 g, 1.05 mmol, 1.05 equivalent) was poured into a 50 mL Schlenk tube and the solvent was removed under vacuum. CoBr_2 (0.219 g, 1.00 mmol, 1 equivalent) was added and dissolved in 20 mL of absolute EtOH. The resulting violet solution was stirred overnight at room temperature. The CO was bubbled into the solution by cannula. The solution turned brownish and then green.

The solvent was removed under vacuum and the residue extracted with THF. The solvent was removed and the solid washed with heptane. The resulting dark green solid is dried under vacuum.

Characterization

IR ATR ν (CO): 2006 cm^{-1} ; 1971 cm^{-1} ; 1912 cm^{-1} ; ν (NH): -, ν (CH): 2957 cm^{-1} ; 2929 cm^{-1} ; 2871 cm^{-1} .

4.2.8 Synthesis of carbonyl-tetrahydroborato-bis[(2-diisopropylphosphino)ethyl]amine-cobalt(I) (F)



Procedure

In a 100 mL Schlenk tube, $\text{CoBr}_2(\text{CO})[\text{HN}((\text{CH}_2\text{CH}_2)\text{P}(\text{CH}(\text{CH}_3)_2)_2)]$ (475.1 g, 0.86 mmol) and a solution of NaBH_4 in absolute EtOH (160.4 mg in 45 mL) were added. The solution turned dark brown with reddish glares.

The solvent was removed under vacuum. The solid was suspended in Et_2O and filtered. The Et_2O was removed in vacuo and the residue extracted several times with Heptane (~40mL). The heptane was removed to leave a reddish solid.

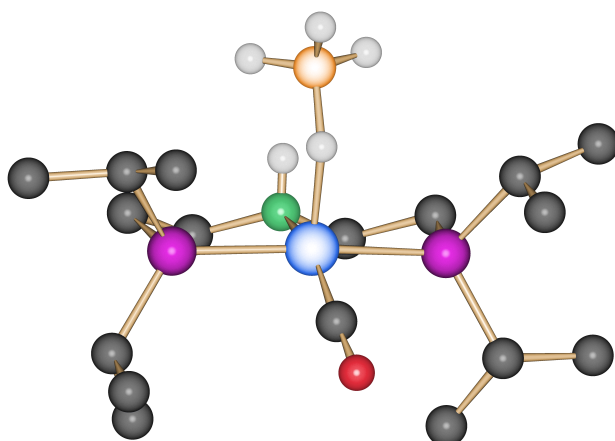
Yield: 158.1 mg (45 %).

Characterization

IR ATR ν (CO): 2971 cm^{-1} ; 1914 cm^{-1} ; 1871 cm^{-1} ; ν (NH): 3400; ν (CH): 2959 cm^{-1} ; 2871 cm^{-1} ; 2783 cm^{-1} ; ν (BH): 2368 cm^{-1} .

$^1\text{H-NMR}$ (300 MHz, C_6D_6) δ (ppm): 3.58 (m, 2H, NH); 3.25 (m, 4H, CH_2), 2.1 (4H, $\text{CH}(\text{CH}_3)_2$); 1.8 (m, 4H, CH_2); 1.35–1.00 (m, 24H, $\text{PCH}(\text{CH}_3)_2$); -1.4 (broad, 4H, BH_4).

Pure red crystals suitable for a single X-Ray diffraction were grown from a solution of ethyl ether layered with heptane.



SCHAKAL

Figure 36. Crystal structure of complex **F**.

Table 10. Crystal data of complex **F**.

Identification code	
Crystal description	Red prism
Empirical formula	$C_{17}H_{37}Cl_2CoNO_2P_2$
Formula weight	$407.19 \text{ g}\cdot\text{mol}^{-1}$
Temperature	150(2) K
Wavelength	0.71073 \AA
Crystal system	Monoclinic
Space group	$P2(1)/n$
Unit cell dimensions	$a=8.0249(2)$ $\alpha= 90.00^\circ$ $b=27.3200(8)$ $\beta= 97.101(1)^\circ$ $c=10.3546(3)$ $\gamma= 90.00^\circ$
Volume	$2252.73(11) \text{ \AA}^3$
Z	4
Density (calculated)	$1.201 \text{ mg}/\text{m}^3$
Absorption coefficient	0.907 mm^{-1}
F(000)	880
Crystal size	$0.38 \times 0.32 \times 0.14 \text{ mm}^3$
Distances	
Co-C	$1.6949(17) \text{ \AA}$

C-O	1.163(2) Å
Co-N	2.0555(12) Å
N-H	0.823(19) Å
Co-H _{1-BH4}	1.66(2) Å
H ₁ -B	1.27(2) Å
H _{2,3,4} -B	1.10(2) Å
Co-P ₁	2.1869(4) Å
Co-P ₂	2.1863(4) Å
Angles	
C-Co-N	154.31(8) °
Co-N-H	103.8(13) °
C-Co-P ₁	95.61(6) °
C-Co-P ₂	90.14(6) °
C-Co-H _{BH4}	112.2(7) °

4.3 HYDROGENATION REACTION

Hydrogenation reactions were carried out using an autoclave (Parr Instrument series) reactor (300mL) equipped with a mechanical stirrer (0-1200 rpm) and provision for measurement of temperature and pressure. The autoclave was modified adding a new red valve, where a small tube was inserted in order to have an argon flow during charging (Figure 36). This prudence was necessary due to the expected high sensibility of the catalyst. In a typical experiment reaction vial and autoclave were flashed with argon several times. Substrate (0.5 mmol) is added to the vial depending on his state of matter:

- solid, the substrate is directly added to reaction vial then flashed with argon;
- liquid, the substrate is dried under CaH_2 , distilled and degassed by freeze-pump-thaw cycles.

A catalyst solution in THF is prepared and added to the vial (2 mL). Autoclave was charged with reaction vial very fast under an argon flow in order to reduce air/oxygen contamination. The autoclave was connected to a Schlenk line, the small tube removed and the red valve left open in order to remove any traces of air by argon flow.

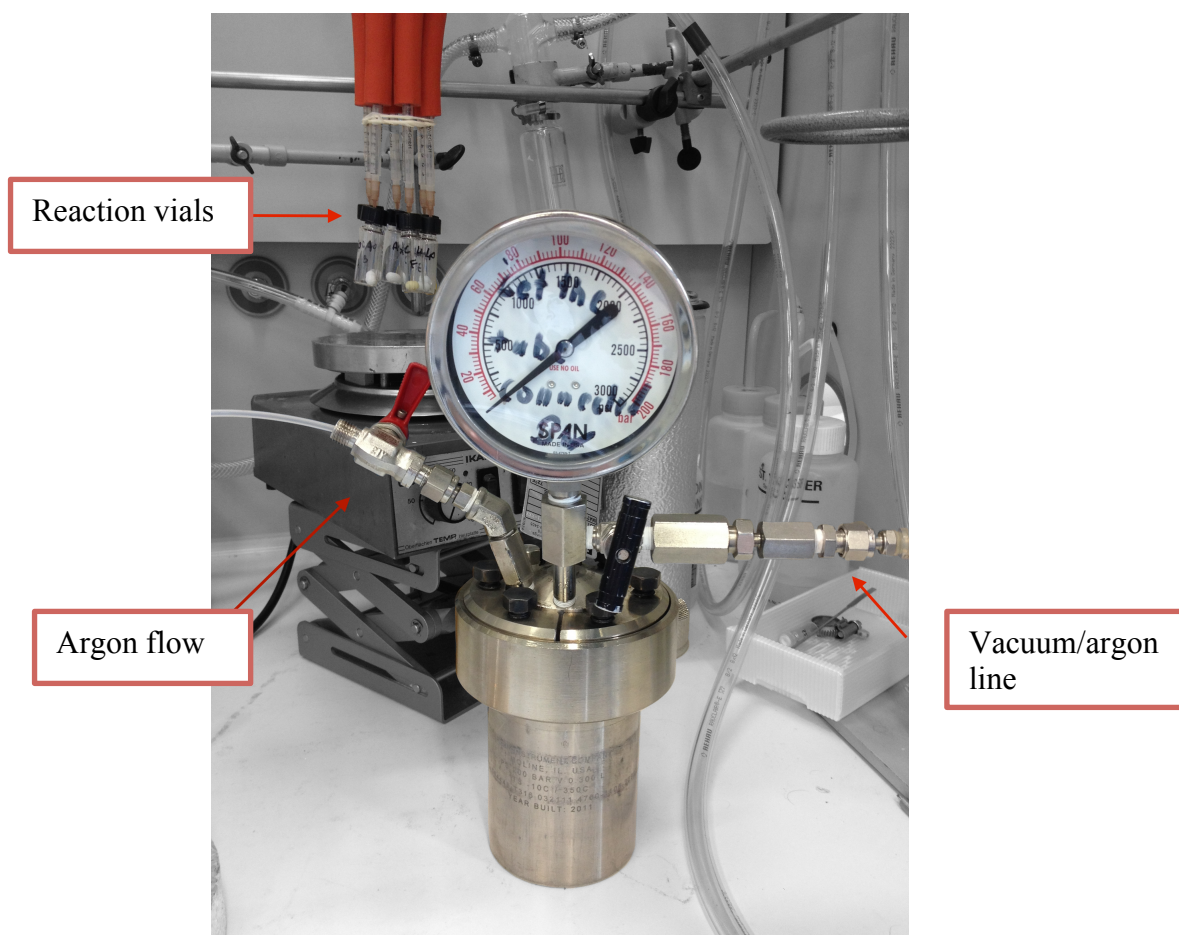
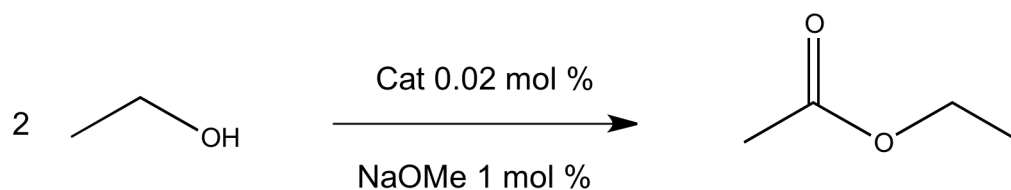


Figure 37. In the foreground, the autoclave with connections to vacuum/argon line (right) and argon flow (left). In the background, reaction vials connected to the vacuum/argon line.

The autoclave was closed, purged several times (at least 6) with H₂ to avoid any traces of argon and then pressurized at 30 bar (H₂). Temperature was set to 100°C and reaction mixture was stirred at 1000 rpm until the end of reaction time.

At the end, the autoclave was cooled down in an ice bath and depressurized. Hexadecane was added as a standard to the reaction solution and samples analyzed by GC and GC/MS.

4.4 ACCEPTORLESS DEHYDROGENATIVE COUPLING OF ETHANOL



In a typical ADC experiment, a catalyst solution was addedⁱⁱ to a 25 mL Schlenk tube and solvent was removed under vacuum. The stopper was replaced with a finger-type condenser connected to circulating fresh water (see Figure 37).

A septum was placed on the side-arm of Schlenk tube and pierced with a needle, connected to a vacuum/argon line, to let the argon flow in and out. EtOH was added with a syringe through the septum. The flask was placed into an oil-bath preheated to 90 °C and left under reflux for 24 h. During reaction, H₂ gas eventually produced passed through vacuum/argon line and a mineral oil bubbler.

At the end of reaction time, cyclooctane was added as a standard and conversion to product was monitored by ¹H-NMR and GC analysis.

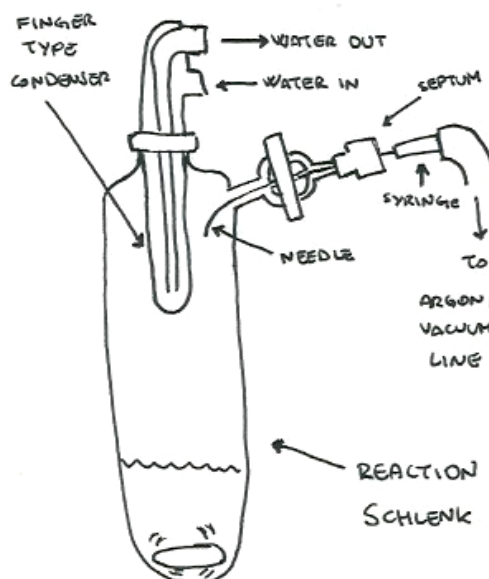
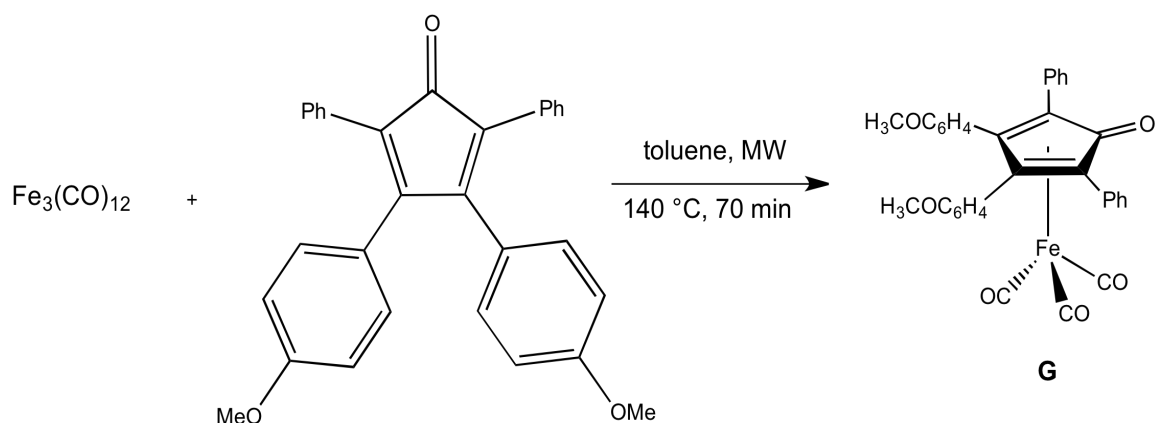


Figure 38. Assemblage for ADC of ethanol.

ⁱⁱ When NaOMe was used as an additive, it was added before catalyst solution.

4.5 IRON COMPLEXES

4.5.1 Synthesis of triscarbonyl-(η^4 -3,4-bis(4methoxyphenyl)-2,5-diphenylcyclopenta-2,4-dienone)iron (G)



Procedure

In a 75 mL Teflon tube equipped with magnetic stirrer, 3,4-Bis(4-methoxyphenyl)-2,5-diphenylcyclopenta-2,4-dienone (0.53 g, 1.2 mmol) and $\text{Fe}_3(\text{CO})_{12}$ (0.20 g, 0.40 mmol) were dissolved in 40 mL of toluene. The container is closed with a cap, equipped with a temperature sensor, and placed into microwave.

The reaction is heated to 140 °C for 70 min. At the end of reaction time, the solvent is removed under vacuum and the solid re-dissolved in minimum amount of CH_2Cl_2 . The crude is purified by column chromatography on alumina ($h = 3$ cm). The unreacted ligand was eluted with CH_2Cl_2 , then a yellow fraction was recovered by EtOAc, finally further triscarbonyl product was recovered by a EtOAc/MeOH (1:1) mixture. Last two fractions were mixed and solvent removed in vacuo to leave a yellow solid identified as Triscarbonyl-(η^4 -3,4-bis(4methoxyphenyl)-2,5-diphenylcyclopenta-2,4-dienone)iron **G** by IR and $^1\text{H-NMR}$.

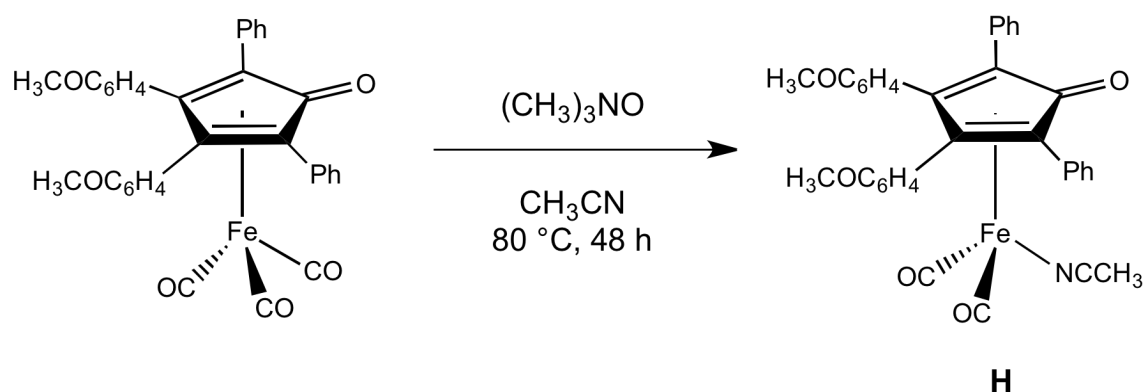
Yield: 0.063 g (27.5 %)

Characterization

IR (CH_2Cl_2) $\nu(\text{CO})$: 2067 cm^{-1} , 2013 cm^{-1} , 1998 cm^{-1} , $\nu(\text{C}=\text{C})$: 1609 cm^{-1} , 1518 cm^{-1} .

$^1\text{H-NMR}$ (399.9 MHz, CDCl_3) δ (ppm): 7.53-6.67 (m, 18H, CH aromatici); 3.77 (s, 6H, $-\text{OCH}_3$).

4.5.2 Synthesis of dicarbonyl-(η^4 -3,4-bis(4-methoxyphenyl)-2,5-diphenylcyclopenta-2,4-dienone)(acetonitrile)iron (**H**)



Procedure

In a 50 mL Schlenk tube, tris-carbonyl-(η^4 -3,4-bis(4-methoxyphenyl)-2,5-diphenylcyclopenta-2,4-dienone)iron (0.055 g, 0.095 mmol) was dissolved in 15 mL of anhydrous acetonitrile. Triethylamine-N-oxide (0.007 g, 0.095 mmol) was added to the solution. Reaction mixture was left under reflux at 80 °C for 48 h. The solution turned red.

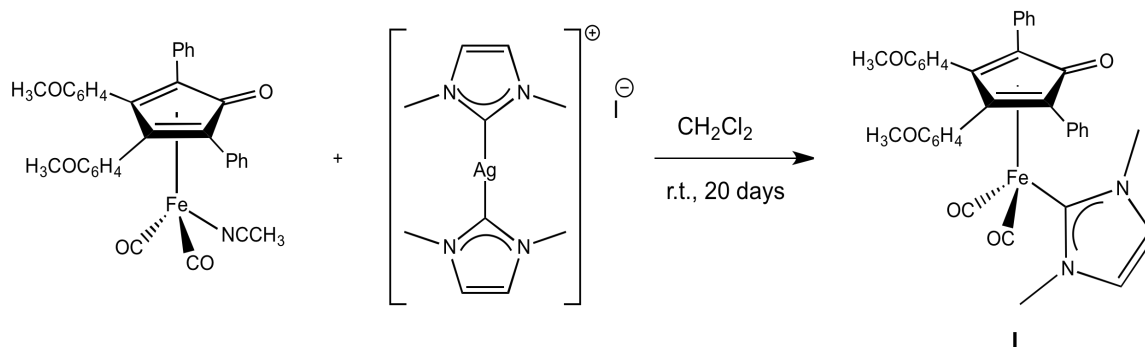
At the end of reaction time, the solvent was removed under vacuum to leave a solid, identified as dicarbonyl-(η^4 -3,4-bis(4-methoxyphenyl)-2,5-diphenylcyclopenta-2,4-dienone)(acetonitrile) iron **H** by IR and $^1\text{H-NMR}$ analysis.

Characterization

IR (CH_2Cl_2) $\nu(\text{CO})$: 2008 cm^{-1} , 1954 cm^{-1} , $\nu(\text{C}=\text{C})$: 1608 cm^{-1} , 1515 cm^{-1} .

$^1\text{H-NMR}$ (399.9 MHz, CDCl_3) δ (ppm): 7.64-6.63 (m, 18H, CH aromatici); 3.74 (s, 6H, $-\text{OCH}_3$); 2.01 (s, 3H, $-\text{NCCH}_3$).

4.5.3 Synthesis of dicarbonyl-(η^4 -3,4-bis(4-methoxyphenyl)-2,5-diphenylcyclopenta-2,4-dienone)(1,3-dimethyl-imidene)iron (I)



Procedure

In a 50 mL Schlenk tube, dicarbonyl-(η^4 -3,4-bis(4-methoxyphenyl)-2,5-diphenylcyclopenta-2,4-dienone)(acetonitrile)iron (0.056 g, 0.095 mmol) and 20 mL of a solution of 1,3-dimethylimidazol-ylidene silver iodide complex (0.021 g, 0.047 mmol in 20 mL) in CH_2Cl_2 were added. Reaction mixture was left under stirring at room temperature for 20 days. Reaction was followed by IR spectroscopy.

At the end of reaction time, the solution was dark red and a yellow precipitate was formed. Solution was filtered through a pad of Celite under inert atmosphere and the solvent removed under vacuum. The solid left was analyzed by $^1\text{H-NMR}$ and ESI-MS analysis and identified as dicarbonyl-(η^4 -3,4-bis(4-methoxyphenyl)-2,5-diphenylcyclopenta-2,4-dienone)(1,3-dimethyl-imidene)iron I. Quantitative yield.

A crystallization attempt in CH_2Cl_2 double layered with petroleum ether was made without success.

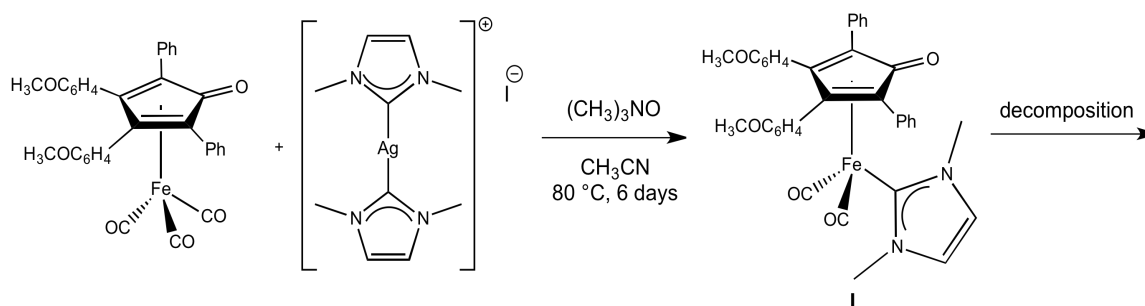
Characterization

IR (CH_2Cl_2) $\nu(\text{CO})$: 1987 cm^{-1} , 1931 cm^{-1} , $\nu(\text{C}=\text{C})$: 1606 cm^{-1} , 1515 cm^{-1} .

$^1\text{H-NMR}$ (399.9 MHz, CDCl_3) δ (ppm): 7.72-6.70 (m, 18H, CH aromatics); 3.75 (s, 6H, $-\text{OCH}_3$); 3.18 (s, 3H, $-\text{NCH}_3$).

ESI-MS (m/z) (+) = 653 [M+H]^+ ; 675 [M + Na]^+ ; 691 [M + K]^+ .

4.5.4 Attempt of synthesis of dicarbonyl-(η^4 -3,4-bis(4-methoxyphenyl)-2,5-diphenylcyclopenta-2,4-dienone)(1,3-dimethyl-imidene)iron *in situ*

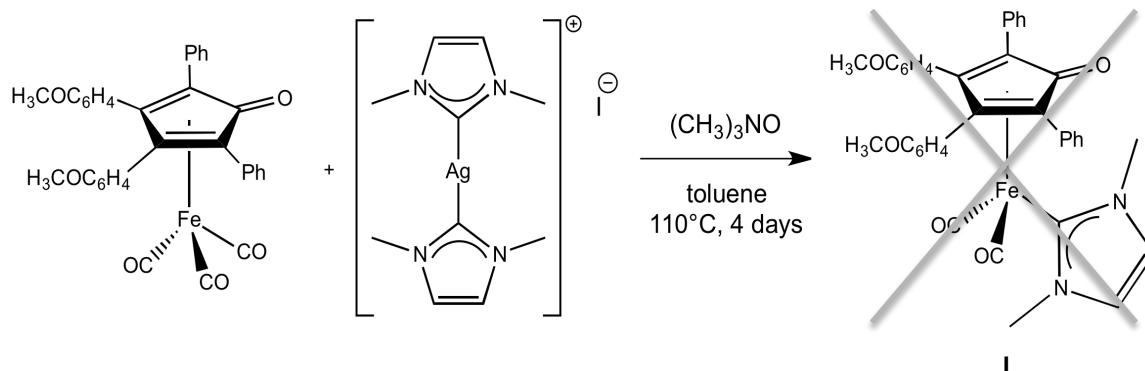


Procedure

In a 100 mL Schlenk tube, triscarbonyl-(η^4 -3,4-bis(4-methoxyphenyl)-2,5-diphenylcyclopenta-2,4-dienone)iron (0.056 g, 0.095 mmol), $(\text{CH}_3)_3\text{NO}$ (7.1 mg, 0.095 mmol) and 30 mL of a solution of 1,3-dimethylimidazol-ylidene silver iodide complex (0.021 g, 0.047 mmol in 30 mL) in CH_3CN were added. Reaction mixture was left under reflux at $80\text{ }^\circ\text{C}$ for 6 days and followed by IR spectroscopy (IR (**I**) $\nu(\text{CO})$: 1989 cm^{-1} ; 1932 cm^{-1}).

The solvent was removed under vacuum. Solid was analyzed by IR and $^1\text{H-NMR}$ spectroscopy, then dissolved in toluene double-layered with hexane. Under these conditions the product (**I**) decomposed.

4.5.5 Attempt of synthesis of dicarbonyl-(η^4 -3,4-bis(4-methoxyphenyl)-2,5-diphenylcyclopenta-2,4-dienone)(1,3-dimethyl-imidene)iron *in situ*



Procedure

Tris-carbonyl-(η^4 -3,4-bis(4-methoxyphenyl)-2,5-diphenylcyclopenta-2,4-dienone)iron (0.056 g, 0.095 mmol), $(\text{CH}_3)_3\text{NO}$ (7.1 mg, 0.095 mmol) and 20 mL of a solution of 1,3-dimethylimidazol-ylidene silver iodide complex (0.021 g, 0.047 mmol in 30 mL) in anhydrous toluene were added to a 100 mL Schlenk tube. Reaction mixture was left under reflux at 110°C for 4 days and followed by IR spectroscopy.

Crude is purified by column chromatography. Free unreacted cyclopentadienonic ligand was eluted by CH_2Cl_2 , then polarity of eluent was increased by a $\text{CH}_2\text{Cl}_2/\text{Et}_2\text{O}$ mixture with increasing ratio (10:1, 10:2, 2:1, 1:1). Finally EtOAc was used as eluent and a fraction of tris-carbonylic iron precursor **G** was recovered. Carbonylic carbenic iron complex **I** was not recovered.

5. Bibliography

- (1) T. W. Solomons, C. B. Fryhle, *Chimica Organica* 3° Ed. Zanichelli, pag 285
- (2) Ege, S. N. *Organic Chemistry*; D. C. Health and Company:Lexington, **1989**; p 596
- (3) Kubas, G. J. *Chem. Rev.* **2007**, 107, 4152.
- (4) Jia, G.; Lau, C. P. *Coord. Chem. Rev.* **1999**, 190–192, 83.
- (5) Clapham, S. E.; Hadzovic, A.; Morris, R. H. *Coord. Chem. Rev.* **2004**, 248, 2201.
- (6) Bullock, R. M. *Chem.Eur. J.* **2004**, 10, 2366.
- (7) *Topics in Organometallic Chemistry: Bifunctional Molecular Catalysis*; Ikariya, T., Shibasaki, M., Eds.; Springer: New York, **2011**; Vol. 37.
- (8) Ikariya, T. *Bull. Chem. Soc. Jpn.* **2011**, 84, 1.
- (9) Denis H. James William M. Castor, “Styrene” in *Ullmann’s Encyclopedia of Industrial Chemistry*, Wiley-VCH, Weinheim, **2005**.
- (10) Newkome, G. R.; Puckett, W. E.; Gupta, V. K.; Kiefer, G. E. *Chem. Rev.* **1986**, 86, 451.
- (11) Bertoli, M.; Choualeb, A.; Gusev, D. G.; Lough, A. J.; Major, Q.; Moore, B. *Dalton Trans.* **2011**, 40, 8941.
- (12) Moreno, I.; SanMARTin, R.; Ines, B.; Churruca, F.; Dominguez, E. *Inorg. Chim. Acta* **2012**, 363, 1903.
- (13) Benito-Garagorri, D.; Kirchner, K. *Acc. Chem. Rev.* **2008**, 41, 201.
- (14) Van Koten, G. *Pure Appl. Chem.* **1989**, 61, 1681.
- (15) Mohammad, H. A. Y.; Grimm, J. C.; Eichele, K.; Mack, H. G.; Speiser, B.; Novak, F.; Quintanilla, M. G.; Kaska, W. C.; Mayer, H. A. *Organometallics* **2002**, 21,5775.
- (16) Gelman, D.; Musa, S. *ACS Catal.* **2012**, 2, 2456.
- (17) Noyori, R.; Okhuma, T. *Angew. Chem., Int. Ed.* **2001**, 40, 40.
- (18) Teunissen, H. T.; Elsevier, C.J. *Chem. Commun.* **1997**, 667.
- (19) Hanton, M. J.; Tin, S.; Boardman, B. J.; Miller, P. J. *Mol. Catal. A: Chem.* **2011**, 70.
- (20) (a) Geilen, F. M. A.; Engendahl, B.; Harwardt, A.; Marquardt, W.; Klankermayer, J.; Leitner, W. *Angew. Chem.* **2010**, 122, 5642.
(b) Geilen, F. M. A.; Engendahl, B.; Harwardt, A.; Marquardt, W.; Klankermayer, J.; Leitner, W. *Angew. Chem. Int. Ed.* **2010**, 49, 5510.
(c) Geilen, F. M. A.; Engendahl, B.; Hölscher, M.; Klankermayer, J.; Leitner, W. *J. Am. Chem. Soc.* **2011**, 133,14349.
- (21) Corma, A.; Iborra, S.; Velty, A. *Chem. Rev.* **2007**, 107, 2411.

- (22) Huber, G. W.; Chheda, J. N.; Barrett, C. J.; Dumesic, J. A. *Science* **2005**, 308, 1446.
- (23) Huber, G. W.; Iborra, S.; Corma, A. *Chem. Rev.* **2006**, 106, 4044.
- (24) Serrano-Ruiz, J. C.; Wang, D.; Dumesic, J. A. *Green Chem.* **2010**, 12, 574.
- (25) Zhang, J.; Leitus, G.; Ben-David, Y.; Milstein, D. *Angew. Chem.* **2006**, 118, 1131;
Angew. Chem, Int. Ed. **2006**, 45, 1113.
- (26) Fogler, E.; Balaraman, E.; Ben-David, Y.; Leitus, G.; Shimon, S. J. W.; Milstein, D. *Organometallics* **2011**, 30, 3826.
- (27) Werkmeister, S.; Junge, K.; Beller, M. *Org. Process Rev. Dev.* **2014**, 18, 289.
- (28) Langer, R.; Leitus, G.; Ben-David, Y.; Milstein, D. *Angew. Chem. Int. Ed.* **2011**, 50, 2120.
- (29) Nielsen, M.; Alberico, E.; Baumann, W.; Drexler, H.-J.; Junge, H.; Gladiali, S.; Beller, M. *Nature*, **2013**, 495, 85.
- (30) Alberico, E.; Sponholz, P.; Cordes, C.; Nielsen, M.; Drexler, H.-J.; Baumann, W.; Junge, H.; Beller, M. *Angew. Chem. Int. Ed.* **2013**, 52, 14162.
- (31) Werkmeister, S.; Junge, K.; Wendt, B.; Alberico, E.; Jiao, H.; Baumann, W.; Junge, H.; Gallou, F.; Beller, M. *Angew. Chem. Int. Ed.* **2014**, 53, 1.
- (32) Chen, L.; Ai, P.; Gu, J.; Jie, S.; Li, B.-G. *Journal of Organometallics Chemistry* **716** **2012** 55.
- (33) Wang, M.; Yu, X.; Shi, Z.; Qian, M.; Jin, K.; Chen, J.; He, R. *Journal of Organometallics Chemistry* **645** **2002** 127.
- (34) Zhang, G.; Scott, B. L.; Hanson, S. K. *Angew. Chem. Int. Ed.* **2012**, 51, 12102.
- (35) Rozenel, S. S.; Kerr, J. B.; Arnold, J. *Dalton Trans.*, 2011, **40**, 10397.
- (36) Zhang, D. L.; Deng, Y. F.; Li, C. B. *Chen, J. Ind. Eng. Chem. Res.* **2008**, 47, 1995.
- (37) Conley, B. L.; Pennington-Boggio, M. K.; Boz, E.; Williams, T. J. *Chem. Rev.* **2010**, 110, 2294.
- (38) (a) Warner, M. C.; Casey, C. P.; Backvall, J.-E. *Top. Organomet. Chem.* **2011**, 37, 85.
(b) Conley, B. L.; Pennington-Boggio, M. K.; Boz, E.; Williams, T. J. *Chem. Rev.* **2010**, 110, 2294.
(c) Karvembu, R.; Prabhakaran, R.; Natarajan, N. *Coord. Chem. Rev.* **2005**, 249, 911.
- (39) Cesari, C.; Sambri, L.; Zacchini, S.; Zanotti, V.; Mazzoni, R. *Organometallics* **2014**, xxx

- (40) Busetto, L. Fabbri, D.; Mazzoni, R.; Salmi, M.; Torri, C. Zanotti, V. *Fuel* **90** **2011**, 1197.
- (41) Pasini, T.; Solinas, G.; Zanotti, V.; Albonetti, S.; Cavani, F.; Vaccari, A.; Mazzanti, A.; Ranieri, S.; Mazzoni, R. *Dalton Trans.* **2014**, 43, 10224.
- (42) Iron hydrogenase enzymes: (a) Peters, J. W.; Lanzilotta, W. N.; Lemon, B. J.; Seefeldt, L. C. *Science* **1998**, 282, 1853. (b) Nicolet, Y.; Piras, C.; Legrand, P.; Hatchikian, C. E.; Fontecilla-Camps, J. C. *Structure* **1999**, 7, 13. (c) Fan, H.-J.; Hall, M. B. *J. Am. Chem. Soc.* **2001**, 123, 3828.
- (43) Casey, C. P.; Guan, H. *J. Am. Chem. Soc.* **2007**, 129, 5816.
- (44) Conti, S. *tesi di laurea magistrale* (II sessione A.A. 2012-2013): Nuovi complessi carbenici N-eterociclici di argento e rutenio: il ruolo del sale di imidazolio.
- (45) Johnson, T. C.; Clarkson, G. J.; Wills, M. *Organometallics* **2011**, 30, 1859.